

Department of Civil and Environmental Engineering

Stanford University

Seismic Risk to Major Industrial Facilities

By

Anne Kiremidjian,
Keith Ortiz,
Richard Nielsen,
and Bahram Safavi



Report No. 72
January 1985

The John A. Blume Earthquake Engineering Center was established to promote research and education in earthquake engineering. Through its activities our understanding of earthquakes and their effects on mankind's facilities and structures is improving. The Center conducts research, provides instruction, publishes reports and articles, conducts seminar and conferences, and provides financial support for students. The Center is named for Dr. John A. Blume, a well-known consulting engineer and Stanford alumnus.

Address:

The John A. Blume Earthquake Engineering Center
Department of Civil and Environmental Engineering
Stanford University
Stanford CA 94305-4020

(650) 723-4150
(650) 725-9755 (fax)
racquelh@stanford.edu
http://blume.stanford.edu

©1985 The John A. Blume Earthquake Engineering Center

SEISMIC RISK TO MAJOR INDUSTRIAL FACILITIES

by

Anne S. Kiremidjian, Keith Ortiz, Richard Nielsen

and Bahram Safavi

Report to the

National Science Foundation

Grant No. CEE-8116997

and

Grant No. CEE-8400479

January, 1985

ABSTRACT

Seismic risk to major industrial facilities has been studied primarily in relation to nuclear power plants. Recently, however, attention has been focused on other large industrial plants due to the increasing awareness of the potential of damage of such plants and the consequences from faiures at such plants.

The overall goal of this study is to develop a general methodology for seismic risk evaluation at major industrial facilities. Such a methodology includes (1) methods for estimating the damage to structures and equipment, (2) methods for evaluating the performance of the overall system, and (3) formulations for estimating the economic and other losses. This report focuses on the first of these aspects of the general risk methodology.

Currently existing methods for evaluating the performance of structures at major industrial facilities when subjected to earthquake ground motion were reviewed. The advanced first order reliability approach be used for that purpose. The main advantages of this approach is that reliability computations are mathematically invariant and uncertainties included in the analysis relate to physical parameters which can be quantified more readily. Simplified formulations for the limit state equations are presented which can be standardized for classes of structures with similar design configurations. The methods for failure probability (or reliability) estimates are illustrated through specific examples. For the purpose of presenting application examples, typical structures found at oil refineries are identified. Reliability estimates are obtained specifically for tall isomerization columns of uniform and non-uniform cross sections. Various degrees of complexity are introduced in the structural response formulations to assess the adequacy of the simplified approach.

Currently, methods for system performance are being investigated for potential use in the general seismic risk methodology. The attention is focused on incorporating component dependencies within the system and multiple performance states of components. The systems analysis method will be tested through an application to a simplified hypothetical oil refinery.

ACKNOWLEDGEMENTS

The research reported herein is part of the project "Seismic Risk to Major Industrial Facilities" conducted under the sponsorship of the National Science Foundation. The authors are greatful for the financial support of NSF which made the project possible. The continued encouragements of Dr. Mike Gaus and Dr. S.C. Liu of NSF is especially acknowledged.

The authors would like to also thank Chevron Corporation and in particular Warren Mitchell and Ben Burke of Chevron Corporation, San Francisco for continual technical advise on the design and performance of facilities at oil refineries, critical review of several manuscripts and encouragement through the course of this research.

As the research extended over several years, a number of graduate students and faculty of the John A. Blume Earthquake Engineering Center have made significant contributions. The help of Professors Haresh C. Shah, James M. Gere and Helmut Krawinkler is greatfully acknowledged. Thalia Anagnos actively participated at the early stages of the project and her help and advice is especially acknowledged.

The computer program on structural component reliability evaluations provided by Dr. Rudiger Rackwitz of the University of Munich was particularly helpful to this project.

Most of all the authors would like to thank Theadora Kennedy for very patiently typing the manuscript after several revisions.

TABLE OF CONTENTS

	Page
ABSTRACT	i
ACKNOWLEDGEMENTS	ii
LIST OF FIGURES	v
LIST OF TABLES	vii
1. INTRODUCTION	1
1.1 Statement of the Problem	1
1.2 Scope of the Project	2
1.3 The General Risk Analysis Problem	3
1.4 Report Organization	6
2. DAMAGE FROM PAST MAJOR EARTHQUAKES	8
2.1 Introduction	8
2.2 Damage Summaries	9
2.3 Discussion and Conclusion	18
3. METHODS FOR SYSTEMS ANALYSIS	23
3.1 Fundamentals of Systems Analysis	23
3.2 Identification of System Failure Modes	29
3.3 Calculation of Failure Mode Probabilities	31
3.4 Probability of System Failure	34
3.5 Summary	35
4. COMPONENT RELIABILITY FORMULATION	36
4.1 Structural Relibility Theory for Component Failures	36
4.1.1 First Order Second Moment (FOSM) Methods	37
4.1.2 Advanced First Order Reliability (AFOR) Methods	38
4.2 Lognormal Fragility Approach	41
4.3 Application of AFOR Methods	43
4.4 Summary and Conclusions	47

		Page
5.	APPLICATION OF METHODOLOGY TO OIL REFINERY	49
	5.1 General Refinery Layout	49
	5.1.1 Two Stage Crude Unit	55
	5.1.2 Atmospheric Column	58
	5.1.3 Side Cut Strippers	60
	5.1.4 Vacuum Column	60
	5.1.5 Piping and Fittings	61
	5.1.6 Pipe Stanchions	62
	5.1.7 Cylindrical Storage Tanks	63
	5.1.8 Spherical Storage Tanks	65
	5.1.9 Support Frames	65
	5.1.10 Occupied Buildings	66
	5.1.11 Furnaces	66
	5.1.12 Cooling Towers	67
	5.2 Seismic Design Criteria	67
	5.2.1 Structures	68
	5.2.2 Equipment	70
	5.2.3 Cylindrical Storage Tanks	71
	5.2.4 Comments and Summary	75
6.	COMPONENT RELIABILITY COMPUTATIONS	77
	6.1 Introduction	77
	6.2 Bolt Yield Analysis	77
	6.2.1 Equivalent Static Analysis	79
	6.2.2 Random Vibrations Analysis	84
	6.3 Skirt Buckling	90
	6.4 Weld Tear	92
	6.5 Nonuniform Vessel	96
	6.6 Summary and Conclusions	98
7.	SUMMARY, CONCLUSIONS AND FUTURE WORK	101
	7.1 Summary	101
	7.2 Future Work	103
REFERENCES		105

LIST OF FIGURES

		Page
1.1	Steps in seismic risk analysis of major industrial facilities	4
2.3.1	Collapsed tank	20
2.3.2	Elephant foot buckling	20
2.3.3	Diamond Buckling	21
2.3.4	Buckled roof	21
2.3.5	Broken piping connection	22
2.3.6	Anchor bolt yield	22
3.1	a) Example system Z b) Subsystem X c) Subsystem Y	24 24 24
3.2	Simple system in (a) series, and (b) in parallel	26
3.3	a) Fault tree representation for subsystem in Figure 3.1(b) b) Fault tree represnetation for subsystem in Figure 3.1(c)	28 28
3.4	Event tree example for system Z	30
3.5	Integration regions for multistate correlation components	33
4.1	Definition of the Hasofer and Lind reliability index	39
4.2	Two story frame supporting equipment E_1 and E_2	43
4.3	Ground motion spectra	45
5.1	Simplified system flow showing basic equipment	50
5.2	Simplified refinery flow diagram and typical equipment	51
5.3	Two stage crude unit	56
5.4	Typical atmospheric column	57
5.5	Reinforced conrete pipe support structure	62
5.6	Typical tanks	64
5.7	Effective weight of tank contents	72
5.8	Effective height to centroid of tank contents	72

5.9	K-factor for period calculations	72
6.1	Atmospheric column	78
6.2	Fragility curve for equivalent static analysis	81
6.3	Sensitivity analyses for bolt yield	82
6.4	Sensitivity of bolt yield fragility to anchor bolt design	83
6.5	Cross section and stress distribution at base of supporting skirt	88
6.6	Stress in bolts versus applied base moment as predicted by equations 6.8 and 6.9	89
6.7	Equivalent static buckling fragilty curve for uniform column	93
6.8	Sensitivity analysis for buckling of uniform column	95
6.9	Nonuniform vessel	97
6.10	Fragility curves for equivalent static analysis of nonuniform column	99
6.11	Lognormal approximations for fragility curves	100

LIST OF TABLES

2.1	Structural Damage to Tanks	11
2.2	Structural Damage to Tall Columns	15
2.3	Structural Damage to Other Equipment	16
2.4	Summary of Typical Damages	19
5.1	Major Oil Refinery Components and their Contribution to Failure	52
5.2	Earthquake and Seismic Zone Factors	68
5.3	Structure Coefficient (K)	69
6.1	Basic Random Variables for Analysis of Nonuniform Vessel	98

CHAPTER 1

INTRODUCTION

The need for a comprehensive methodology for evaluating the risks from failure of major industrial facilities due to earthquakes has recently been recognized. This need stems from the increased awareness of the damage potential of large earthquakes, the greater number of industrial plants in seismically active regions, the proximity of those plants to highly populated areas, and the growing public concern for the consequences of such failures.

Among the many different types of industrial plants, of primary interest are these facilities for which failure can result in either major direct losses (e.g., fires) or major indirect losses (e.g., discontinuation of service to a community). Examples of such facilities are chemical plants, oil refineries, electric power plants (other than nuclear), electronics and automobile manufacturing plants, food processing plants, chemical and biological laboratories, etc. These types of facilities are classified as large according to the volume of production, dollar value of production, degree of economic impact, degree of biological impact, etc., or a combination of them. (Nuclear power plants can be included with this definition of major industrial facilities. However, the unique nature of the design and the severity of failures from nuclear power plants requires separate analysis. For these reasons they are excluded from this study.)

The overall objective of this study is to develop a general risk methodology suitable for application to major industrial facilities subjected to large earthquakes. The results of such a risk analysis can be used to rehabilitate existing facilities by identifying weak components to be upgraded or components to be made redundant; existing design procedures can be evaluated and upgraded; and emergency procedures can be developed for the most likely major failures.

1.1 Statement of the Problem

Major industrial facilities are often conglomerates of interconnected structural, mechanical, and electrical subsystems. These subsystems are functionally and physically dependent. The subsystems form complex systems

themselves which can be analyzed by advanced systems analysis methods. Of primary concern is the risk to the many subsystems as well as the overall system. The definition of risk depends on the type of facility and the goal of the risk analysis.

Seismic risk analysis techniques have been developed for conventional buildings, which generally are single structures. These techniques cannot be applied directly to major industrial facilities because of the complexity of such facilities. Considerable work has been done in developing systems analysis techniques for nuclear power plants. The Reactor Safety Study (1975) was the first major study of such complex systems. The most recent study is the Seismic Safety Margins Research Program (SSMRP) conducted by the Lawrence Livermore Laboratory, Livermore, California (Smith et al., 1981; Bohn et al., 1980). Even though many of the techniques used in these studies may be applied to major industrial facilities, the commitment of large resources (manpower, money, and time) may not always be justified when compared with the design effort. Furthermore, new theoretical developments in structural and systems reliability analysis have been implemented to a very limited extent. Finally, the objective of the risk analysis for major industrial facilities may differ considerably from that for nuclear power plants. For these reasons industrial facilities need to be studied separately from nuclear power plants.

In summary, a general risk methodology suitable for application to major industrial facilities must treat the facility as a system. Physical and functional dependencies must be considered. However, the resources demanded by the methodology must be consistent with the prevailing structural analysis and design practices in each industry. At this time no such general methodology exists.

1.2 Scope of the Project

Within the overall goal of developing a general methodology for large industrial facilities, this study concentrates on the evaluation of the performance of component structures in large systems subjected to earthquake ground motion. The study investigates the implementation of recent developments in structural reliability theory and proposes standardized formulations for application to multiple component reliability computations. The feasibility of the proposed approach is demonstrated through example applications to components at an oil refinery subsystem.

1.3 The General Risk Analysis Problem

The main steps in a general seismic risk methodology for large industrial facilities include (a) evaluation of the site hazard; (b) evaluation of the component performance; (c) assessment of the overall plant performence; and (d) computation of losses. These aspects of the methodology are further subdivided as shown in Figure 1.1

Site Hazard. At present numerous methods are available for the evaluation of the potential ground motion at a site. Most of these methods can be used as part of the risk analysis of industrial plants. The criteria which will govern the selection of one method over another include the tectonic regime of the region, the variability of soil conditions over the site and the seismic hisotry of the site. For example, review of the geologic and tectonic setting of a region and its seismic history will reveal if subduction zones are present, if geologic faults are well identified and if seismicity is characterized by large or small events. Thus the models selected need to reflect as many of these aspects as possible. Resulting site hazard computations should be expressed in terms of ground motion parameters suitable for component and systems reliability analysis such as peak ground acceleration, response spectral acceleration power spectral acceleration, etc. Similarly, forecasts should be for annual hazard and hazard over the life of the facility.

Component Reliability Analysis. A major step prior to the overall system reliability is the identification of all components, identification of their correlation and identification of their function within the system. Recent developments in structural reliability theory provide the tools for assessing the failure probabilities (or reliabilities) of such components. Advanced first order reliability analysis (AFOR) methods are particularly useful for that purpose and are discussed in Chapter 4.

System Reliability Analysis. Classical systems analysis methods have been developed in relation to mechanical and electrical systems. The mathematical tools developed for system reliability assessment include event/fault tree, graph and network analysis. The techniques were originally developed for systems in which random component failures, also known as primary components failures, were the main source of system failure. The component failures in

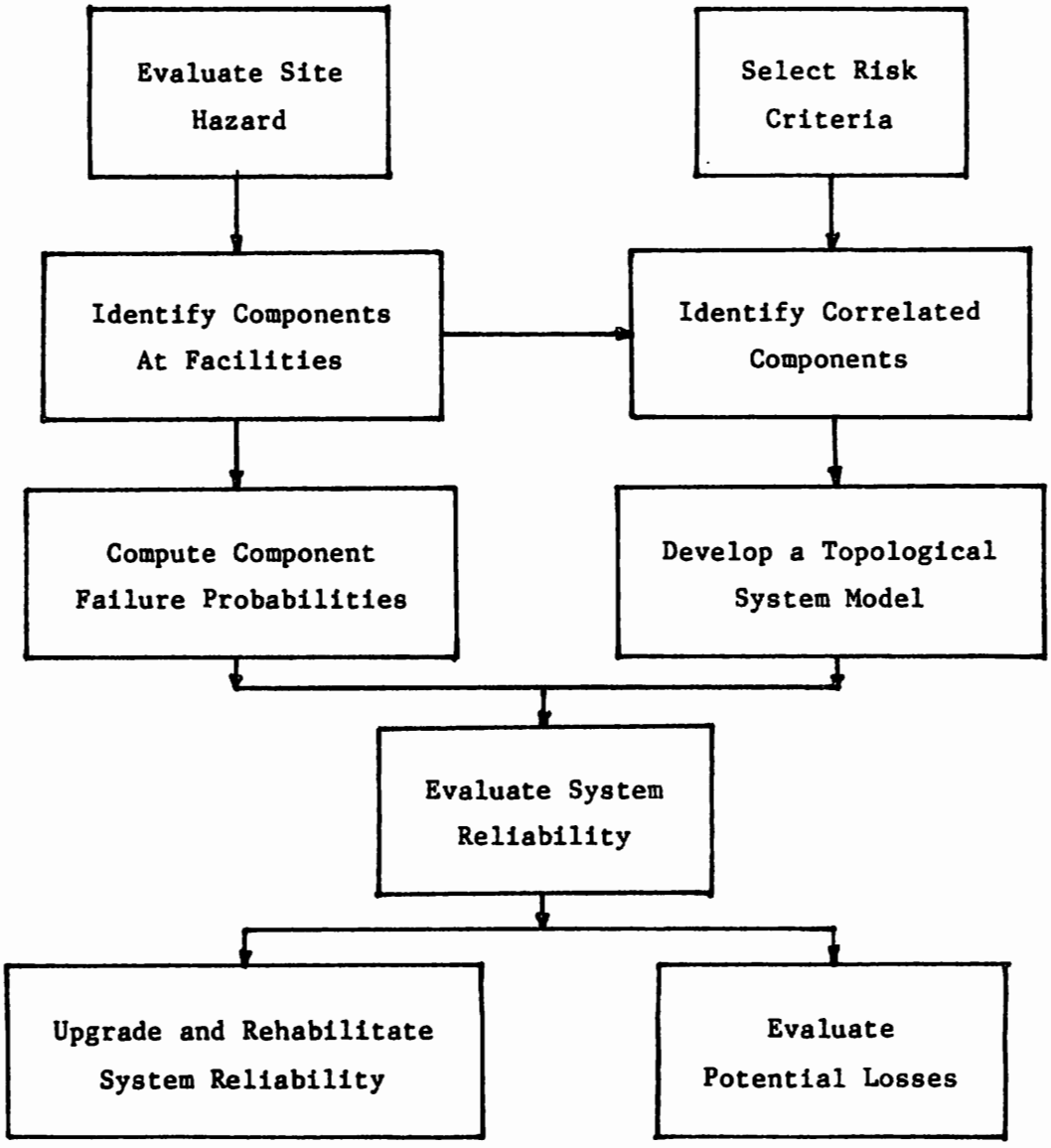


Figure 1.1 Steps in seismic risk analysis of major industrial facilities

graph and network analysis. The techniques were originally developed for systems in which random component failures, also known as primary components failures, were the main source of system failure. The component failures in these analyses could reasonably be assumed to occur independently of each other. In contrast, component failures at industrial plants can be highly correlated.

Most systems are usually complex combinations of systems in parallel and in series. Often, however, such complex systems can be simplified by considering series systems in parallel or parallel systems in series combinations. Methods for analysis of these systems are discussed in greater detail in Chapter 3. Among the goals of such analyses are the identification of most likely failure sequences and upgrading of the system for optimal performance.

Risk Criteria and Systems Representation. In order to model a facility as a network of nodes and links, it is necessary to select a risk criteria, identify the physical layout of the system and the functional layout of the facilty.

Several risk criteria are identified as being particularly useful for large industrial facilities. These include total capital loss, production volume loss, risk of fires and risk from the release of hazardous substances. The systems representation of a facility will be highly dependent on the selected risk measure. Each of these criteria are discussed in the following paragraphs.

a. Capital Loss. Under the assumption that the cost of damage repair for a component is independent of the state of damage to other components. This is the simplest criterion to estimate. The total capital loss or damage repair cost is the sum of the expected costs for all components. "Total" risk in its simplest form will be the arithmetic sum of component risks. A more comprehensive measure of capital loss, however, would include dollar loss due to production loss from down time (or time of inoperation).

b. Release of Hazardous Material. The risk from release of hazardous materials is similar to the risk of radioactive release from nuclear power plants. Such releases are expressed in terms of some measure indicative of the quantity of release and severity of its consequences. In order to assess the risk of release, it is first necessary to determine the sequences leading to the release and their probabilities. Considerations of safety systems are particularly important for this type of analysis.

c. Fire. The potential for fire is almost synonimous with the release of cumbustible material (e.g., butane gas from a storage tank). In that respect the analysis for fire potential will be similar to that for release of hazardous materials. In addition, however, a source of ignition must be present simultaneously and any fire safety systems must be included in the analysis. For example, a spark from an electric motor could ignite a butane gas leak. The evaluation of fire potential and losses from fire can be very complex since the release of combustible material as well as the presence of an ignition source are usually dependent on time and space. A simplified analysis might only consider the release of combustible material, thus reducing the problem to the risk from release of hazardous material.

d. Loss of Production. The evaluation of losses from production interruption requires intimate knowledge of the production systems. In addition to normal production operation of the system, it is necessary to know and understand redundant production routes which may enable the continuation of operation at reduced levels. As an example, consider a system that separates crude oil and water. The oil and water mixture is heated and held in a separation tank. Then oil is drawn off into several oil tanks before shipping. Upon the failure of one of the separator units one of the oil tanks may be modified to serve as a separator, thus allowing the system to operate, perhaps, at a reduced level. Thus while it may be straightforward to estimate component and subsystem downtime, the impact on production capacity or loss is more difficult to evaluate. Ascribing a monetary value to lost production is difficult with any confidence due to the dynamic nature of a production system and the uncertainty in economics over long periods of time.

1.4 Report Organization

In order to achieve the goal of this project several investigations were conducted concurrently. The results of these investigations are reported in the following order.

Chapter 2 of this report presents a synthesis of the observed damage that has occurred to major industrial facilities during past earthquakes as reported in the literature. The system analysis problem is formulated in Chapter 3. The component reliability problem is discussed in Chapter 4. In Chapter 5

the major components of an oil refinery are discussed. In that chapter design methods are reviewed to the extent that they pertain to the reliability problem. Applications of component reliability analysis methods are presented in Chapter 6. Summary, conclusions and future work are discussed in Chapter 7.

CHAPTER 2

DAMAGE FROM PAST MAJOR EARTHQUAKES

2.1 Introduction

In order to study the behavior and identify failure modes of structures and equipment at major industrial facilities, it is important to review the damage observed at such plants during past earthquakes. In this chapter, we present a summary of reported damage to structures and equipment from past earthquake events. The emphasis in this review is on damage to structures at oil refineries. Available information on the factors influencing the type and severity of damage are also included in the damage summaries. A brief general discussion on the factors influencing damage is presented in this section.

Damage to structures and equipment at industrial facilities depends on the characteristics of the earthquake ground motion, the characteristics of the structure or equipment and the local soil conditions. Acceleration, velocity or displacement amplitudes, frequency content, duration and number of peaks above a specified amplitude are some of the characteristics of the ground motion related to damage. The ground motion parameter most widely used in current practice is the peak ground acceleration, PGA. Intuitively, PGA should be proportional to the damage level of a structure. Existing data, however, are too sparce and uncertain to confirm that assertion. Nevertheless, the ground motion parameter reported most often is the peak ground acceleration. Other ground motion parameters, such as frequency content, duration of motion, root-mean-square acceleration, etc., are equally, if not more important for damage assessment. These parameters can be evaluated provided strong ground motion records exist at the site. Standaradized definitions, however, are not yet available for some of these parameters resulting in discrepancies between reported values. For the purposes of this study, peak ground acceleration values are included in the damage summaries whenever these are available. The remaining ground motion parameters are not reported even though their importance is recognized. They are not readily available and their computation is beyond the scope of this study.

Structural characteristics important for damage assessment include predominant frequencies of the structure, damping, ductility and other material

and geometric properties. Structures with similar physical and functional characteristics are grouped together. Available information from the literature on the structural parameters is summarized based on the review of damage data.

Input ground motion at a site depends on the local soil conditions. The frequency content, amplitude and duration of ground motion are altered according to the properties of the local soil. Similarly, the response of the structure depends on the interaction between the soil at the foundation and the structure. Liquefaction or subsidance of the soil are important failure modes and must be considered even though there may not be any direct damage to the structure. Thus, the review of damage from past earthquakes includes information on the local soil properties. Failures of the soil are summarized and the effect of the soil on the type and degree of damage to the structure or equipment are included whenever that information is available.

2.2 Damage Summaries

In the past, several major earthquakes have affected major industrial facilities. A careful examination of their impact on these facilities can be extremely valuable as one attempts to assess the probable risks to an industrial facility in a future earthquake. The performance of structures and equipment in past earthquakes can serve as a guide to identify potential problems and weaknesses in components and systems. Possible and likely failure modes of components and the effects of these failure modes on the overall system can be identified through such a survey.

A major effort by Yanev and Swan (1982) to summarize the performance of a variety of components in power plants subjected to major earthquakes has been recently completed. Their study reviews the design standards of typical components, evaluates the response of these components to given known ground motions from past earthquakes and reports the impact of their response to the overall system. The main conclusion from their study is that equipment designed to sustain peak ground accelerations of up to 0.2g performed very well even when they were subjected to greater accelerations. Many of the component types discussed in their study, such as pumps, valves, motors, etc., can be found in a variety of large industrial facilities.

In addition to their findings, this report presents a damage summary for some typical oil refinery and refinery-type equipment as an example of the information and insight to be gathered from past earthquakes. This summary describes damages due to direct earthquake effects only. Secondary effects such as tsunami and landslides are not included. Earthquake reports from the past fifty years are most relevant in this evaluation since equipment and construction methods previous to that time may differ substantially from current usage. For this reason, earthquake damage reports from the following earthquakes were examined:

1. Long Beach, California, March 10, 1933
2. Kern County, California, July 21, 1952
3. Alaska, March 27, 1964
4. Niigata, Japan, June 16, 1964
5. San Fernando, California, February 9, 1971
6. Managua, Nicaragua, December 23, 1972
7. Miyagi-Ken-Oki, Japan, June 12, 1978
8. Imperial County, California, October 15, 1979
9. Greenville, California, January 24, 1980
10. Central Greece, February 24, 1981
11. Coalinga, California, May 2, 1983

The damage summaries are presented in Tables 2.1, 2.2, and 2.3. These include damage to tanks (Table 2.1), tall columns (Table 2.2), and other equipment (Table 2.3). Table 2.2.1 is an amplification of the data in the last column of Table 2.2.

The data were originally gathered by a variety of persons and organizations including engineers, earthquake researchers, industry representatives, and insurance underwriters. The specific reference for each section is cited below the name of the earthquake in the first column. The second column is the location of the facility and/or the distance from the epicenter to the facility along with any known intensity parameters at that site. The third column lists any pertinent descriptions of the structure or piece of equipment including dimensions where known. The fourth column describes the reported damage. The last column provides any other pertinent information including secondary effects of the damage and description of local soil conditions. The summaries are grouped by type of structure or piece of equipment and then subdivided by earthquake events in reverse chronological order.

Table 2.1 Structural Damages to Tanks

Name of Earthquake (Reference)	Site Intensity/ Magnitude & Location	Tank Description							Structural Damage	Comments
		No. of Tanks	Dia (ft)	Ht (ft)	H/D	Roof Type	Pad Type	Fluid Level (ft)		
Coalinga 5/2/83 (Nielsen, 1983, unpublished)	M = 6.5 3 mi from epicenter	1	48	30	.625	fixed	gravel	24.5	Bulging and rupture of of shell at fluid level	Dikes contained spill. Riveted plate construction.
		1	48	30	.625	fixed	gravel		Outflow pipe disconnected from tank.	
Greenville 1/24/80 (Stratta, 1980)	MMI = VI PGA = 0.2 - 0.3g	1	25.0	50.2	2.0	fixed	concrete		Elephant foot	Tank anchored to mat by 20 - 5/8 in. diameter-wejits
Greenville 1/24/80 (Stratta, 1980)	M = 5.5 18 km from epicenter PGA = 0.3g	10							No damages	All tanks were anchored to concrete pads.
		24							Light damages: minor spalling of concrete pad, failed anchorage welds, minor local buckling.	All tanks were encased in a cooling jacket.
		70							Medium damages: concrete spalling of pads, failed anchorage welds or bolts, Some buckling (2 in. peak to peak).	
		26							Severe damages: anchors failed, extensive buckling uplift of base.	
Imperial Co. 10/15/79 (Reconnaissance Report, Imperial Co., 1980)	M = 6.6 25 mi NW of epicenter PGA = 0.3g	1	48.0	48.0	1	floating	earth	25.5	Dents in shell from roof Elephant foot, 3/4 in. bulge Settlement of tank ± 1 in.	Leaking fluids filled dike, no fire resulted, but 1 mi. radius was evacuated and fire department was called.
		1	47.75	48.0	1.0	floating	earth	34.9	Dents in shell from roof Elephant foot, 3/4 in. bulge Settlement of tank ± 1 in.	Tanks were unanchored.
		1	61.0	48.0	0.79	floating	concrete ringwall	39.4	Leak in tank at floor Settlement of tank ± 1 in.	Tanks were designed to API standard 650 including earthquake forces.
		1	46.5	40.0	0.86	fixed	concrete	34.4	Settlement of tank 1-2 in. on S. W. side.	
		1	41.25	49.0	1.19	fixed	concrete ringwall	43.53	Elephant foot, 6 in. bulge. Leak in tank at floor-wall junction. Crack in floor coating, no leak.	

Table 2.1 (continued)

Name of Earthquake (Reference)	Site Intensity/ Magnitude & Location	Tank Description						Structural Damage	Comments
		No. of Tanks	Dia (ft)	Ht (ft)	H/D	Roof Type	Fnd Type	Fluid Level (ft)	
Imperial Co. 10/15/79 (Reconnaissance Report, Imperial Co. 1980)	M = 6.6 25 mi. NW of epicenter PGA = 0.3g	1	48.16	49.0	1.02	fixed	concrete ringwall	29.9	Ringwall cracked
		1	49.83	49.0	0.98	fixed	concrete	29.8	Ringwall cracked
		1	48.0	48.0	1.0	fixed	concrete ringwall	39.9	Elephant foot, 6 in. bulge. Ringwall cracked.
		1	21.25	24.0	1.13	floating	earth	9.4	Probable floor leak.
Imperial Co. 10/15/79 (Reconnaissance Report, Imperial Co. 1980)	M = 6.6 15 mi from epicenter PGA = 0.51g N-S 0.37g E-W 0.93g V	1	135.0	45.0	0.33	fixed	asphalt base w/ rock ring wall		Buckling of roof plate, roof stringers collapsed. Separation of roof and wall at perimeter weld. Some fuel spilled
		1	73.0	20.0	0.27	fixed	same		Some buckling of roof plate.
Sendai Japan 6/12/78 Reconnaissance Report, Miyagi Ken-Oki 1978)	M = 7.5 100 km from epicenter PGA = 0.27g N-S 0.29g E-W 0.17g V	3							Break at wall-floor junction. Oil released, dike overflowed inundating adjacent facilities
		3							Damaged No fire resulted since plant was shut down at time of earthquake.
Managua 12/23/72 (Ferrer, 1975)	M = 62 50 km from epicenter PGA = 0.39g E-W 0.34g N-S 0.33g V	3							Elephant foot Tanks contained water and were left in service.
San Fernando 2/9/71 (Western Oil, 1971, unpublished)	M = 6.6 El Segundo PGA	1	60	30	0.5	floating		28.25	Roof seals caught on tank rim
		1	80	48	0.6	floating		44.79	Roof seals caught on tank rim
		1	110	48	0.44	floating		46.71	Roof seals caught on tank rim
		1	78	35	0.45	floating			Buckled roof plate
		1							Cracked deck plate
		1							Cracked rim plate
		2	114	30	0.26	floating		28.00	Oil slopped out of roof

Table 2.1 (continued)

Name of Earthquake (Reference)	Site Intensity/ Magnitude & Location	Tank Description						Structural Damage	Comments
		No. of Tanks	Dia (ft)	Ht (ft)	H/D	Roof Type	Fnd Type	Fluid Level (ft)	
Alaska 3/27/64 (Johnson, unpublished)	M = 8.4 130 mi from epicenter	1	30.0	48.0	1.6	fixed			Collapse due to buckling
		1	70.0	48.0	0.68	floating			Roof rotated, damaged roof seal, and gage well
		1	144.0	56.0	0.39	floating			Roof rotated, damaged roof seal, and gage well
		1	90.0	48.0	0.53	floating		full	Roof buckled
		1	90.0	48.0	0.53	floating		full	Roof buckled
		1	64.0	48.0	0.75	fixed		full	Elephant foot and uplift of foundation.
Alaska 3/27/64 (Johnson, unpublished	M = 8.4 130 mi from	1	28.0	40.0	1.4	fixed			Collapse due to buckling Leaking at wall-bottom junction
		1	42.0	40.0	0.95				Buckling and failure at pad Leaking at wall-bottom junction
Alaska 3/27/64 (Johnson, unpublished)	M = 8.4 130 mi from epicenter	1	39.0	40.0	1.3			full	Elephant foot and uplift Break at wall-bottom junction
		1	30.0	40.0	1.3			full	Elephant foot
Alaska 3/27/64 (Committee on the Alaska Earthquake, 1973)	M = 8.4 Location unspecified	1	100	32	.32			full	Damage to roof, top of shell and roof columns
		1	45	32	.71			full	Damage to roof, top of shell and roof rafters. Elephant foot.
		1	120	32	.27			full	Damage to roof, top of shell and roof columns
		1	55	23	.42			full	Damage to roof rafters.
		1	20	40	2.0				Elephant foot
		1	112	56	.50	floating			Roof pontoon damaged
		1	49	48	.98				Elephant foot
		1	160	56	.35				Support columns twisted and rafters damaged.

Table 2.1 (continued)

Name of Earthquake (Reference)	Site Intensity/ Magnitude & Location	Tank Description						Structural Damage	Comments
		No. of Tanks	Dia (ft)	Ht (ft)	H/D	Roof Type	Pad Type	Fluid Level (ft)	
Niigata 6/16/64 (Kawasumi, 1968)	M = 7.5 51 km from epicenter								Shell plates cracked Oil drained
		1							Some buckling at top
		1				floating			Tank contents ignited (no leakage)	Resulting fire buckled adjacent tanks.
		1							Tank cracked, draining oil buckling tank	Leaked contents inundated adjacent facilities and dwellings.
Long Beach 3/10/33 (NBFU, 1933)	M = 6.3 various locations	13							Tanks separated from water draw-off drain	Oil lost down water draw-off drain.
Long Beach 3/10/33 (NBFU, 1933)	M = 6.3 Huntington Beach	1							Collapse
		Many							Distortion, elongation, Buckling of roof plate, strain in riveted joints.
		2							Riveted joint failed, tank leaked
		1							Floating roof damaged.

Spherical Tanks

Name of Earthquake (Reference)	Site Intensity/ Magnitude & Location	Tank Description No.	Size	Damage	Comments
Central Greece 2/24/81 (Carydis, 1982)	MMI = VIII M = 6.7 ± 50 km from epicenter	1		Cracking & Spalling at base of concrete columns and footings. Stretched diagonal ties and turn buckles.	
Kern Co. 7/21/52 (Johnston, 1955)	M = 7.7 16 mi SW of Bakersfield	2	2500 bbl	Support legs collapsed. Lead-in lines ruptured.	Ignition of released gasses caused fire which severely damaged plant.

Table 2.2 Structural Damage to Tall Columns

Columns

Name of Earthquake (Reference)	Site Intensity/ Magnitude & Location	Description No.	Description Type	Damage	Comments
Managua 12/33/72 (Ferrer, 1975)	M = 6.2 50 km from epicenter PGA = 0.39g EW 0.34g NS 0.33g V		Reactor and Furnace columns	Cracked foundations	
Alaska 3/27/64 (Johnson, unpublished)	M = 8.4 130 mi from epicenter	1	Crude column	Anchor bolt yielding 3/16 in.	
Kern Co. 7/21/64 (Steinbrugge, 1954)	M = 7.7 130 mi west of	?	Tall columns	Anchor bolt yielding	No repairs needed for skirts. See Table 2.2.1 for summary of bolt yielding

Table 2.2.1

Description							Damages			
							Bolt stretch (in)			
No.	Dia (ft)	HT (ft)	Gross wt (kips)	No.	Bolt Size (in)	Bolt Cir (in)	NE	SW	NW	SE
1	5.0	52.0	200	16	1-3/4	53.0	1.563	0.563	0.625	0.750
1	3X4	65.5	50	8	1-1/2	56.5	0.375	0.250	0.188	0.125
1	3X4	65.5	50	8	1-1/2	56.5	0.5	0.5	0.469	0.469
1	6.5	84.4	220	16	1-3/4	88.0	E 0.969	W 0.531	0.438	0.5
1	6.5	84.4	220	16	1-3/4	88.0	E 0.938	W 0.50	0.5	0.5
1	7.5X4	112.5	110	16	1-3/4	98.0	0.25	0.25	0.25	0.25
1	3.0	33.6	15.5	8	1-1/4	41.88	0.125	0.125	0.125	0.125
1	3/5	94/9	30	12	2	49.0	0.125	0.125	0.125	0.125

Table 2.3 Structural Damage to Other Equipment

Smoke Stacks

Name of Earthquake (Reference)	Site Intensity/ Magnitude & Location	Description	Damage	Comments
Imperial Co. 10/15/79 (Reconnaissance Report, Imperial Co. 1980)	M = 6.4 15 mi from epicenter PGA = 0.51g N-S = 0.37g E-W = 0.93g V	3 - Gunite-lined steel stacks	Anchor bolt yielding	
Kern Co. 7/21/52 (Steinbrugge, 1954)	M = 7.7 16 mi SW of Bakersfield	Steel heater stack	Local buckling Anchor bolt yielding	

Heat Exchangers

Name of Earthquake (Reference)	Site Intensity/ Magnitude & Location	Description	Damage	Comments
Imperial Co. 10/15/79 (Reconnaissance Report, Imperial Co., 1980)	M = 6.4 10 mi east of epicenter	Long tube heat exchangers	Dislocation at fixed-end tube-to-tube-sheet	Dislocation caused leakage.
Kern Co. 7/21/52 (Steinbrugge, 1954)	M = 7.7 16 mi SW of	Horizontally mounted	Foundation rocked, 5 piers cracked	Piers were replaced.

Pipes and Pipe Supports

Name of Earthquake (Reference)	Site Intensity Magnitude & Location	Description No.	Size/ Type	Damage	Comments
Alaska 10/27/64 (Johnson, unpublished)	M = 8.4 130 mi from epicenter	1	10 in	Pulled apart 30 inches	
Kern Co. 7/21/52 (Steinbrugge, 1954)	M = 7.7 3 mi west of Bakerfield	1	Steam pipe	Broken	

Table 2.3 (continued)

Pipes and Pipe Supports (continued)

Name of Earthquake (Reference)	Site Intensity Magnitude & Location	Description No.	Size/ Type	Damage	Comments
Kern Co. 7/21/52 (Steinbrugge, 1954)	M = 7.7 1 mi radius from Enidio	4		Pulled apart and telescoped	
		3		Pulled apart of weld broke	
		1		Buckled	
Kern Co. 7/21/52 (Steinbrugge, 1954)	M = 7.7 16 mi south of Bakerfield	1	High pressure	8 in. split	
		1	Field line	Broken	
Long Beach 3/10/33 (NBFU, 1933)	M = 6.3 Watsonville		Oil and Vapor	Broken	
Long Beach 3/10/33 (NBFU, 1933)	M = 6.3 Los Angeles, Harbor		Oil Lines	Broken	

Pumps

Name of Earthquake (Reference)	Site Intensity Magnitude & Location	Description No.	Size	Damage	Comments
Alaska 10/27/64 (Johnson, unpublished)	M = 8.4 40 mi east of epicenter	1	Small pump	Flange broke, gasoline leaked.	Gasoline ignited by downed power lines.

Wharf Facilities

Name of Earthquake (Reference)	Site Intensity Magnitude & Location	Description	Damage	Comments
Alaska 3/27/64 (Johnson, unpublished)	M = 8.4 130 mi from epicenter		Catwalks pulled loose, sank at end.	

NOTE: Blank areas indicate that no information was available.

2.3 Discussion and Conclusion

An examination of the data presented on the previous section reveals that the extent of the damage to different plants can vary considerably for a given earthquake and even more so from earthquake to earthquake. However, some patterns can be observed as summarized below.

Tables 2.2 and 2.3 summarize the types of equipment and structures observed to fail most often and the resulting damage. Usually the impact is limited to lost inventory and production, and damaged equipment. However, in a few notable instances the impact was more severe. In the Alaska, Niigata, and Kern County earthquakes, leaking fluids ignited and burned tanks and adjacent buildings. In the Niigata and Miyagi-Ken-Oki earthquakes, the released fluids overtopped the dikes and flooded adjacent industrial and residential areas. In the Niigata and Imperial County earthquakes, adjacent areas had to be evacuated.

Even a cursory examination of the damage will reveal that the component most frequently and severly damaged is the storage tank (see Table 2.4). In only a few cases components other than tanks were damaged to an extent that they could not be repaired within a short period of time. For example, the spherical tanks burned in the Kern county earthquake had to be replaced. The catwalk at the wharf in Anchorage damaged by the Alaska earthquake also required extensive repairs. The damage to these pieces of equipment was nearly total and production time was lost during their repair.

Other types of damage were relatively minor such as stretched bolts on atmospheric columns, cracked foundations and piers, displaced equipment and broken pipes. The impact of these types of damage is fairly small since they could be corrected during the inspection shutdown that follows a major earthquake.

After examining the damage reports presented earlier, one can conclude that, with the notable exception of the tanks, the components of an oil refinery have, on the whole, performed as intended. Damage to production facilities has been minor. Damage to storage and, in some cases, transport facilities has been severe and would indicate the need to upgrade their performance.

Table 2.4

Summary of Typical Damages

Type of Equipment	Typical Damage
Cylindrical Tanks	Collapse (Fig. 2.3.1)
	Elephant Foot Buckling (Fig. 2.3.2)
	Diamond Buckling (Fig. 2.3.3)
	Roof Buckling (Fig. 2.3.4)
	Floating roof rotation
	Foundation settlement
	Broken piping connections (Fig. 2.3.5)
Spherical Tanks	Damage to legs and foundation
Smoke Stacks	Local buckling
	Anchor bolt yield
Columns	Anchor bolt yield (Fig. 2.3.6)
Heat Exchangers	Connection broken
	Foundation damage
Pumps	Broken flange
Pipes & pipe supports	Pipes pulled apart
Wharf Facilities	Catwalk pulled loose

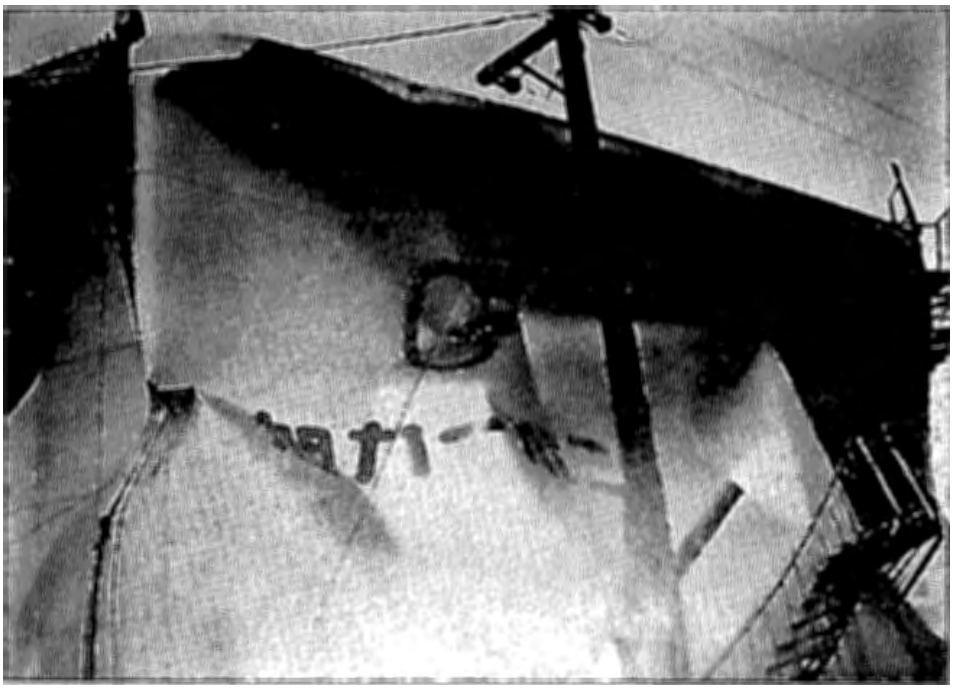


Figure 2.3.1 Collapsed tank (from Kawasumi, 1968)

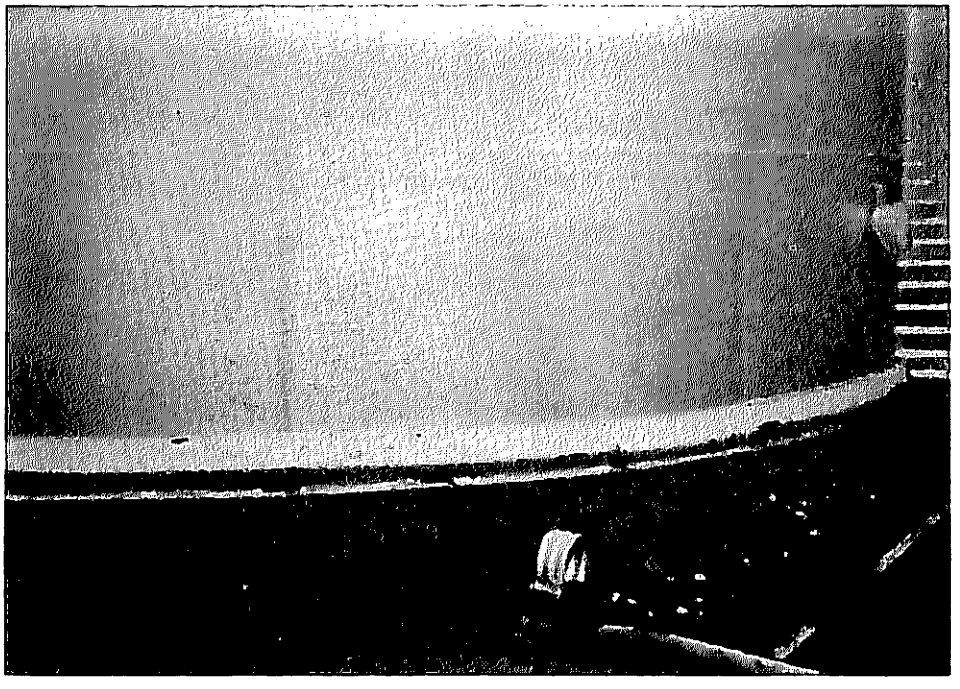


Figure 2.3.2 Elephant foot buckling
(from Committee on the Alaska Earthquake, 1973)

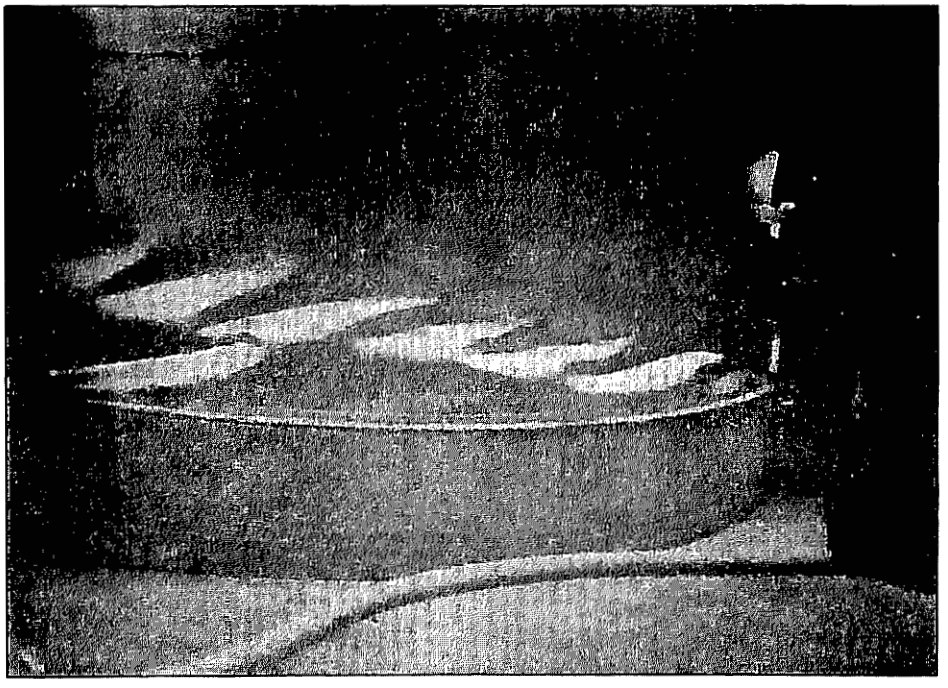


Figure 2.3.3 Diamond buckling (from Stratta, 1980)

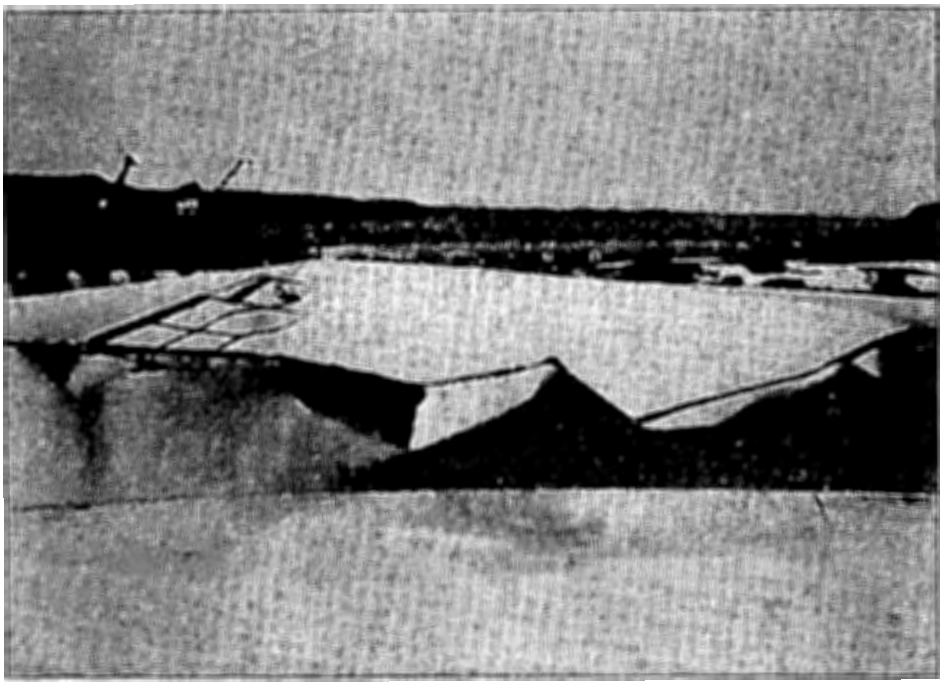


Figure 2.3.4 Buckled roof (from Committee on the Alaska Earthquake, 1973)

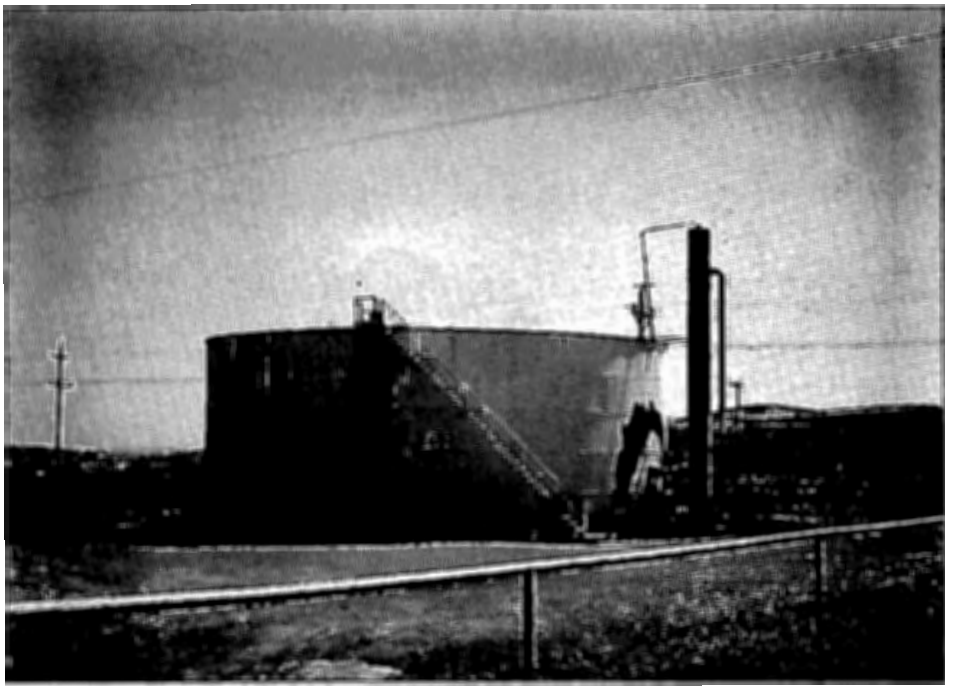


Figure 2.3.5 Broken piping connection, Coalinga May, 1983 earthquake (Photo by R. Nielsen)

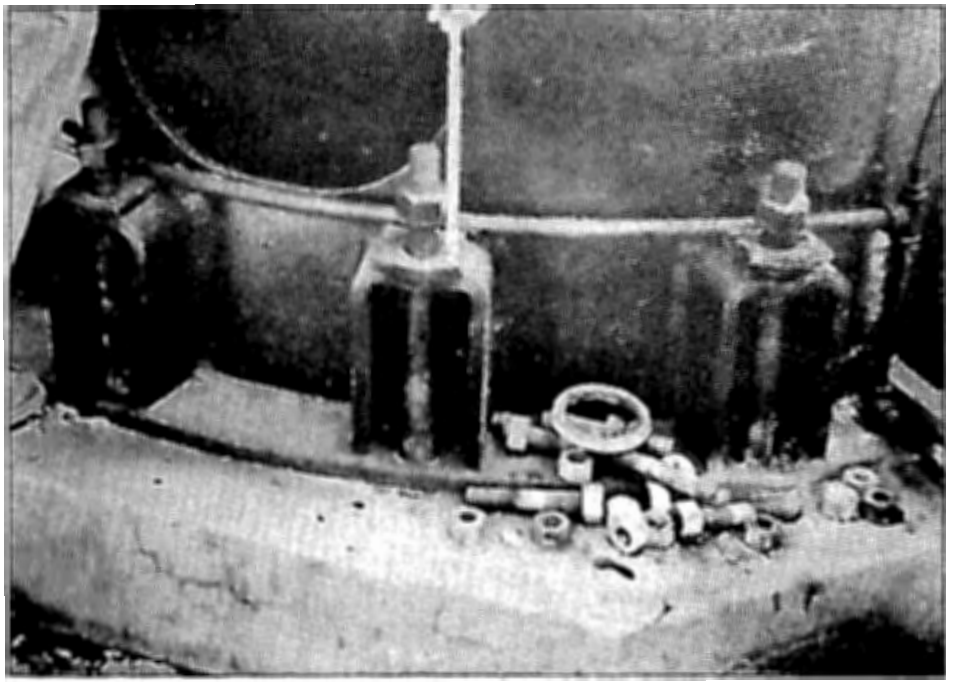


Figure 2.3.6 Anchor bolt yield (from Steinbrugge, 1954)

CHAPTER 3

METHODS FOR SYSTEMS ANALYSIS

Classical systems analysis methods have been developed in relation to mechanical and electronic systems. Many of these analysis techniques have been extended for applications to nuclear power plant systems. Differences, however, exist in the analysis objectives and design technology between nuclear power plants and other industrial facilities. Consequently, it may be difficult and particularly cost ineffective to apply component reliability and systems analysis methodology for nuclear power plants to evaluate the risk to other major industrial facilities. The scope of the study is concentrated on the development of component reliability methods to be discussed in Chapter 4. Thus, in this chapter systems analysis methods are only summarized.

The chapter begins with a brief review of the concepts of classical systems analysis theory. Then methods for analysis of large systems are presented with an emphasis on their applicability to major industrial facilities.

3.1 Fundamentals of Systems Analysis

The successful operation of a system depends on the successful operation of some or all of its components. For example, an emergency fire water delivery system, Z, is shown in Figure 3.1a. It is composed of two subsystems, a primary system, X, and a back up system, Y. Subsystem X is itself composed of two redundant (parallel) sources of water, tanks B and D, and the accompanying valves A, B, and C (see Figure 3.1b). Subsystem Y (Figure 3.1c) relies on the water in a lake which must be taken out using pump F and passed through valve G. The successful operation of system Z, i.e., the delivery of water to a fire, requires either subsystem X or subsystem Y to operate. These in turn depend on the operation of components A through G in various combinations. The study of the operation of such a system in relation to its components is called systems analysis.

The analysis of systems has become an important field of study. Numerous mathematical techniques have been developed to evaluate the reliability of systems. These techniques include event tree/fault tree, graph, and network

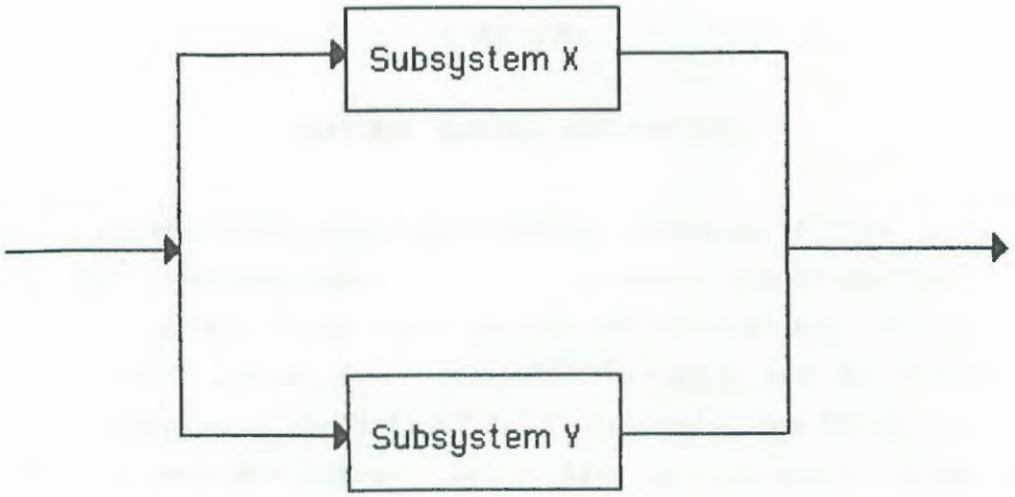


Figure 3.1(a) Example system Z

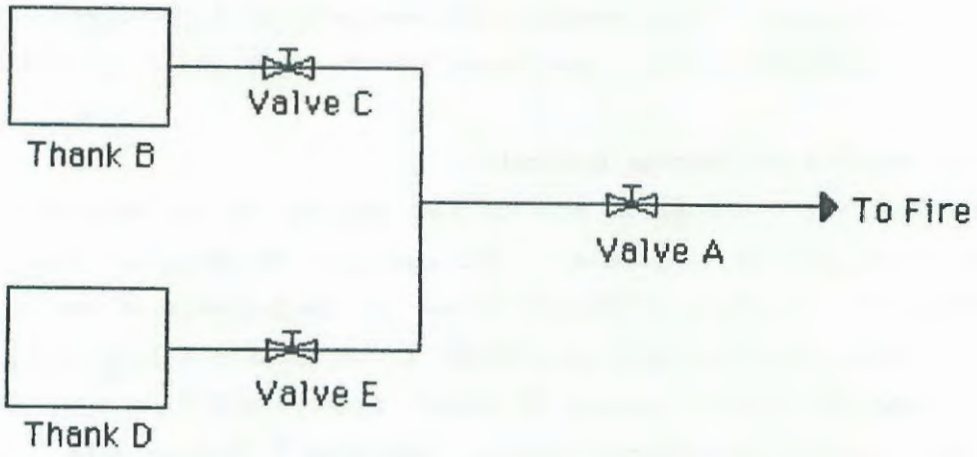


Figure 3.1(b) Subsystem X



Figure 3.1(c) Subsystem Y

analysis. The techniques were originally developed for systems in which random component failures, such as faulty switches, also known as primary component failures, were the main source of system failure. The component failures in these analyses could reasonably be assumed to occur independently of each other.

The primary objective in a systems analysis is to determine the reliability of the system. Reliability is defined as the probability that the system will perform its function over the projected operation time subjected to normal and/or adverse conditions. For seismic risk analysis, the conditions under which the system operates are those resulting from earthquake ground vibration.

The two fundamental types of systems are the series and parallel systems. A system of single elements is a series system if it fails whenever any of its elements fails. Such a system is also called a weakest-link-system (Thoft-Christensen and Baker, 1982). Figure 3.2a shows a typical example of a system in series. Let C_i denote the event "failure of component i". If we denote by $P_{f,S}$ the probability of system failure for a simple system in series, that probability is obtained as follows:

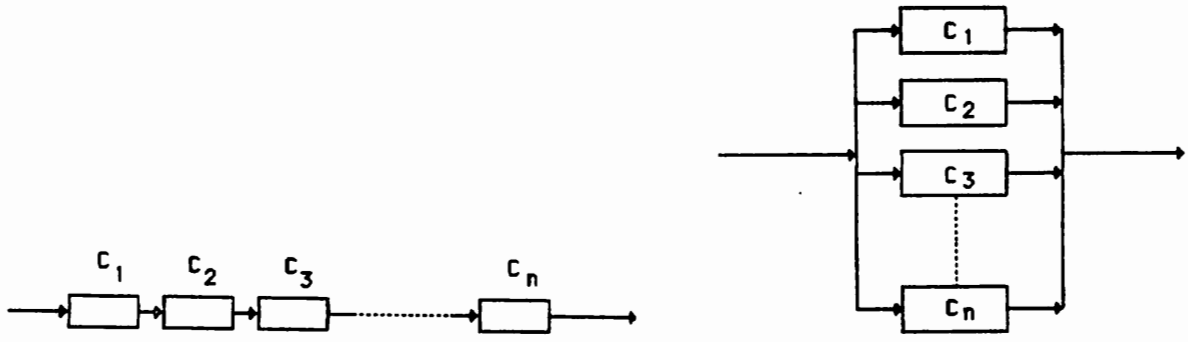
$$P_{f,S} = \Pr\{\text{system fails}\} = P[\bigcup_{i=1}^{n} C_i] = 1 - P[\bigcap_{i=1}^{n} C_i'] = 1 - \prod_{i=1}^{n} (1 - P(C_i)) \tag{3.1}$$

assuming components are independent. If the components are not independent, the bounds are given by

$$\max_i\{P(C_i)\} < P[\bigcup_{i=1}^{n} C] < \sum_{i=1}^{n} P(C_i) \tag{3.2}$$

A system which requires all n components to fail in order for the system to fail is defined as a parallel system. Such a system is shown in Figure 3.2b. The failure probability of a system with n components in parallel is given by

$$P_{f,S} = P[\bigcap_{i=1}^{n} C_i] = \prod_{i=1}^{n} P(C_i) \tag{3.3}$$



(a) (b)

Figure 3.2 Simple system in (a) series, and (b) in parallel.

assuming all components are independent. The corresponding bounds for system with dependent components are given by

$$\prod_{i=1}^{n} P(C_i) \leq P[\bigcap_{i=1}^{n} C_i] \leq \min_i \{P(C_i)\} \tag{3.4}$$

Most systems are usually complex combinations of systems in parallel and in series. Often, however, such complex systems can be simplified by considering series systems in parallel or parallel systems in series combinations. Probability bounds for each of these basic system combinations are given as follows:

(a) series system in parallel

$$\prod_{i=1}^{n} \max_j\{P(C_{ij})\} \leq \prod_{i=1}^{n} P[\bigcup_{j=1}^{m} C_{ij}] \leq P[\bigcap_{i=1}^{n} \bigcup_{j=1}^{m} C_{ij}]$$

$$\leq \min_l \{P[\bigcup_{j=1}^{m} C_{ij}]\} \leq \{\sum_{j=1}^{m} P(C_{ij})\} \tag{3.5}$$

(b) parallel systems in series

$$\max_j\{\prod_{j=1}^{m} P(C_{ij})\} \leq \max_i\{P[\bigcap_{j=1}^{m} C_{ij}] \leq P[\bigcup_{i=1}^{n}\bigcap_{j=1}^{m} C_{ij}]$$

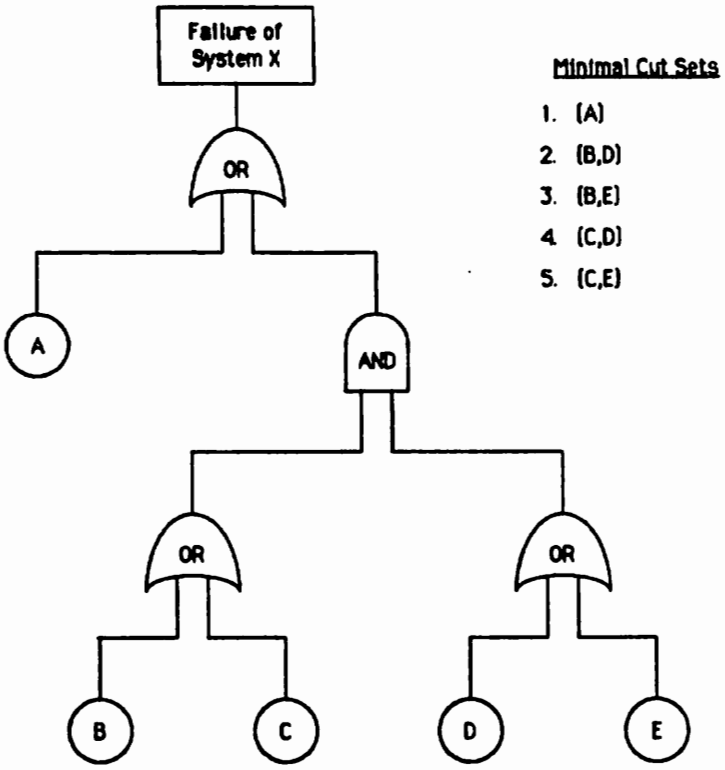
$$\leq \sum_{i=1}^{n} P[\bigcap_{j=1}^{m} C_{ij}] \leq \sum_{i=1}^{n} \min_j \{P(C_{ij})\} \qquad (3.6)$$

The bounds given in equations 3.5 and 3.6, however, become very wide for large systems, and thus they are of limited use.

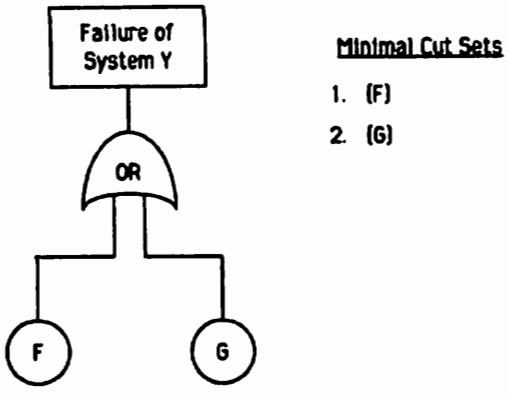
In order to simplify the analysis, especially when large systems are being studied, it is most often assumed that component failures are independent. In addition, components are usually assumed to be bi-modal, i.e., they are either functional or not (C_i = 0 or 1). In seismic risk analysis, however, the correlation of component failures is very important. For example, suppose valves A and G in system Z shown in Figure 3.1, were located next to each other in the same building. Then, if the building were to collapse in an earthquake, both valves would be inoperable; that is, both components would fail together. In that case the correlation coefficient between the two failures equals one (ρ = 1.0). In the cases where one valve or the other may fail alone under direct seismic loading, the correlation is less than one (ρ < 1).

Thus, an important aspect of systems analysis, particularly in relation to seismic risk analysis of such systems, is the treatment of component dependencies. The first source of component failure correlation is due to the simultaneous loading of all components by an earthquake. Such failures are called common mode failures and have been studied in relation to nuclear power plant reliability assessment (PRA Guide, 1982).

In order to uncouple the component failures, component failure probabilities are evaluated conditional on the earthquake loading. The systems reliability analysis is then performed for a given seismic loading, which is usually the peak ground acceleration (PGA), and repeated for all possible levels of the seismic load. The total probability of system failure is then the weighted integral of the conditional probabilities of failure given by



(a)



(b)

Figure 3.3 (a) Fault Tree representation for subsystem X of Figure 3.1b
(b) Fault tree representation for subsystem Y of Figure 3.1c

$$P_{f,S} = \Pr\{\text{system failure}\} = \int_{\text{all } A} \Pr\{\text{system failure}/A\}\, f_A(a)\, da$$

$$= \int_{\text{all } A} P_{f,S/A}\, f_A(a)\, da \qquad (3.7)$$

where A is the global seismic loading parameter simultaneously affecting all components in an earthquake.

In addition to being correlated, most components in real systems can be in an intermediate state other than failure/no failure which can be of importance to the survival of the overall system. For example, if a pipe is connected to a vessel which has moved several inches from its original design position causing a break in the pipe-vessel connection, the subsystem can be considered to have failed even though the vessel or the pipe are not in a failure state. Another example is leakage through a valve. The valve is neither in failure or functional state, but is partially functional (or failed). With the currently available systems analysis techniques, multi-state components and subsystems cannot be easily included. In relation to structural reliability, approximate methods of systems analysis have been developed which provide for such cases (e.g. Cornell, 1967; Ditlevsen, 1979; Rackwitz, 1978; Thoft-Christensen and Sorensen, 1982). The objective of subsequent studies will be to investigate the feasibility of applying existing structural reliability methods to large systems, thus enabling considerations of correlation and multiple component states.

Assuming that the conditional probabilities of component failure and the appropriate correlation coefficients can be determined, the conditional probability of system failure can be computed. Three logical steps are required: (1) identify the failure modes of the system; (2) calculate the probability of occurrence of each failure mode; and (3) combine these probabilities to find the probability of system failure.

3.2 Identification of System Failure Modes

For simple systems the failure modes might be enumerated by inspection. However, for moderately complex systems it is necessary to use the tools of fault tree and event tree analysis. Consider first the fault tree.

A fault tree describes the logical (and, or) combination of component failures, called basic events, which cause system failure, called the top

event. Figure 3.3a shows a fault tree for the failure of the example subsystem X described in Section 3.1. For instance, subsystem failure would result if tank B, tank D, and valve A all failed, i.e., the logical combination of events A and B and D. In set notation this is written as {A ∩ B ∩ D}, where " ∩" means the intersection of two events. An intersected set of events (component failures) such as this that leads to the top event (system failure) is called a cut set. Note, however, that {A} or {B ∩ D} separately will also cause subsystem failure, so that they are themselves cut sets. The smallest sets that result in the top event of a fault tree are called minimal cut sets. These are the cut sets used in the evaluation of the system failure probabilities.

It can be shown that the minimal cut sets of a system are unique. Thus, the task of finding all of a subsystem's failure modes is equivalent to enumerating its minimal cut sets. For subsystem X the minimal failure mode cut sets are {A}, {B ∩ D}, {B ∩ E}, {C ∩ D}, and {C ∩ E}. Figure 3.3b shows a fault tree for subsystem Y for which the failure modes are {F} and {G}. A number of computer programs are available for fault tree generation and reduction to minimal cut sets (e.g. Fussell, 1975; Powers et al., 1975).

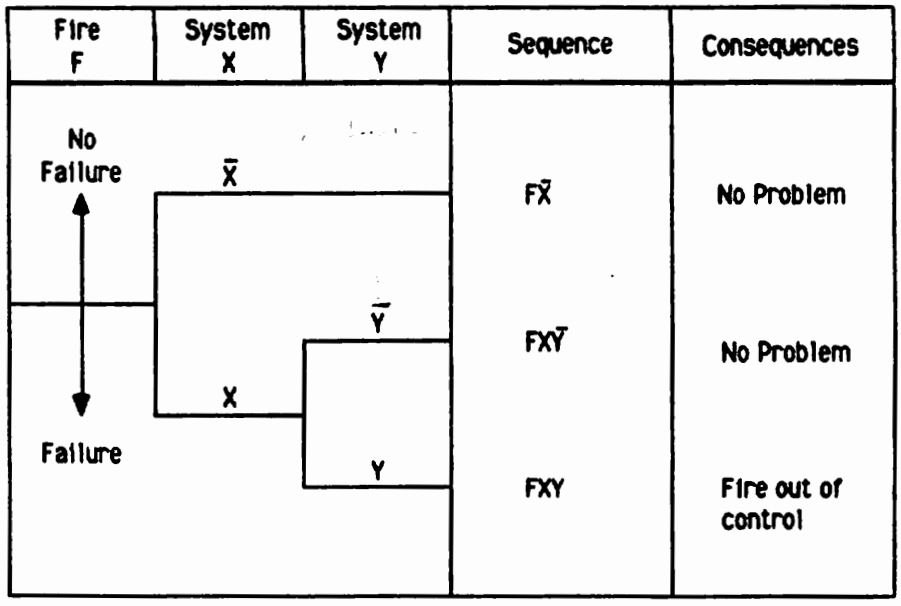


Figure 3.4 Events tree example for system Z

An event tree is useful for study of the interaction of different subsystems. An event tree describes the logical sequences, or combinations, of subsystem failures and the consequences of each sequence to the system. Figure 3.4 shows an event tree for the example of Figure 3.1. Of the four possible failure sequences, it is necessary to consider in detail only the sequence: subsystem X fails and subsystem Y fails, i.e. $\{X \cap Y\}$. Thus, system Z fails for the events resulting from the intersection of subsystem X minimal cut sets with the subsystem Y minimal cut sets; namely, $\{F \cap A\}$, $\{F \cap B \cap D\}$, $\{F \cap B \cap E\}$, $\{F \cap C \cap D\}$, $\{F \cap C \cap E\}$, $\{G \cap A\}$, $\{G \cap B \cap D\}$, $\{G \cap B \cap E\}$, $\{G \cap C \cap D\}$, and $\{G \cap C \cap E\}$. These are the ten failure modes of the system. The event tree techniques for reducing the problem size increases in usefulness as the number of subsystems increases.

3.3 Calculation of Failure Mode Probabilities

Let C_i denote the event "failure of component i" as defined previously. For failure mode F_j, consisting of n component failures the probability of failure is

$$P_{f,F_j} = \Pr\{\text{failure mode } F_j \text{ occurs}\} = \Pr\{\bigcap_{i=1}^{n} C_i\} \qquad (3.8)$$

where $\bigcap_{i=1}^{n}$ represents the intersection of all events in the minimal cut set.

If all components in the minimal cut set are independent and described by two states (fail/no fail), then equation 3.8 reduces to equation 3.3. When components are correlated and their failures are multistate, evaluation of equation 3.8 requires the calculation of an n-dimensional integral. Numerical integration can be used for that purpose as long as the number of components in the minimal cut set is small. A problem encountered much more commonly in practical applications is the determination of correlation and the forms of the joint distributions for all components in a cut set. Failure data are usually very limited especially when the components are large structures (e.g. tall columns or furnaces) which cannot be tested in the laboratory and which have not failed in the past when subjected to earthquake ground motion. For sufficiently small number of components in a cut set which are correlated, equation 3.8 can be evaluated using the tools developed for structural reliability. The basic theory of structural reliability is described at a greater

depth in Chapter 4. In this section, the techniques relevant only to systems analysis are discussed with an emphasis on correlated multistate components.

Consider the simple case when there are three correlated multistate components in the cut set. Figure 3.5a shows the intersected region for three hypothetical components in two dimensions. (Figure 3.5b shows the region that is the union of the same failure regions for comparison). The probability of F_j occurring is the integral of the joint probability density function over the intersected failure domain. Again this integral is difficult to evaluate due to the arbitrary shape of the failure domain.

Based on the first order reliability approach, the failure probability of component i can be approximated by

$$P_{f,C_i} = \Pr\{g(x) < 0\} = \Pr\{h(\underline{U}) < 0\} \simeq \Pr\{\ell(\underline{U}) < 0\} \qquad (3.9)$$

where $\ell(\underline{U})$ is the equation of the supporting hyperplane in the U-space which approximates the failure surface, $h(\underline{U})$, at the checking point. The checking point is defined as the minimum distance from the origin to the failure surface for component i. Note that the failure surface $g(\underset{\sim}{X}) = 0$ has been transformed to the normal U-space using the appropriate transformation (e.g., Rosenblatt transformation). In the U-space all variables are standard normal variates. The coordinates of the checking point are given by $\{\beta_i \ \underline{\alpha}_i\}$, where β_i is the length of the β-vector and $\underline{\alpha}_i$ is the vector of direction cosines to the i^{th} surface. With the above linearization, the problem is reduced to one dimension along a line parallel to the vector $\underline{\alpha}_i$, with $Z_i = \underline{U}\ \underline{\alpha}_i$:

$$P_{f,C_i} \simeq \Pr\{\underline{U}\ \underline{\alpha}_i + \beta_i < 0\} = \Pr\{Z_i < -\beta_i\} = \Phi(-\beta_i). \qquad (3.10)$$

Thus, for an n-component cut set, an n-dimensional Z-space in standard normal coordinates can be constructed. Each Z_i has a standard normal density. Figure 3.5 shows the case of two components. The probability of the failure mode is then the integral over the rectangular failure domain in the Z-space, which is given by the standard multinormal integral,

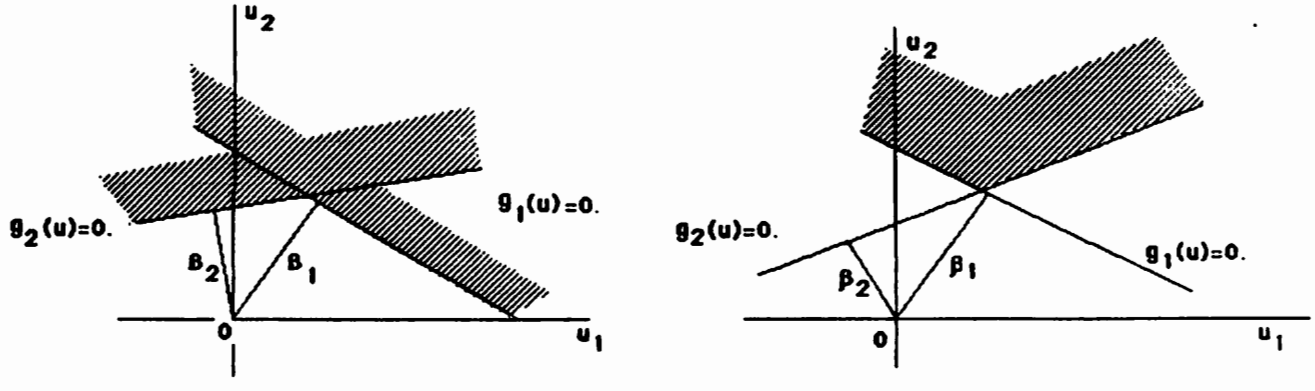
$$P_{f,C_i} \simeq \Pr\{\bigcap_{i=1}^{n} C_i\} = \Pr\{\bigcap_{i=1}^{n} [Z_i < -\beta_i]\} = \Phi_n(-\underline{\beta}; R_Z) \qquad (3.11)$$

where $\underline{\beta}$ is the vector of β_i's and R_Z is the matrix of correlation coefficients. The correlation coefficients may be calculated from the direction cosines of the β-vectors:

$$\rho_{ij} = \mathrm{Cov}[Z_i, Z_j] = E[Z_i Z_j] = E[(\underline{U}\ \underline{\alpha}_i)] = \underline{\alpha}_i \cdot \underline{\alpha}_j \qquad (3.12)$$

The fact that U_i is an independent standard normal variable for each component is used above.

The integral of the multinormal probability density function over an arbitrary failure domain is difficult when there is correlation between component failures. Numerical integration is the most widely used technique. However, as the number of dimensions increases the number of integration points grows exponentially. Therefore numerical integration is prohibitively expensive for failure modes with more than four or five components (SSMRP, 1981). Other techniques including Monte-Carlo integration and series expansion have been applied without great benefit. Rackwitz (1978) reports that the integral can be bounded, but the bounds are not necessarily narrow.



(a) (b)

Figure 3.5 Integration regions for multistate correlated components

Thus, it appears that for the present, the analyst is limited to failure modes containing at most four or five components. It is likely, though, that larger failure modes have probabilities which are much smaller. As long as the correlations are not strong the inclusion of each additional component reduces the failure mode probability by a factor on the order of magnitude of the component's probability of failure. (Recall that if the component failures were independent, the failure mode probability would be the product of the individual probabilities). If the size of the system is kept small and the components are chosen carefully, the present limitation of at most four or five components per failure mode may be acceptable.

3.4 Probability of System Failure

The system failure probability can be calculated from the failure mode and component probabilities. The system failure event is the union of all failure mode events. Thus,

$$P_{f,S} = \Pr\{\bigcup_{j=1}^{m} F_j\} = \Pr\{\bigcup_{j=1}^{m} [\bigcap_{i=1}^{n} C_i]_j\} \qquad (3.13)$$

The problem of correlation arises again because the failure modes are not independent. Consider the example in Figure 3.1. Two of the failure modes for the example system Z are {F ∩ A} and {G ∩ A}, the failure of valve {A} appearing in both. The probability of either of these two failure modes occurring is given by

$$\Pr\{(F \cap A) \cup (G \cap A)\} = \Pr\{F \cup G) \cap A\} \qquad (3.14)$$

Therefore, to properly calculate the system failure probabilities the intersection between failure modes must not be counted twice. This is difficult to avoid for large systems.

Generally, three upper bounds on the system failure probability can be calculated (Smith et al., 1981).

$$B_1 = 1 - \prod_{j=1}^{k} (1 - P_{f,F_j}) \qquad (3.15a)$$

$$B_2 = \sum_{j=1}^{k} P_{f,F_j} \qquad (3.15b)$$

$$B_3 = \sum_{j=1}^{k} P_{f,F_j} - \sum_{(i,j)} \Pr\{F_i \cap F_j\} \qquad (3.15)c$$

The first upper bound would be the exact probability if the failure modes were independent. The second is an upper bound on the probability of a union. The third approximation is known as Hunter's bound and substracts some of the intersections from the union {A U B}. Note that B_2 and B_3 may be greater than unity. A lower Hunter's bound can also be calculated (Hunter, 1977).

Thus, a bound on the conditional probability of failure of the system at a given level of seismic loading can be found. The systems analysis should also include the calculations of sensitivity and importance measures. The sensitivity of a component to changes in the basic loading and resistance variables may be measured by the derivative of the failure surface (at the checking point in the AFOR method). The relative importance of a component failure to the failure of the system may be measured by taking the ratio of the sum of the failure mode probabilities which include these component, to the total system failure probability. The relative importance of a given failure mode to the system may be measured by the failure mode probability divided by the system failure probability (SSMRP, 1981).

3.5 Summary

The structural reliability approach to systems analysis has been adopted for this project. It was chosen because of the need to treat correlated multivaried component failures due to earthquake loadings. The probability of system failure is computed as the probability of the union of the failure modes. Failure modes are identified as minimal cut sets of component failures. Probabilities of failure modes are obtained from the intersections of component failure events. Fault trees and event trees are useful for identifying failure modes and enumerating the minimal cut sets of a system.

Key to this approach is (1) the estimation of the conditional failure probability of components for a given level of earthquake loading, and (2) the correlations between component failures. These calculations are described in detail in the next section for typical industrial facility components.

CHAPTER 4

COMPONENT RELIABILITY FORMULATION

4.1 Structural Reliability Theory for Component Failures

Structural failures occur when the load on a structure is greater than the structure's resistance. In general, the random variables will be either loading or resistance variables or both. Resistance variables can be further reduced to geometrical or strength variables. Next, a mathematical model describing the interaction of loads and resistances is formulated. In principle, this interaction is usually defined in terms of a margin of safety, M

$$M = R - S$$

where

R = Resistance

S = Load.

When $M > 0$, the structure is safe. It is unsafe for $M < 0$. Since the resistance and the load are functions of many random variables, the margin of safety is generalized to a function $g(\underline{X})$ where $\underline{X} = \{X_1, X_2, \ldots X_n\}$ is the vector of basic random variables. The region defined as $\omega_S = \{\underline{X}: g(\underline{X}) > 0\}$ is the safe domain, $\omega_f = \{\underline{X}: g(\underline{X}) < 0\}$ is the failure domain and $\partial\omega = \{\underline{X}: g(\underline{X}) = 0\}$ is the failure surface. Figure 4.1 shows the failure and safe domains for the case of two random variables. In an "exact" analysis probability of failure is found as follows

$$P_f = \int_{\underline{X}\epsilon\omega_f} f_{\underline{X}}(\underline{X})\, d\underline{X} \qquad (4.1)$$

where $f_{\underline{X}}(\underline{X})$ is the joint probability density of the basic random variables.

However, in most practical cases the integrations involved are unwieldy even with numerical techniques. For this reason, some approximate methods have evolved for estimating the total probability of failure. The method presented here follows the ideas proposed by Cornell (1969), Hasofer and Lind (1974) and Rackwitz and Fiessler (1977). Essentially, they combine to create an invariant first-order approximation to the probability of failure.

4.1.1 First Order Second Moment (FOSM) Methods:

The most widely used approximation technique was introduced by Cornell (1969). Since probability distribution data for structural problems is often limited to the first few moments of the distribution of a variable, a distribution-free measure of structural reliability, called the safety index β, was proposed. Assuming R and S to be independent and the failure event to be $M = R - S < 0$, the safety index is defined by

$$\beta = \frac{\mu_R - \mu_S}{\sqrt{\sigma_R^2 + \sigma_S^2}} \tag{4.2}$$

where μ_R and μ_S are the expected values (means) of R and S, and σ_R^2 and σ_S^2 are the variances of R and S. Furthermore, if R and S both have normal (Gaussian) probability distributions then the probability of failure is given by

$$P_f = 1 - \Phi(\beta) = \Phi(-\beta) \tag{4.3}$$

where $\Phi(\cdot)$ is the cumulative probability of the standard normal variate.

A similar definition of β can be made for the failure event defined by $M = \{\ln(R/S) < 0\}$ where R and S are independent lognormally distributed random variables. In that case the probability of failure, P_f, is again calculated from β as above. However, if neither R nor S are both normally or lognormally distributed, equation 4.3 is only an approximation of P_f. The quality of the approximation will depend on the degree of non-linearity of the failure surface and the deviation of the distributions for R and S from a normal distribution. A Chebichev upper bound can also be obtained for the probability of failure (Veneziano, 1977). This bound however is very wide, and insufficient for most practical cases when a probability estimate is required. Thus, it is suggested in the literature (Ang and Cornell, 1973) that β itself be the measure of structural reliability, rather than P_f.

Approaches such as the safety index, β, are known as first-order second moment (FOSM) approximations, because all the probability information is based on the first and second moments, i.e., means and variances. Consider the limit state function $g(\underline{X})$. Expanding $g(\underline{X})$ about the mean values $\{\mu_{X_1}, \mu_{X_2}, \ldots, \mu_{X_n}\}$ of the variables $\underline{X}$ in a Taylor series

$$g(\underline{X}) = g(\underline{\mu}_X) + \sum_{i=1}^{n} (X_i - \mu_{X_i}) \frac{\partial g}{\partial X_i} +$$

$$\frac{1}{2} \sum_{i=1}^{n} \sum_{j=1}^{n} (X_i - \mu_{X_i}) (X_j - \mu_{X_j}) \frac{\partial^2 g}{\partial X_i \partial X_j} + \ldots \qquad (4.5)$$

where the derivatives are evaluated at the means, μ_{X_i}. The following approximations can be made for the mean and variance of $g(\underline{X})$ by taking only the first order terms of the series (Ang and Tang, 1975).

$$E[g(\underline{X})] \simeq g(\underline{\mu}_X) \qquad (4.6)$$

and

$$\text{Var}[g(\underline{X})] \simeq \sum_{i=1}^{n} \left(\frac{\partial g}{\partial X_i}\right)^2 \text{Var}(X_i) + \sum_{i \neq j}^{n} \sum^{n} \left(\frac{\partial g}{\partial X_i}\right) \left(\frac{\partial g}{\partial X_j}\right) \text{Cov}(X_i, X_j) \qquad (4.6b)$$

The safety index, β can thus be generally defined using these approximations as

$$\beta = \frac{E[g(\underline{X})]}{D[g(\underline{X})]} \qquad (4.7)$$

where $D[\cdot]$ is the square root of the variance of the function $g(\underline{X})$. The safety index β defined by equation 4.2 corresponds to the FOSM approximation for two basic uncorrelated variables. Further discussion of these approximate methods can be found in Cornell, 1969; Ang and Cornell, 1973. The main problem with the safety index as defined is that its value will change depending on the form of the failure function $g(\underline{X})$.

4.1.2 Advanced First Order Reliability (AFOR) Method

A new approximate method has been developed which estimates a much closer bound on the probability of failure than the one obtained from the first order second moment approach. This method is refered to as the advanced first-order reliability (AFOR) approach.

In the advanced first order reliability method, the basic random variables describing the failure surface are transformed to standard normal variables. The random variable X_i with cumulative distribution function,

$F_{X_i}(X_i|X_1, X_2, \ldots, X_{i-1})$, is replaced by a standard normal variable U_i via the transformation:

$$X_i^* = F^{-1}\ [\Phi(U_i|X_1, X_2, \ldots X_{2-1})] \tag{4.8}$$

where X_i^* is a given point in the domain, Rackwitz (1977). This transformation will be exact at all points for a normally distributed basic random variable. For a non-normal variable, the probability density and distribution of the transformed variable will equal the density and distribution of the original variable only at X_i^*. It is important to note that this transformation explicitly accounts for dependent random variables.

Once the transformation is completed, the shortest distance from the origin to the transformed failure surface is calculated (see Figure 4.1). The Hasofer and Lind (1974) reliability index, β_{HL}, is calculated as follows:

$$\beta_{HL} = \min_{U \in \partial\omega} \left(\sum_{i=1}^{n} U_i^2 \right)^{1/2} \tag{4.9}$$

where $\partial\omega$ is the failure surface in the transformed space.

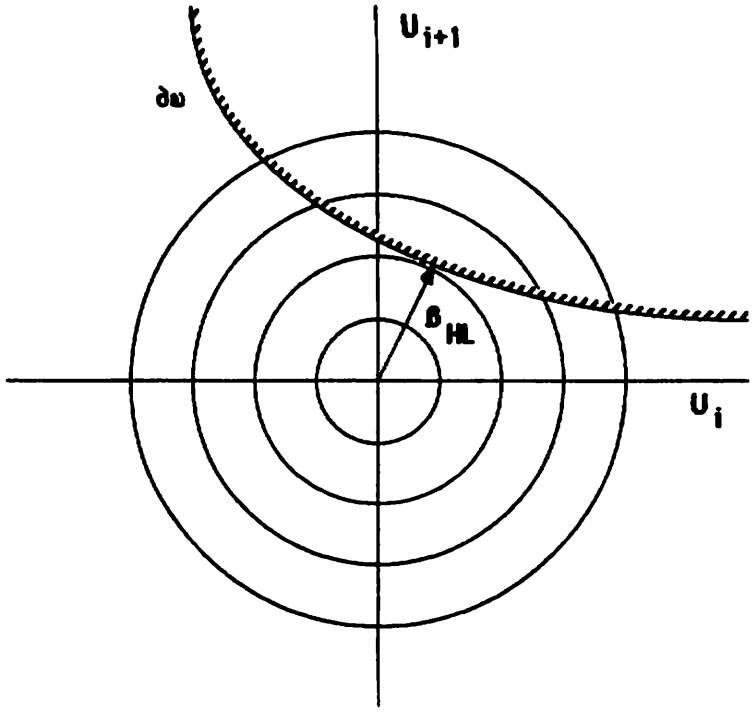


Figure 4.1 Definition of the Hasofer and Lind reliability index

The point at which β_{HL} touches the failure surface is known as the design point or most-likely failure point. β_{HL} and the design point are usually calculated iteratively.

The failure surface is approximated by a hyperplane taking the first terms of a Taylor series evaluated at the most likely failure point. Then the integral given by equation 4.1 is evaluated by

$$P_f = 1 - \Phi(\beta) = \Phi(-\beta) \tag{4.10}$$

Ditlevsen (1977) has shown that this approximation is almost always close to the correct value of the failure probability if the failure surface is not highly nonlinear.

The AFOR method, therefore, depends on finding the design point on the failure surface in the U-space. As with most non-linear equations several different search algorithms are available. An iterative procedure with fast convergence rate has been used by Hohenbichler and Rackwitz (1981) and is adopted in this study.

In summary, the two main approximation methods currently used in structural reliability applications have been discussed above. The first-order second moment approach estimates the mean and the variance of the safety margin, R-S, or its generalization, $g(\underline{X})$, by a first order approximation evaluated at the mean values of $\underline{X}$. The safety index β is estimated in terms of the mean and variance of the random variables. The failure probability can be computed with accuracy only in the case when all random variables are uncorrelated and normally distributed and the function $g(\underline{X})$ is almost linear.

The advanced first-order reliability approach, on the other hand, estimates a probability of failure through a linearized approximation of the failure surface at the design point in a standard normal space. The main advantage of the AFOR method is that the reliability index β is invariant under transformations. The approximation of failure probability is poor only when the failure surface is very highly nonlinear. The AFOR method achieves better estimates of the failure probability than the FOSM approaches, however, computational cost could be higher for complex problems.

4.2 Lognormal Fragility Approach

A component's conditional probability of failure distribution has come to be known as its "fragility curve". For seismic loadings the conditioning variable is usually taken as either the peak ground acceleration or the local loading variable acting on the component, (e.g., moment, axial force, etc.). The determination of fragility curves is one of the central concerns of the systems analysis.

Different forms have been proposed for the shapes of fragility curves, such as step functions and ramp functions (PRA Guide 1982). The currently popular lognormal distributional form was proposed by Kennedy et al. (1980). Using the notation described in the previous section, the fragility of a component is given by

$$f = \text{frequency } \{R < S\} \tag{4.11}$$

where R is the resistance (capacity) of the component and S is the load at the location of the component for a given input load to the overall system. Following the first-order second moment method, the value of f is obtained by considering the following:

$$f = \Phi \left[\frac{\ln (\tilde{R}/\tilde{S})}{\sigma_{\ln R}} \right] \tag{4.12}$$

where $\tilde{R}$ and $\sigma_{\ln R}$ are respectively the median and logarithmic standard deviation of the capacity of a component for a given failure mode. In order to further simplify the evaluation of equation 4.12, the capacity is assumed to be related to the load. This relationship is usually represented as follows:

$$R = S\, F_S\, F_R \tag{4.13}$$

where F_S and F_R are factors of safety corresponding to factors relating to the load, S, and the resistance capacity, R, (e.g. ductility, strength, etc). Each of these factors of safety can be further expanded into a product of other safety factors reflecting basic influences to the load or the resistance. All of the safety factors are treated as lognormally distributed random variables with corresponding median and logarithmic standard deviation

values. In addition, the variability is assumed to be due to "randomness" and "uncertainty". For example, the safety factor F_S can be written as:

$$F_S = \tilde{F}_S \, \varepsilon_{S_R} \, \varepsilon_{S_U} \tag{4.14}$$

where ε_{S_R} is a unit median random variable reflecting the inherent randomness in the median load, S, and ε_{S_U} is a unit median random variable reflecting the uncertainty in the calculation of F_S. Both of these variables are assumed to be lognormally distributed with logarithmic standard deviations β_{S_R} and β_{S_U}. Similar quantities can be defined for F_R and any other safety factor that may be required in the analysis process. Following Kennedy et al. (1980), we define

$$Q = \Pr \{f < f' | S_o\} \tag{4.15}$$

to be the conditional probability that the failure frequency, f, is less than an arbitrary value, f', given a load of S. Using equation 4.12 the frequency f' is computed as follows:

$$f' = \Phi \left[\frac{\ln(\tilde{S}/\tilde{R}) + \beta_{R_U} \, \phi^{-1}(Q)}{\beta_{R_R}} \right] \tag{4.16}$$

In the above equation β_{R_U} and β_{R_R} correspond to the standard deviations of the random variables ε_{R_U} and ε_{R_R} for the resistance factor of safety.

The advantage of assuming lognormally distributed factors of safety lies in the fact that the product of lognormally distributed independent random variables is also lognormal. This feature becomes very attractive especially when many factors of safety are included in the computations. In addition, the separation of "randomness" and "uncertainty" makes possible the prediction of confidence intervals on the probability estimates of system failure.

The parameters of the lognormal fragility curve, however, are very difficult to estimate, even for experts. Considerable subjective judgement is required to develope the appropriate factors of safety and to separate the variance into "randomness" and "uncertainty". The results are inconsistent formulations of different fragility curves, which are worsened when several

analysts develop fragilities for different components. This methodology has been through several revisions defining strength, ductility, and structure response safety factors, as well as randomness and uncertainty.

4.3 Application of AFOR Methods

The application of AFOR methods to seismic reliability of code-designed structures will now be presented. In order to illustrate the particulars of this analysis, a simple structure will be introduced. The example structure shown on Figure 4.2 consists of a two-story frame supporting two pieces of equipment, E_1 and E_2. The failure mode to be considered is the shear between the equipment bases and the floor. As explained earlier, the failure surface, $\partial\omega$, is given by

$$\partial\omega = \{X_R^{(1)}, X_S^{(1)} : g(X_R^{(1)}, X_S^{(1)}) = 0\} \tag{4.17}$$

where

$$g(X_R^{(1)}, X_S^{(1)}) = X_R^{(1)} - X_S^{(1)} \tag{4.18}$$

and $X_R^{(1)}$ is shear resistance between E_1 and the floor (see Figure 4.2); $X_S^{(1)}$ is earthquake-induced shear at the same location.

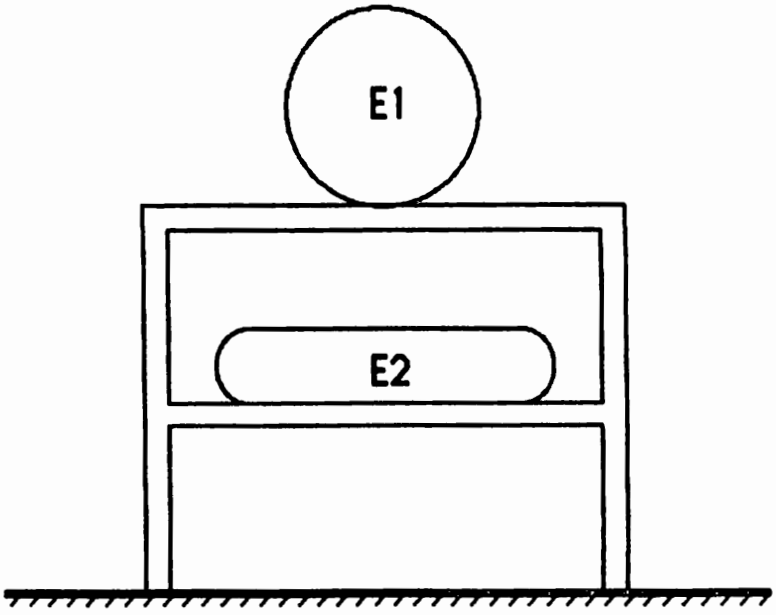


Figure 4.2 Two story frame supporting equipment E_1 and E_2

An expression for $X_R^{(1)}$ in terms of basic random variables can be easily derived from mechanics. An expression for $X_S^{(1)}$ is more difficult to develop. Current codes do not specify directly the design shear between a pump and the floor. They do, however, describe the total base shear, X_{base}, to be applied to the structure and provide the means of relating this quantity to the shear between E_1 and the floor, $X_S^{(1)}$. Based on assumptions for mode shapes, the relationship between base shear, X_{base}, and floor shear, $X_S^{(1)}$, can be expressed in terms of function G_1

$$X_S^{(1)} = G_1(X_{base}). \tag{4.19}$$

where

$$G_1(X_{base}) = F_t + (X_{base} - F_t) \frac{W_1 H_1}{W_1 H_1 + W_2 H_2} \tag{4.20}$$

$$= C_1 \cdot X_{base}$$

where $F_t = .07T X_{base}$

$$C_1 = .07T + (1 - .07T)(W_1 H_1)/(W_1 H_1 + W_2 H_2),$$

and T = period of structure. (4.21)

In order to provide a common load parameter, the base shear must then be related to some measure of ground motion intensity, most often the peak ground acceleration (PGA). To arrive at a simple relationship between X_{base} and PGA, most static design codes assume the structure to be a linear single degree-of-freedom oscillator. The ground motion is then represented by a spectral envelope or dynamic amplification factor (DAF) (Figure 4.3) which is scaled by the PGA. With these assumptions, the relationship between X_{base} and PGA becomes a function G_2:

$$X_{base} = G_2(PGA) \tag{4.22}$$

where

$$G_2(PGA) = DAF(T) \cdot PGA$$

$$= C_2 \cdot PGA \tag{4.23}$$

Combining these expressions, the failure surface can be described by the functions:

$$g(\underline{X}) = X_R^{(1)} - C_1 \cdot C_2 \cdot PGA \qquad (4.24)$$

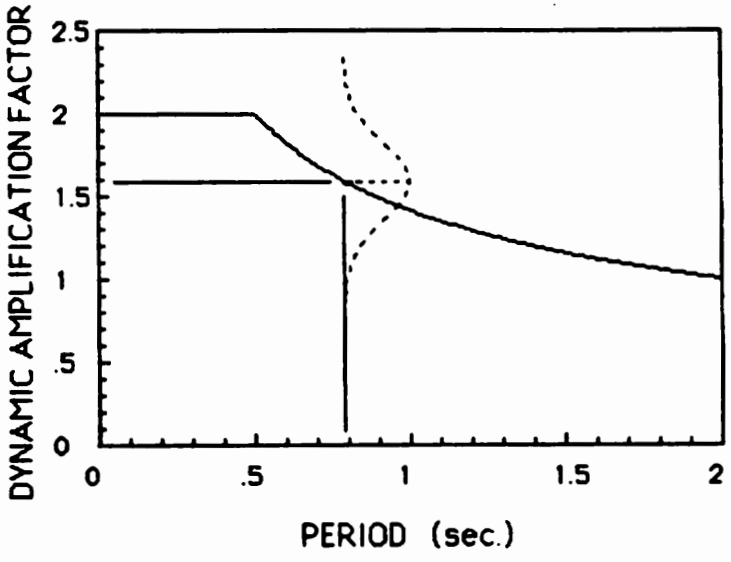


Figure 4.3 Ground motion spectra

The randomness in C_1 is due to the scatter of the actual load $X_S^{(1)}$ around the predicted load for a given base shear. The randomness in C_2 results from the scatter of the DAF around the predicted DAF for a given T (Figure 4.3).

Because the system analysis requires a probability of failure conditional on an external event, this failure surface is calculated conditional on a given PGA. In other words P_f is calculated given an assumed value of PGA. The calculations are repeated for several values of PGA in order to plot the conditional probablity of failure curve (i.e., fragility curve).

Correlation

There are two aspects of correlation to be dealt with in a reliablity analysis. First, for a given failure mode of a component, the basic random

variables may be dependent. Second, there may be correlation between failure modes of the same components or among similar components.

For the structure described above, C_1 and C_2 are functionally dependent on the period of the structure, T. Thus, the distributions on C_1 and C_2 are expressed in terms of T and are then transformed to standard normal space using the Rosenblatt transformation. The transformed variables are still functions of T. The period,T, would then be described by its distribution in the transformed space.

Correlation between failure modes can also be described quantitatively. For each failure mode, the direction cosines, $\underline{\alpha}$, for the vector from the origin to the design point are defined by:

$$\alpha_i = \frac{U_i}{|\beta|} \tag{4.25}$$

where $|\beta|$ is the length of the vector from the origin to the design point and U_i is the i^{th} component of that vector. For multiple failure modes, the limit state is composed of the union of the hyperplanes for all modes. The correlation between any two failure modes is the dot product of their direction cosine vectors:

$$\rho_{k\ell} = \sum_{i=1}^{n} \alpha_i^{(k)} \cdot \alpha_i^{(\ell)} \tag{4.26}$$

where $\rho_{k\ell}$ is the correlation between failure modes k and ℓ. $\alpha_i^{(k)}$ is the i_{th} component of the direction cosine vector for failure mode k. For the example problem above, let failure mode 1 be failure in shear at the base of E_1. Failure mode 2 is the same at the base of E_2. The basic random variables are transformed as follows:

Basic Variable		Transformed to	Basic Variable		Transformed to
$C_1^{(1)}$	→	$U_1^{(1)}$	$C_1^{(2)}$	→	$U_1^{(2)}$
$C_2^{(1)}$	→	$U_2^{(1)}$	$C_2^{(2)}$	→	$U_2^{(2)}$
$V_R^{(1)}$	→	$U_3^{(1)}$	$V_R^{(2)}$	→	$U_3^{(2)}$
T	→	$U_4^{(1)}$	T	→	$U_4^{(2)}$

(4.27)

The magnitudes of $\underline{U}^{(1)}$ and $\underline{U}^{(2)}$ are respectively $\beta^{(1)}$ and $\beta^{(2)}$

Noting that $C_2^{(1)} = C_2^{(2)}$, then

$$\begin{aligned} U_2^{(1)} &= U_2^{(2)} \\ U_4^{(1)} &= U_4^{(2)} \end{aligned} \tag{4.27}$$

The correlation between failure modes 1 and 2, ρ_{12}, is given by:

$$\begin{aligned} \rho_{12} &= \alpha_2^{(1)} \alpha_2^{(2)} + \alpha_4^{(1)} \alpha_4^{(2)} \\ &= \frac{(U_2^{(1)})^2 + (U_4^{(1)})^2}{|\beta^{(1)}| \cdot |\beta^{(2)}|} \end{aligned} \tag{4.28}$$

4.4 Summary and Conclusions

Several methods for evaluating component reliabilty for an industrial facility have been outlined. They are the First-Order Second Moment (FOSM) method including the special case of FOSM methods known as the lognormal fragility curve and the Advanced First Order Reliabilty (AFOR) method. Both methods are first order approximations of the failure domain. The AFOR method, however, has some advantages over the FOSM approach. The AFOR method includes information on all probability distributions in the failure domain rather than just the moments of the random variables. Correlations among basic random variables as well as between failure modes are included in the AFOR formulation.

The AFOR method, however, can be computationally inefficient. Computational difficulties arise in the evaluation of both the component and system failure probabilities. Cut set failure probabilities of a system are estimated by considering the intersection of all events in the cut set. Since lognormal distributions are multiplicatively regenerative, the evaluation of cut set probabilities is relatively easy. For other distributions, however, the calculation of cut set probabilities can be difficult, requiring numerical integration over a large number of variables. The AFOR fragility curve, however, often approaches a lognormal fragility curve. In the applications presented in Chapter 6, the lognormal approximations are made by matching the median and standard deviation from the AFOR fragility curve. By making such

an approximation, the probability distribution is estimated from the first two moments similar to the FOSM analysis. The advantage of this approximation over the FOSM approximation is that the estimates of correlation are preserved and the uncertainties are related to the basic random variables rather than numerous safety factors. With these considerations, the AFOR approach is selected for all subsequent applications.

CHAPTER 5

APPLICATION OF METHODOLOGY TO OIL REFINERY

In this chapter the major structures and equipment at oil refineries are identified. A brief description of each component and its relation to the refining process is provided. The seismic design criteria for structures at the refinery are reviewed. The summaries presented in this chapter will be utilized in Chapter 6 where reliability computations are presented for several structures found at oil refineries.

5.1 General Refinery Layout

The refinery is subdivided into many parts, with each subregion dedicated to a single product or function related to a product. The general flow in a refinery process is shown schematically in Figure 5.1. The flow of a product, however, is not always uni-directional. Crude oil is stored in tanks in one location from where it is piped to the crude unit refining section of the plant. From the crude unit the various basic products (e.g., gas, gasoline, kerosene, diesel oil, and fuel oil) are piped in differnt directions. Each product goes through a series of processes, not necessarily physically adjacent to one another, and finally reaches its storage tanks. The storage tanks are connected to truck terminals, pipelines, etc, which again are not necessarily physically adjacent.

The actual process flow in a refinery is obviously very complex. In fact, the process flow is continuously being adjusted to convert input crude oils of varying composition into the constantly changing product demand. By necessity, there is a large variety of specialized production equipment. To introduce the typical structures and equipment in a refinery, a simplified flow diagram is represented in Figure 5.2. The numbers in Figure 5.2 refer to items in Table 5.1 which lists some of the major components of a refinery and the contribution they make to the overall risk of the refinery.

The refinery is a spatially distributed system. From the seismic risk assessment point of view it is expected that an entire oil refinery will not be subjected to the same base rock excitation due to an earthquake. Since the

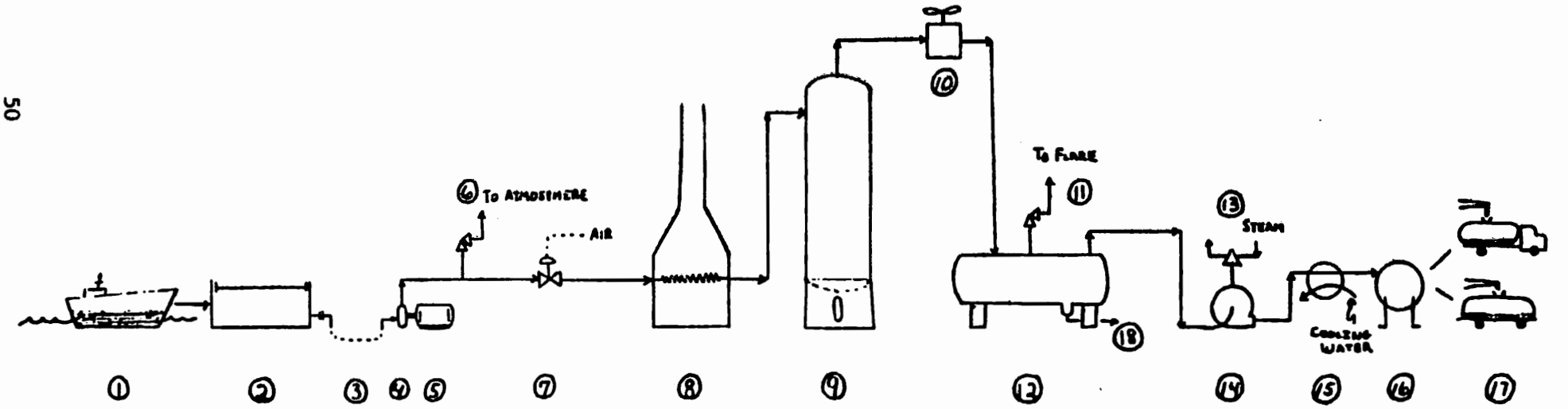


Figure 5.1 Simplified system flow showing basic equipment.
(Table 5.1 identifies the components according to the specific number.)

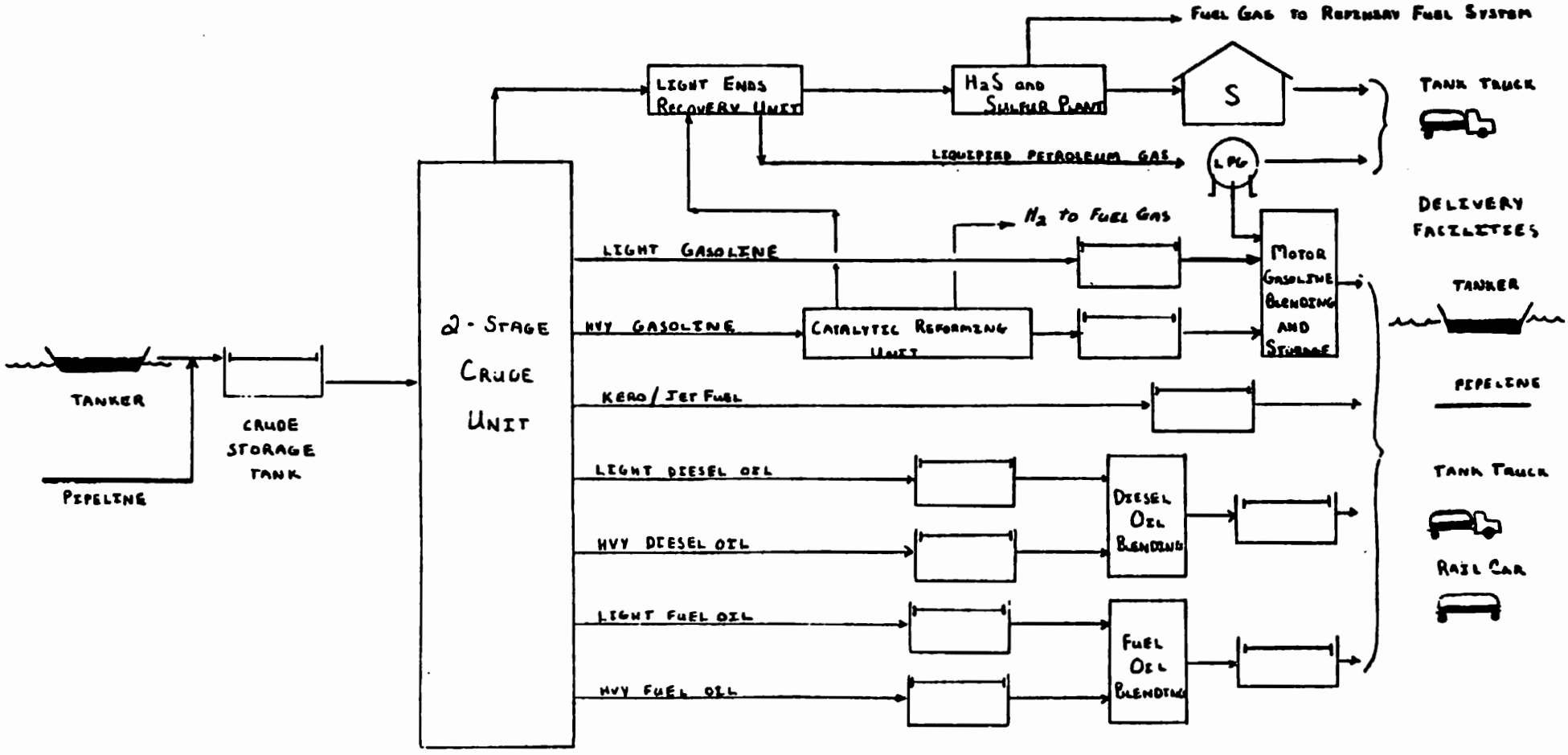


Figure 5.2 Simplified refinery flow diagram and typical equipment

Table 5.1 Major Oil Refinery Components and their Contribution to Failure.

Component	Modes of Failure	Consequences of Failure
*1. Wharf Unloading Facilities	- Structural damage or collapse - Wharf piping damage	- hazard to personnel/barge break loose - possible hydrocarbon (HC) release on water, potential fire hazard
2. Tanks	- surging - roof or pan damage - roof sink - shell buckling or rupture - bottom rupture	- HC release - exposed HC in tank, fire hazard - HC release, potential fire hazard
3. Piping Systems (Including piping valves, flanges, nozzles, etc.)	- flange separation - valve case ruptures - piping supports fail - underground piping rupture - rupture at connections to equipment (i.e., nozzles on tanks, header box equip.)	- HC or hazardous chemical release personnel hazard and potential inigition hazard
4. Pumps	- packing gland/mech. seal failure - pump case rupture	- HC release, fire hazard
5. Motors	- interruption of electrical supply - damage to electrical substation and equipment (transformers, etc.)	- possible electrocution hazard - electrical failure leading to process upset
6. Atmospheric Pressure Relief (PRV)	- response to pressure build-up cause by other equipment failure	- HC gas or liquid or hazardous chemical release to atmosphere

* Numbers correspond to components identified in Figure A1.

Table 5.1 (continued)

Component	Modes of Failure	Consequences of Failure
7. Control valve and system	- improper operation due to control system malfunction (air or power system problems) - control room and panel damage	- process upset downstream equipment failure - loss of operator control on process
8. Furnace	- damage to structural supports - stack buckling or collapse - tube support failure	- structural hazard to personnel - HC release into fire of furnace
9. Column	- shell or skirt buckling - foundation damage or overturning	- possible HC release and/or structural hazard to personnel
10. Air-cooled heat exchanger	- pipeway bent buckling or overturning - tube failure	- same as 9 above
11. PRV to relief system	- excess liquid buildup in system - failure of expansion joints - flare buckling or collapse	- possible flaring malfunction "fire rain" - possible HC liquid or gas release - structural hazard - relief system inoperable
12. Vessel	- displayed from foundation - foundation damage	- possible HC release or hazardous chemical release
13. Steam turbine Driver and stem system	- steam system interruption or steam pressure collapse	- equipment shutdown-process upset - interruptions of critical pumping services

Table 5.1 (continued)

Component	Modes of Failure	Consequences of Failure
14. Compressor	- seal or lube oil system interruption - foundation damage - damage to compressor structure	- compressor down-process upset - possible release of hazardous gases
15. Shell and tube exchanger Cooling water system	- foundation structural damage - tube failure - interruption of cooling water supply due to cooling tower damage	- possible HC release - possible HC release to atmosphere via cooling tower
16. Storage sphere	- foundation failure or collapse	- HC release, potential fire hazard - structural hazard to personnel
17. Delivery facility Tank truck loading racks	- structural damage - overhead line rupture	- same as in 16 above
18. Water treatment ponds	- structural damage to dike	- flooding of plant causes building damage, personnel hazard, process upset, etc.

local geology may change dramatically from one place to another within the refinery, each location will be subjected to different surface ground motions for the same earthquake. The distribution of ground motion at the refinery is very difficult to describe analytically. Variations with soil condition, however, can be considered to be the most important contributors to the change in ground motion at different locations. Thus, discrimination by soil types and modification of the base rock motion for various soil conditions is a viable approach to the characterization of the surface ground motion.

In order to reduce the complexities inherent in dealing with such a large distributed system, a subsystem of the refinery known as a two-stage crude unit will now be introduced and examined in greater detail.

5.1.1 Two Stage Crude Unit

Figure 5.3 shows schematically the flow in a two-stage crude unit. Its main function is to separate crude oil into its various fractions, each with roughly the same weight. Crude oil is heated in a furnace and then fed into a distilling column, the atmospheric column, where the various components or "cuts" rise or fall to their appropriate levels under heat and pressure. The stratified column of fluid is tapped at various levels to draw off gasses (light ends), gasoline, kerosene/jet fuel, diesel oil, and fuel oil.

The second stage of the two-stage crude unit refers to the sidecut strippers through which the components pass after leaving the main distilling column. The strippers are themselves distilling columns in which the same thermodynamic process occurs. However, these columns are much smaller in size compared to the atmospheric column. The sidecut strippers can recirculate fluid back to the atmospheric column, so the fractioned fluid entering a stripper at the right weight is passed to the product line and the rest is sent back to the atmospheric column.

A specialization of this pattern of flow is used for the heavy fuel oil. After leaving the atmospheric column, it is heated and fed to a vacuum column. The vacuum column is of irregular diameter, which has to do with its operation at less than atmospheric temperature.

The crude unit is the first step in the refining process and is designed to thermodynamically separate the various fractions approximately by weight.

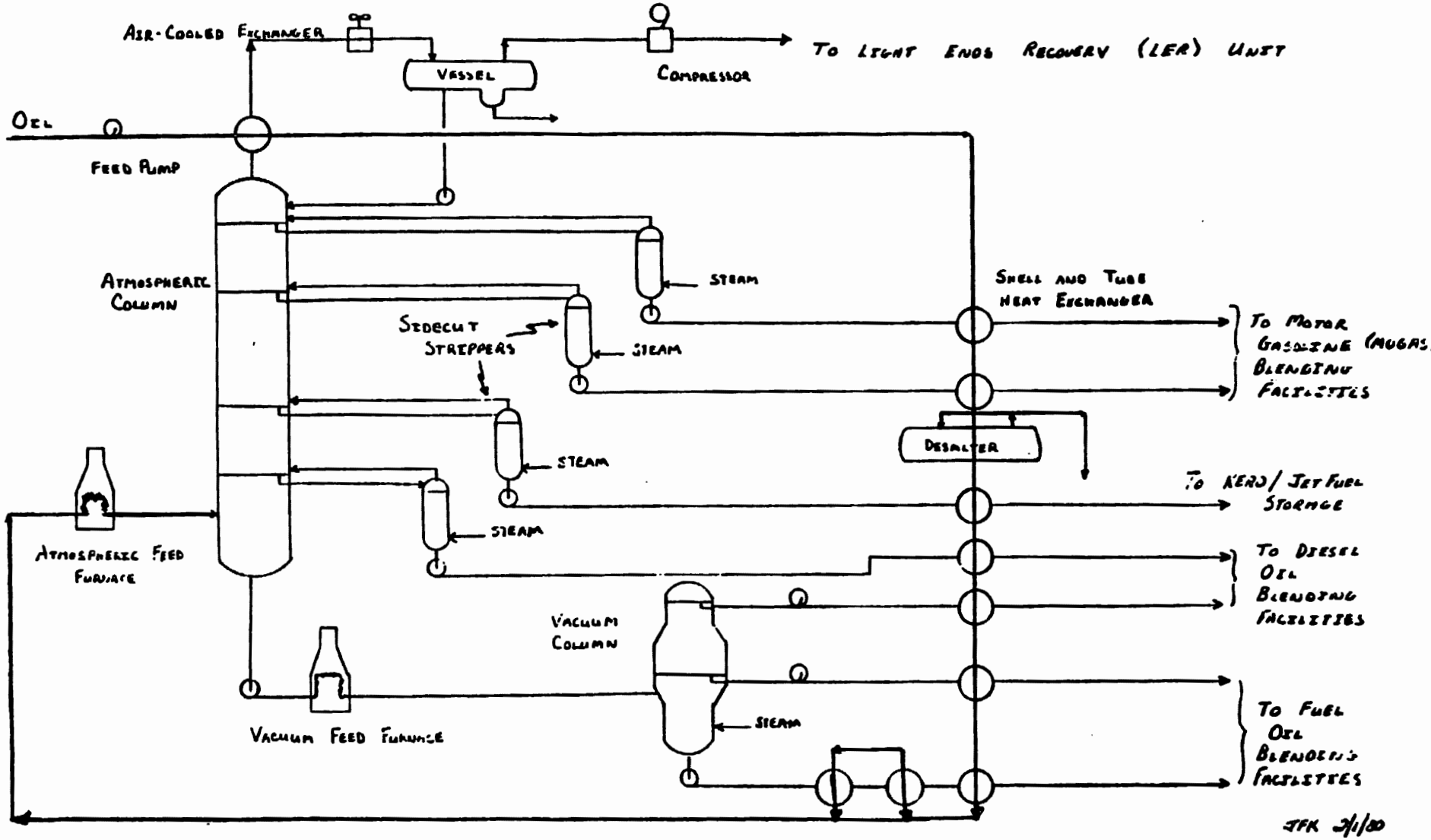


Figure 5.3 Simplified Refinery Flow Diagram - 2 Stage Crude Unit

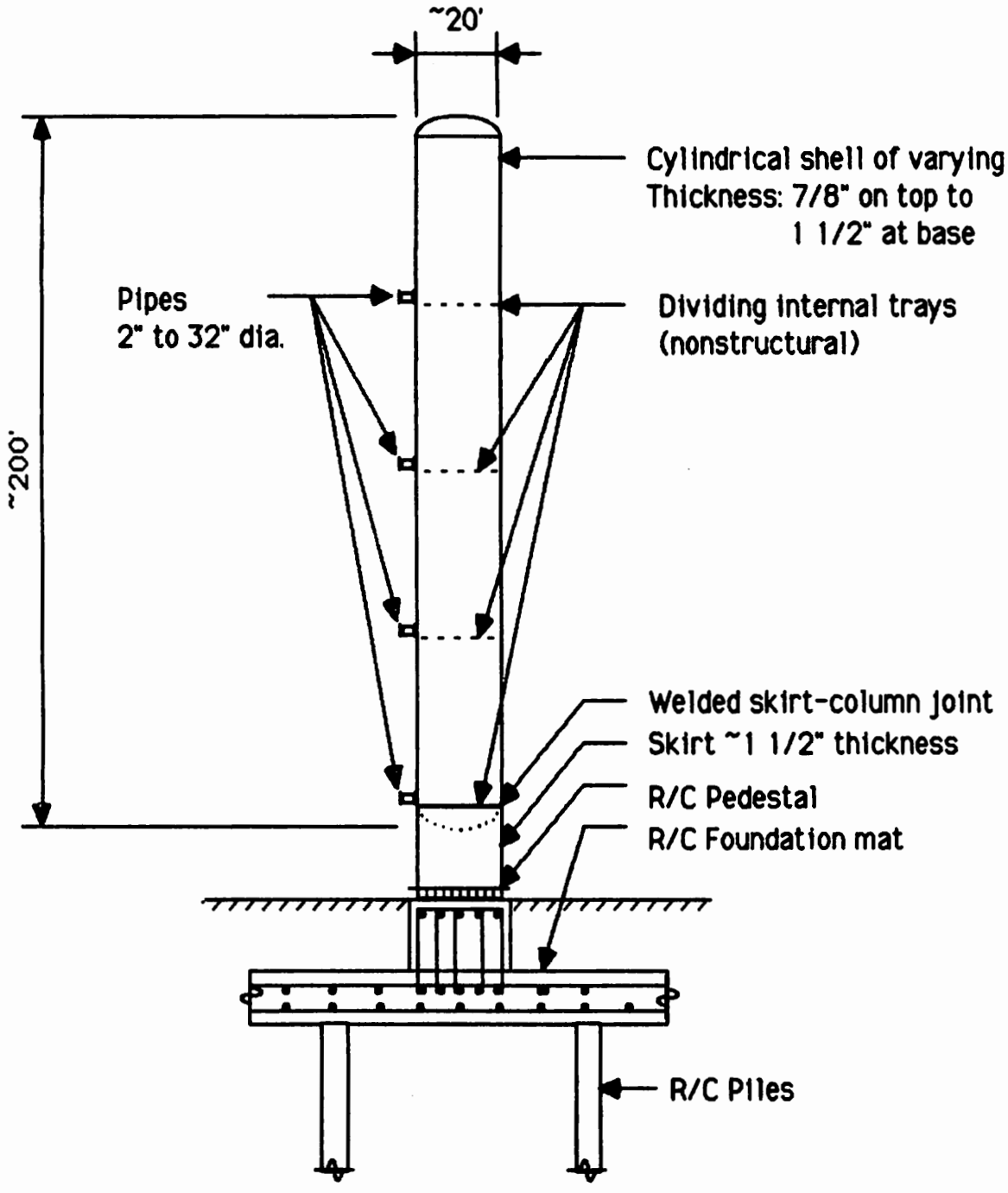


Figure 5.4 Typical Atmospheric Column

Subsequent steps will involve further separation in columns, removal of impurities such as sulfur, chemical processes, and blending the final product. The components comprising the crude are next examined in some detail.

5.1.2 Atmospheric Column

The atmospheric column (Figure 5.4) is likely to be one of the largest and most crucial structures in an oil refinery. Some of these columns can be over 200 ft. tall and approximately 20 ft. in diameter. A typical aspect ratio is about 10 to 1. The column therefore behaves as a cantilever fixed at the foundation. Attached in all directions are pipes of varying diameters (2" to 32") to accomodate flows of gasses and fluids in the distillation process. The contents are at atmospheric pressure.

The functional component of the column is the cylindrical shell of varying thickness capped at the top and bottom, in which stratification occurs. This vessel is welded to a steel skirt which is tied to a concrete pedestal with anchor bolts. The pedestal is integrated with a mat foundation by reinforcing bars.

Under normal operating conditions, the vessel must support its own weight plus the weight and hydrostatic pressure of the contents. Under seismic conditions, the column must withstand the additional overturning moment generated by the earthquake. Buckling failure modes must be considered along with compression. The design must also consider the fact that the vessel will be operating at elevated temperatures which will change the elastic properties of the shell materials. In addition, a corrosion allowance must be included depending on the process involved and the expected life of the vessel. The shell thickness for the 200 foot column for example would vary from 7/8 inch at the top to 1-1/2 inch at the bottom.

The supporting skirt does not have internal hydrostatic pressure nor does it operate at high temperatures. Thus the skirt is often thinner than the shell. In the case of the 200 foot column the skirt thickness is about 1 inch. The skirt normally has cut-outs for the passage of pipes, inspection and maintenance.

A flange and stiffening ring are welded to the base of the skirt. Anchor bolts pass through these rings and are embedded in the pedestal. These anchor

bolts are usually made from mild steel such as A307. The anchor bolts may be up to 3 inches in diameter.

The pedestal is reinforced concrete which is poured after the foundation mat. The reinforcing which integrates the two pours must therefore be set into the mat first. The mat itself is very wide and may support more structures than the atmospheric column. The mat is about 6 or 7 ft. thick and is supported on piles.

As stated above, the column is designed as a cantilever beam. The internal trays which separate the layers of fluid add no stiffness to the shell. The weight of external pipes is accounted for but again no stiffness is added. The region near a nozzle to a pipe is designed for the resultant stress concentrations. Cut-outs in the skirt are reinforced as necessary to maintain the proper stiffness. The mat and pedestal must be designed for overturning.

The bolts are designed to yield before more drastic limit states such as buckling of the skirt are reached. It is intended that the yielding of the bolted connections act as an energy-dissipating mechanism which will forestall further damge. Therefore, the connection must be ductile. It is for this reason that the bolts are made from mild rather than high-strength steel. In addition, the bolts must be long enough, properly embedded, and adequately spaced to avoid brittle failures such as bolt fracture or pop out.

Buckling of the skirt or shell would be a far more costly failure than yielding of the anchor bolts. In the latter case, it would be necessary to retighten or replace the stretched bolts. The buckling failure would entail replacement of all or part of the damaged skirt or vessel.

Other possible failure modes might include: separation of the skirt and the shell at the weld, pulling the anchor bolts out of the pedestal, local damage to the pedestal or mat, overturning of the foundation, soil bearing failure, failure due to soil liquefaction, cracking of a nozzle, and loss of a pipe connection.

Since this is such a key facility, its failure would be very costly in terms of both capital loss and lost production. The fire hazard would undoubtedly be high.

5.1.3 Sidecut Strippers

These columns are typically about 20 ft. high. Their design is similar to the atmospheric column, except that they are smaller and also simpler due to their specialized purpose. The pedestals on which they are erected share the foundation mat for the atmospheric column.

The capital loss due to the failure of a sidecut stripper would be smaller because of its smaller size. Failure of one stripper might only cause loss of production of only one or two products for a limited period of time. The fire hazard would depend on which product the stripper contained, e.g. fuel oil vs. flammable gasses.

5.1.4 Vacuum Column

The vacuum columns are different from the atmospheric columns in several respects. First, their cross-section is often nonuniform. Second, the supporting skirt is mounted on a reinforced concrete support frame. Third, the internal pressure is below the atmospheric pressure and the shell is circumferentially stiffened to prevent buckling inwards.

The skirt is anchored to the frame by anchor bolts. A typical frame consists of eight spiral wrapped columns placed in an octagon and tied together at the top, middle and bottom, by heavy concrete beams.

The failure modes of a vacuum column would include most of those mentioned earlier. These include anchor yielding, buckling, and broken nozzles and connections. An additional failure mode not found in the previously mentioned columns is failure of the concrete frame. The reliabilty of a framed structure is more difficult to analyse simply due to the many possible plastic hinge locations. As a result there will be a multitude of possible failure modes.

Capital loss due to failure of this structure would probably be large. The value of the lost product would depend on many factors since the associated product is fuel oil. Fire hazard would probably be confined to the local area.

5.1.5 Piping and Fittings

There are literally thousands of pipes inside a refinery. Their sizes range from 2 in. or less to 36 in. or possibly larger. They carry not only petroleum products but water, steam, gasses, chemicals and so on. Electrical cables for power and instrumentation also run through small diameter pipes.

According to engineers at Standard Oil Company of California, piping failures due to seismic loads do not constitute a major problem. There are several reasons for their low failure rate.

The first reason is that these pipes are generally long and slender and thus are very flexible between supports. Consequently their predominant periods of vibration are likely to be very different from the periods of the input earthquake motion.

Second, they are very ductile. These pipes may buckle elastically with no harmful effects. Large lateral displacements in general pose no severe problem. Similarly, there is large ductility in the elbows which dissipate energy by becoming oval in shape when bent.

Third, pipes are designed for thermal expansion. They are also checked against the maximum lateral displacements which may occur during an earthquake. When so checked, the two ends of a run of pipe are analytically "fixed ends" with imposed static displacements. Because pipes are so ductile and their dynamic response is minimal, no vibration analysis is performed.

Fourth, a spill caused by pipe rupture should be relatively small (compared to the potential spill from a tank) and is controllable by shutting off valves. Pipes are also easily replaced. Thus the consequences of pipe failure are small when compared with other components.

In summary, the failure of a pipe by buckling, cracking or rupture is not considered likely or of great consequence. The problem with pipes seems to be not with the long stretches, but with the fittings and connections to tanks, towers and the like. Failures of pipe to tank connections have been observed during several past earthquakes. Usually the connection was broken because a valve near it was tied to a concrete support which "didn't follow" the tank. As a result the pipe pulled out of the tank. Other failures of connections might include fracture - especially of cast iron fittings or welds, separation of flanges, and distortion of valves causing malfunction. When developing the

systems representation, the analyst must be careful to designate where the failure of a pipe-vessel connection is considered a failure of the pipe or the vessel. The possible dependence between the pipe-vessel connection failure and other pipe or vessel failure modes must be included in the analysis.

5.1.6 Pipe Stanchions

Running through a refinery are elevated "freeways" of pipes. Generally, pipes run 14 ft above the ground so that vehicles can move freely through the plant. Supporting these pipes overhead are large reinforced concrete stanchions, similar to those that support roadways (see Figure 5.5).

A typical stanchion may carry three levels or trays of pipes. It might be 40 ft. tall and 50 ft. wide. The three trays would be supported by R/C beams 2 ft to 3 ft. deep. The stanchions are placed at 30 ft to 40 ft intervals and are connected by longitudinal reinforced concrete beams.

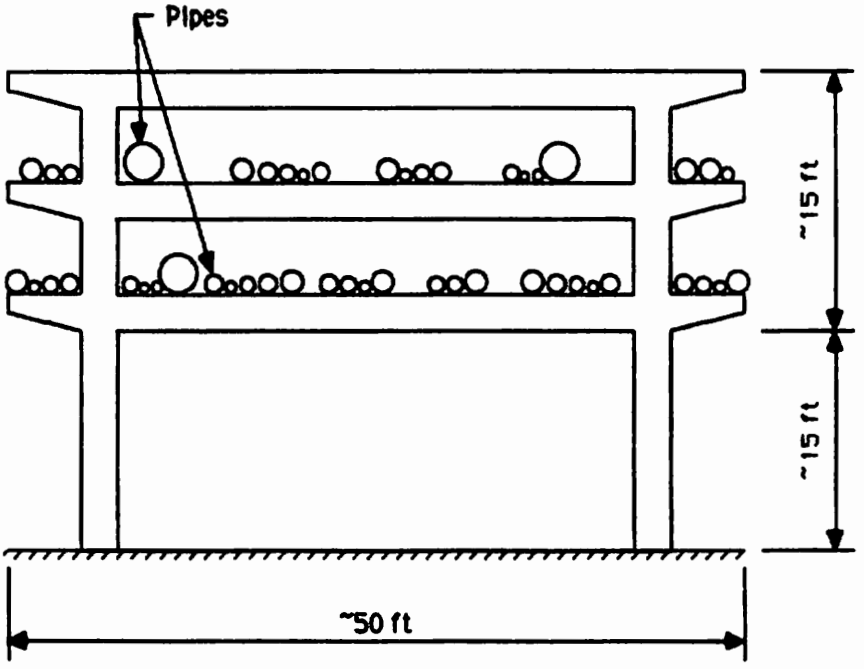


Figure 5.5 Reinforced concrete pipe support structure

The pipes run through guides on the trays but are not tied down. This allows for thermal expansion of the pipes. The thermal displacements are controlled by tying the pipes down to one stanchion only. Thus, longitudinal load on the pipes is resisted by this stanchion. The longitudinal beams tying the stanchions together help to distribute this load, however, it is not designed to brace against dynamic loads. Longitudinal load may also be transmitted to the stanchions by the overhead air coolers.

Steel stanchions are sometimes used, however, concrete is preferred for minimizing the fire hazard. Each stanchion is designed independently of the others ignoring their interaction. If the longitudinal beams and/or air cooling units are stiff enough, however, stanchions may be coupled together and their vibration mode shapes may be altered. This would affect the failure modes of a stanchion.

The failure modes of a stanchion include column failure in shear or buckling, beam (tray) failure, and collapse. It is clear that stanchion failures are not independent. The collapse of one stanchion would increase the loads on the remaining stanchions.

Based on past experience, pipe stanchion failures do not seem to be a serious problem. Likelihood of failure is low and consequences are about equal to the sum of the failures of all the pipes it supports.

5.1.7 Cylindrical Storage Tanks

Based on past experience tanks are regarded as the structures most likely to fail. Depending on the type of failure, large amounts of flammable fluid may be exposed, thus leading to very costly fire damge. There are basically two types of tanks: cylindrical and spherical (see Figure 5.6). The spherical tanks are discussed separately.

The familiar cylindrical storage tank rests on an asphalt, gravel, or ringwall foundation with a steel bottom liner. Occasionally small tanks are supported on rigid concrete mats which may in turn be supported on piles. Except for smaller tanks, it is not feasible to anchor the tank to the foundation. Thus, uplifting at the side of a tank is possible which can lead to failure.

Two types of roofs are commonly used: floating and fixed. The floating roof floats on the fluid contents of the tank. Thus, there is a seal between the roof and the inside wall of the tank. There may be guides for the roof to follow as it rises and falls with the level of the tank. The fixed roof is usually conical in shape and is welded to the upper course of the tank and may be supported by columns inside the tank.

Generally, tank design for seismic loading involves checking the overturning moment caused by sloshing of the contents. Overturning moments are calculated by formulas found in the Recommended Practice No. 11 (RP-11), see Section 5.3. Excess overturning can cause foundation bearing failure or buckling of the lower course known as "elephants foot" because of its appearance. Excess sloshing can cause buckling of the upper course or damage to the roof. Excess sloshing can also cause seal failure in floating roof designs or column failure due to lateral loading by moving fluid in fixed roof designs. Sliding of the tank on its foundation is also possible (see Chapter 2 for examples of these failures during past earthquakes).

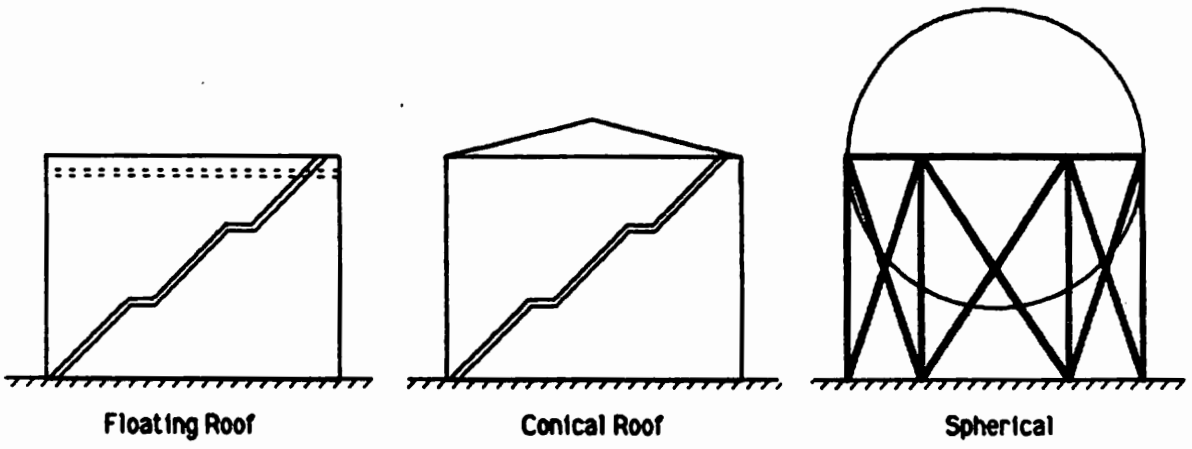


Figure 5.6 Typical tanks

Any of the above failure modes can result in the exposure of flammable fluids or possibly the loss of fire fighting water. Thus, they are all serious. As evidenced from past occurrences, fires in and around tanks are devastating and may go on for days until the fuel is burned. Consequently, tank failures can be considered to be high probabilty events with serious consequences.

Finally, the reader is referred to the discussion of the failure of connections to tanks contained in the section of pipes and fittings. As discussed in Chapter 2 sliding of a tank may cause damage to the connection as an additional failure mode.

5.1.8 Spherical Storage Tanks

Spherical storage tanks are used for contents which must be kept under pressure. The contents might be flammable gasses such as butane. It was the collapse of one such butane tank that led to a costly fire at the Western Gulf Oil Co. Paloma Cycling plant on July 21, 1952 (see Chapter 2).

These tanks are held above the ground by braced frames. Lateral forces are transferred from the frame to the spherical shell by a balcony girder. The structure is considered a single degree of freedom oscillator for calculating the lateral load. This load is distributed to the bracing panels (typically six) depending on their orientation.

The collapse at the Paloma Cycling plant was due to the buckling of a bracing rod. The failure of the rod was a "brittle" failure and was due to poor seismic design considerations. This failure can be predicted easily without any complicated analysis. The current RP-11 now prohibits the use of rods and requires that braces be effective in both tension and compression.

5.1.9 Support Frames

Reactor vessles are sometimes elevated in frames because of functional requirements (e.g. downhill flow to the next vessel) or lack of space on the ground. Such support frames are likely to be constructed of reinforced concrete in consideration of potential fires. They are not enclosed by walls, to allow free air circulation and prevent the build-up of dangerous fumes.

The design of these frames is according to the UBC and RP-11. The performance of these structures is expected to be much closer to their theoretical behavior than ordinary framed buildings due to the lack of architectural walls and due to the smaller uncertainty of the dead loading which is typically mechanical equipment of known weight.

Consequences of failure depend on the product and the process involved. Consideration should also be given to the failure of equipment tie-downs, which may cause damage to the equipment even if the frames are themselves undamaged. Capital loss resulting from such failures should be relatively easy to estimate. Loss of production would only occur on the lines which flow through a failed frame. Fire potential would depend on the considerations above, as well as the presence of an ignition source.

5.1.10 Occupied Buildings

Occupied buildings such as offices and laboratories, are built to local building code requirements for earthquake forces, i.e. UBC. These structures generally do not house processing equipment, thus there is no direct impact on the process in the event of a failure. However, these buildings may house control equipment and/or key personnnel, thus a failure might affect the control or safety of the plant. Failure modes would be dependent on the design of each individual structure.

5.1.11 Furnaces

Furnaces are used to heat the input stock to the desired temperature before introducing them into the pressure vessel. For instance, the crude oil is heated before placing it in the atmospheric column. Although furnaces may vary widely in design depending on the size, a typical furnace would be a one-story framed structure. The furnace would normally be lined with refractory brick.

Typical failure modes would include those found in any framed structure including damage to beams and columns. Damage may occur in the bracing system if the lateral force resisting system is a braced system. Other failure modes would include damage to the heat exchange piping, buckling of the smoke stack, and damage to the refractory lining. Possible consequences include release of hydro-carbons into the furnace from damaged pipes as well as the hazard posed

to personnel by the damaged structure. Capital losses are those which accrue from the damaged equipment. Loss of production would vary depending on the ability to substitute different stock requiring less preheating. Production could possibly continue at a reduced rate allowing for the reduced efficienty of unheated stock.

5.1.12 Cooling Towers

Cooling towers are generally simple framed wood structures. High temperature water is brought to the top of the structure and allowed to trickle down a maze of wooden baffles. Heat is removed from the water through evaporation. The efficiency of the process is enhanced when a fan is used to force air through the tower to increase the rate of evaporation.

Possible failure modes are again related to the failure of the framed structure as well as failure of the piping. Capital losses are a function of the cost of repairing or replacing the structure or piping. Loss of production would result from the impaired efficiency resulting from the reduced rate of cooling of the stock.

5.2 Seismic Design Criteria

The seismic design criteria discussed here is that adapted by the Standard Oil Company of California (SOCAL), which in turn is based on the Uniform Building Code (UBC, 1979). Earthquakes induce dynamic loads on the structures. For the purpose of design, however, equivalent static lateral forces are specified. The dynamic nature of the load is included to the extent that the natural period of the structure is a factor in computing these equivalent static loads. For major structures or critical facilities, it is recommended to use dynamic procedures to verify the above mentioned static approach.

The provisions set by SOCAL in the Recommended Practice No. 11, (1980) and the legal building codes for the region, typically the Uniform Building Code, UBC, determine the lateral forces and their distribution. Based on these codes, structures, vessels, equipments and their supports should be analysed for earthquake loads combined with normal operating gravity loads. Wind and earthquake loads need not be combined with hydrostatic test loads. The structure is then designed for the most adverse loading condition. The

lateral loads are combined with all other loads which may reasonably be expected to occur simultaneously. The wind or earthquake loads are considered to be acting in any general direction. For analysis purposes, however, they may be resolved into components parallel to the principal axes of the structure.

5.2.1 Structures

The total equivalent static lateral load, or the base shear V is given by (UBC or RP-11, 1980).

$$V = ZIKCSW \tag{5.1}$$

where

Z - Seismic zone factor
I - Occupancy importance factor
K - Structural type coefficient
C - Structural period response factor
S - Site-structure interaction factor
W - Total operating weight of structure above ground.

The earthquake zone factor is the same as specified in the Uniform Building Code (1982) (see Table 5.2). The occupancy importance factor I, is selected as unity (I = 1) for the majority of structures. For elevated tanks I = 1.5. Elevated water tanks may be needed for firefighting or emergency generators and are thus considered more important.

Table 5.2

Earthquake and Seismic Zone Factor

Earthquake Zone	Seismic Zone Factor, Z
4	1
3	3/4
2	3/8
1	3/16
0*	0*

* No earthquake design required.

The structural type coefficient, K, indicates how the structure is expected to behave in an earthquake. Table 5.3 gives a list of K values for different types of structures, as used by the Standard Oil Company of California (RP-11, 1980). The relatively high values of K are due to the lower ductility and nonstructural damping used in the design of these structures.

Table 5.3
Structure Coefficient (K) (from R.P.-11, 1980)

Structure Type		Structure Coefficient (K)
Diagonally Braced or Shear-Wall Structures	Steel	2.0
	Concrete	2.0
Rigid Frame Structures	Steel	1.5
	Concrete	1.8
Vertical Vessels on Skirt Support		2.0
Vertical Vessels on skirts when $t_{Skirt} > 3/2\ t_{Skirt}$		2.5
Spheres on Braced Leg Supports		2.5
Vertical Vessels w/unbraced legs		2.5
Pipe Supports		2.0
Concrete Supports for Horizontal Vessels		2.0
Induced Draft Cooling Towers - Timber		1.33

Structure Type		Structure Coefficient (K)		
Pipeway Stanchions		Piping Without Equipment		Piping Plus Equipment**
		Transverse Direction	Longitudinal Direction	Both Direction
Rigid Frame	Steel	1.2	0.8	1.5
	Concrete	1.4	0.9	1.8
Diagonally Braced	Steel	1.5	1.0	2.0
	Concrete	1.5	1.0	2.0

** Equipment: such as air coolers, etc.

The coefficients C and S are computed from functions of the period of the structure and period of soil.

$$C = \frac{1}{15\sqrt{T}} \tag{5.2}$$

$$S = 1.0 + \frac{T}{T_S} - 0.5\left[\frac{T}{T_S}\right]^2 \quad \text{for } T/T_S < 1.0 \tag{5.3}$$

$$S = 1.2 + 0.6\frac{T}{T_S} - 0.3\left[\frac{T}{T_S}\right]^2 \quad \text{for } T/T_S > 1.0 \tag{5.4}$$

where T = period of the structure

T_S = characteristic site period

and $CS < 0.14$, with $C_{max} = 0.12$

The vertical distribution of the earthquake force is triangular, similar to that specified in the UBC. A portion of the total shear is applied at the top of the structure if overall height to base width is greater than 3.0 to account for higher modes of vibrations. In practice this distribution is assumed continuous for uniform structures such as the atmospheric column described in Section 5.1.2. Nonuniform structures, are broken into discrete units along the height of the structure (RP-11, 1980, Appendix V). The force applied to each unit is then calculated.

The horizontal distribution of shear should ensure that torsional forces created by eccentricity between mass and shear centers are accounted for. A minimum eccentricity of 5% of the maximum plan dimension of the structure at the level in question is assumed.

It is recognized that the strength requirements of RP-11 cannot prevent inelastic deformations in structures subjected to moderate earthquake forces. Although it is impossible to specify all the details required to prevent the collapse of a structure under these conditions, RP-11 does give several general guidelines to ensure adequate ductility in the structure. Attention is given to the detailing of concrete connections, steel bracing and the like.

5.2.2 Equipment

The criteria for seismic design of all electrical or mechanical equipment (pumps, switch gear, transformers, control panels, etc.) is to resist seismic forces through anchoring to the foundation or supports. The minimum lateral earthquake force V is given by

$$\text{(i)}\quad V = 0.20\ ZIW \quad \text{Equipment at grade level.} \tag{5.5}$$

$$\text{(ii)}\quad V = 0.30\ ZIW \quad \text{Equipment at elevated levels.} \tag{5.6}$$

where Z, I and W are as defined in Section 5.2.1. The force V is assumed to act at the center of mass of the equipment. The force V is larger for Case (ii) due to an expected amplification of base motion for elevated levels.

Mild steel bolts or other suitable ductile connections should provide the necessary anchorage. Direct welding of a rigid equipment element to a rigid support or foundation will not serve as an allowable ductile anchorage.

5.2.3 Cylindrical Storage Tanks

The response of storage tanks differs significantly from the response of the structures and equipment mentioned earlier. The sloshing of the liquid contents of the tank add significantly to the loads caused by an earthquake. Such forces are not considered by the code provisions discussed in the preceeding sections. For this reason storage tanks are designed according to a separate code such as the API Standard 650, "Weld Steel Tanks for Oil Storage". The provisions of this code are summarized breifly.

The design procedure attempts to account for the two critical response modes of a storage tank. The first is the relatively high frequency response of the structure itself along with the portion of the fluid that is moving in unison with the structure. The second is the low frequency response of the portion of the fluid which is sloshing. Based on these assumptions, the equation for the overturning moment caused by the earthquake motions is:

$$M = ZI(C_1W_sX_s + C_1W_rH_t + C_1W_1X_1 + C_2W_2X_2) \qquad (5.7)$$

where

Z = Seismic zone coefficient.

I = Importance factor. This varies from 1.0 to 1.5 with the higher value recommended for facilities essential for post-earthquake emergency services.

C_1 = Lateral force coefficient related to high frequency response of structure.

C_2 = Lateral force coefficient related to low frequency response of a portion of the fluids.

W_s = Total weight of the tank shell.

X_s = Height from base of shell to center of gravity of shell.

W_r = Weight of roof plus snow load if specified.

H_t = Total height of shell.

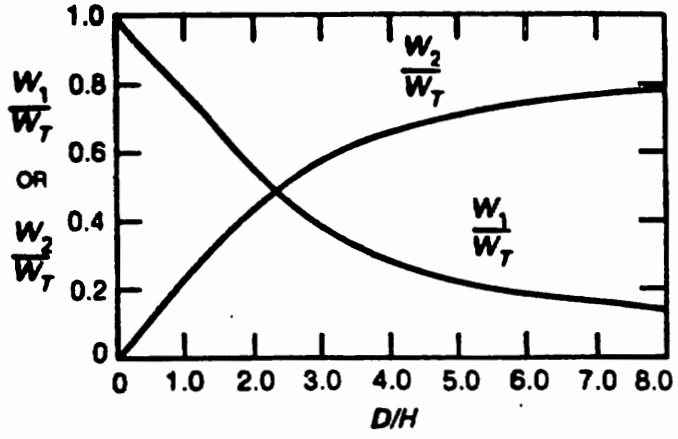


Figure 5.7 Effective weight of tank contents (from API 650)

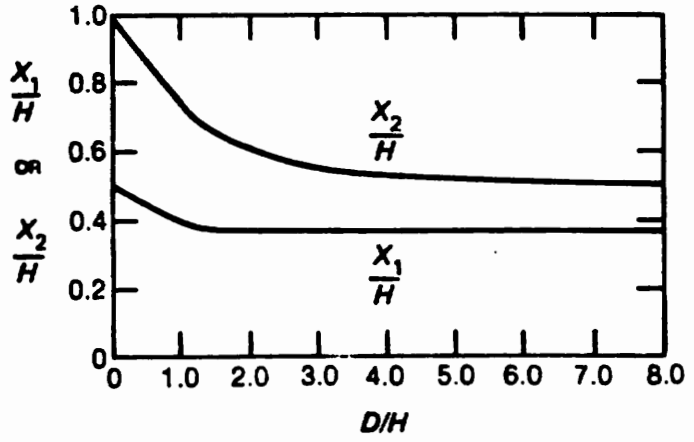


Figure 5.8 Effective height to centroid of tank contents (from API 650)

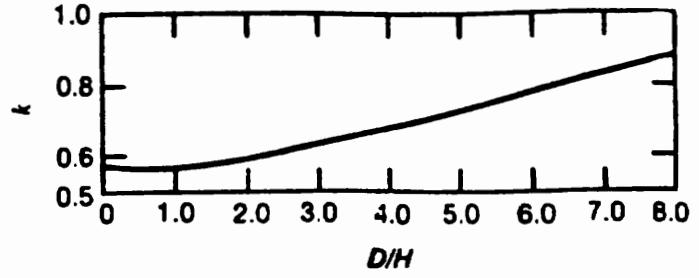


Figure 5.9 k-factor for period calculations (from API 650)

W_1 = Effective weight of tank contents which moves in unison with shell, calculated from Figure 5.7.

X_1 = Height from bottom of tank to centroid of W_1 determined from Figure 5.8.

W_2 = Effective weight of first mode sloshing contents of tank from Figure 5.7.

X_2 = Height from bottom of tank to centroid of W_2 determined from Figure 5.8.

The seismic zone factor, Z, is based on the provisions of ATC-03 rather than the UBC maps. It is felt that the ATC-03 provisions more accurately reflect seismic hazards in the United States.

The factors C_1 and C_2 are functions of the natural frequency of the structure. Since the response of an uplifting tank is extremely difficult to calculate explicitly, a conservative constant value of 0.24 is taken for C_1. This value corresponds to a UBC K-value of 2.0. The high value of K is chosen because a simple structure such as a tank will not have the ductilty and non-structural damping of buildings. This assumption is consistent with the rationale used in selecting the K values presented earlier in Table 5.2.

The factor C_2 is calculated from the following equations

$$C_2 = \frac{0.30\ S}{T} \quad \text{for } T < 4.5 \tag{5.8}$$

$$C_2 = \frac{1.35\ S}{T^2} \quad \text{for } T > 4.5 \tag{5.9}$$

where S is the site amplification factor and T is the period of the first mode sloshing calculated as follows:

$$T = k\sqrt{D} \tag{5.10}$$

where D is the nominal diameter of the tank in feet, and k is taken from Figure 5.9. The variable H in Figure 5.9 is the maximum filling height of the tank in feet.

Figures 5.7 and 5.8 express W_1, W_2, X_1 and X_2 as functions of D/H and W_T. The variables D and H are the same as described in the previous paragraph. W_T is the total weight of the tank contents.

This summarizes the additional loads which must be considered when designing for earthquakes. API Standard 650 also specified the required resistance to overturning and buckling due to longitudinal compressive forces. For unanchored tanks, a portion of the tank contents may be assumed to contribute to the overturning resistance. This portion is calculated as follows:

$$W_L = 7.9 t_b \sqrt{F_{by} G} \quad H \tag{5.11}$$

and

$$W_L < 1.25\ GHD \tag{5.12}$$

wher W_L is the weight of tank contents resisting overturning in pounds per foot of shell circumference, t_b is the thickness of the bottom ring in inches. The thickness t_b must exceed 1/4 in. or the thickness of the bottom shell course. F_{by} is the yield strength of the bottom ring in psi and G is the design specific gravity of tank contents.

The maximum longitudinal compressive force is a function of $M/D_2(W_t + W_L)$ where W_t is the weight of the tank shell per foot of circumference. Thus the maximum compressive force is given by

$$b = W_t + 1.273\ M/D^2 \qquad \text{for } \frac{M}{D^2(W_t + W_L)} < 0.785 \tag{5.13}$$

$$b = \frac{(W_t + W_L)}{W_L} \cdot \frac{1.490}{1 - \left[\frac{0.627M}{D^2(W_t+W_L)}\right]^{1/2}} \qquad \text{for } 1.5 < \frac{M}{D^2(W_t + W_L)} < 1.57 \tag{5.14}$$

When $M/D^2(W_t + W_L)$ is greater than 1.57 or when b/12t is greater than F_a, buckling or yielding may occur. F_a is determined by

$$F_a = \frac{10^6 t}{D} \qquad \text{for } \frac{GHD^2}{t^2} > 10^6 \tag{5.15}$$

$$F_a = \frac{10^6 t}{2.5D} + 600\sqrt{GH} \qquad \text{for } \frac{GHD^2}{t^2} < 10^6 \tag{5.16}$$

and

$$F_a < 0.5\ F_{ty} \tag{5.17}$$

where F_{ty} is the yield strength of the bottom course.

Although no guidelines are specified, the designer should review the thickness of the upper course should the thickness of the lower courses need to be increased for earthquake forces. Attention is also called to the hydrodynamic forces imposed on roof columns of fixed roof tanks by the sloshing liquids. No requirements are made for these forces, however. Freeboard requirements for floating roof tanks are likewise not specified but may be necessary to avoid damage to the roof. Foundations should also accomodate additional forces caused by the overturning moment.

5.2.4 Comments and Summary

It can be readily seen that the earthquake design code used by SOCAL follows very closely the UBC requirements. Storage tanks are a noticable exception. Due to he dynamic loads created by sloshing of the liquids they are designed to API 650 standards. For other structures, the principle deviation from UBC guidelines is the increase in K factors to account for the structures unique to an industrial facility.

It is noted that with the exception of storage tanks, the facilities designed to these codes have withstood earthquakes quite adequately. Their behavior, in general, has been as predicted by the codes. All subsequent comments and observations should be understood in light of this important fact.

RP-11, the UBC, and API 650 are all equivalent static methods. Methods of dynamic analysis such as time-history analysis are not generally used in design of such facilities for the simple reason that they are not economically feasible. The adequate behavior of industrial facilities in past earthquakes coupled with the relatively low cost of materials have made such elaborate analytical methods prohibitively expensive.

Static methods for analysis and design, however, do not provide sufficient insight to the effects of earthquakes on structures. Investigations of failure sequences and the effects of less understood phenomena such as inelastic deformations are pursued only to a limited extent and designers rely on intuition and judgement to anticipate the effects of these factors.

Generally, codes specify safety factors, and attempt to maintain a consistency between safety factors. The aim is to avoid the failures with the

most serious consequences by increasing the safety factors. However, it has been shown that there is no direct link between factors of safety and probability of failure (see, for example, Ravindra and Galambos, 1978). Thus is is possible that for two different limit states designed with identical factors of safety one limit state may be more likely than the other.

With all the shortcomings of the code-based design, structures and equipment at industrial facilities have performed remarkably well during past earthquakes. It is important to note, however, that most of the earthquake events reviewed in this report are of moderate size. Facilities subjected to major or severe earthquakes were located at distances of 40 km or further from the epicenter. Thus, with the exception of the Imperial County, 1979 earthquake event, the ground motions at the site of the facilities have been moderate. It is important therefore to study the behavior of these facilities under extreme conditions in order to determine potential damage to industrial structures and identify specific shortcomings of the design approaches currently in use.

CHAPTER 6

COMPONENT RELIABILITY COMPUTATIONS

6.1 Introduction

The Advanced First Order Reliability (AFOR) methods introduced in Chapter 4 will be illustrated in this chapter through application to some of the structures in the two-stage crude unit described in Section 5.1. The first structure to be analyzed is the atmospheric column. A nonuniform vertical vessel will be examined next.

The dimensions of the atmospheric column to be analysed are given in Figure 6.1. The important limit states for the column are yielding of the anchor bolts at the base of the column, buckling of the supporting skirt, and separation of the weld connecting the skirt to the vessel. The first of these three limit states is the least important in terms of direct economic loss. However, the exceedence of this limit state is very important in terms of the subsequent behavior of the column. As discussed earlier, the column is designed so that the bolts will yield before the other limit states are reached. It is therefore important to calculate the probability of bolt yield before the buckling and weld separation occur. The g-function for this limit state will be formulated using two approaches. The first approach uses a simplified design equation based on equivalent static methods of analysis. The second is a more rigorous random vibrations analysis approach. This is followed by the buckling and weld separation analyses. The last two limit states will be formulated from simplified design equations. The modifications required to adapt the simplified methods to more complicated structures will then be illustrated in the analysis of a non-uniform vertical vessel. A discussion of the results and the role they play in a systems analysis concludes this chapter.

6.2 Bolt Yield Analysis

The limit state equation for bolt yield can be simply stated as:

$$g = \sigma_y - \sigma_b \tag{6.1}$$

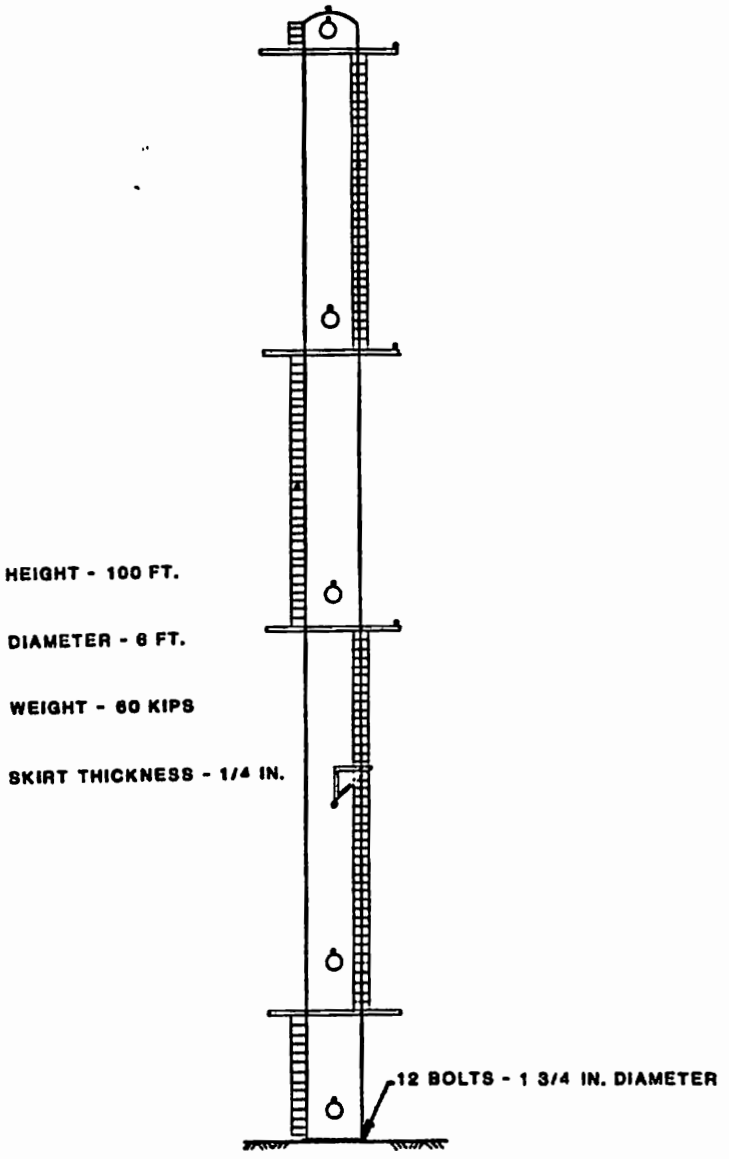


Figure 6.1 Atmospheric column

where σ_y is the yield stress of the bolt material and σ_b is the load imposed on the bolt by the earthquake. This equation is used for both the equivalent static and random vibrations analyses. The differences in the two methods emerge from the formulations of σ_b.

6.2.1 Equivalent Static Analysis

The goal of the equivalent static analysis is to estimate the value of the stress in the bolt due to earthquake ground motions. Since the reliability analysis is performed conditional on a given level of ground motion, peak ground acceleration is used as the ground motion parameter and is assumed to be known. Equivalent static methods similar to those used in design are employed to transform the ground motion into a stress in the bolt. The procedure for evaluating the stress in the bolt is described in the following sections.

Base Shear. Using equivalent static analysis methods the shear at the base of the column is obtained by multiplying the PGA by a dynamic amplification factor (DAF). For purposes of this study, the DAF proposed by ATC-03 is used and is given by

$$V = B \cdot D \cdot Q \cdot W \cdot PGA \tag{6.2}$$

or

$$V = C_1 \, PGA \tag{6.3}$$

where B is the reduction factor which accounts for the ductility and other energy dissipating mechanisms such as soil-structure interaction. Since the column will remain linearly elastic up to the point of bolt yield, the ductility is equal to unity. The factor B then has the maximum value of 0.7. The factor D is the amplification factor derived from the simplified response spectrum. For structures with natural periods greater than 0.3 sec. built on firm soils, D is found to be:

$$D = 2.0 \sqrt{0.3/T} \tag{6.4}$$

where T is the natural period of the structure. Q in equation 6.2 is a quality factor. In order for the DAF to remain at the mean value, the value of Q is equal to one. W is the weight of the structure.

There are several design equations for estimating the natural period of the column. In this case the following equation from RP-11 is used:

$$T = \frac{7.78}{10^6} \left(\frac{\ell^2}{D'}\right) \sqrt{\frac{12\ w\ D}{t}} \qquad (6.5)$$

where ℓ is the height of the column in feet, D' is its diameter also in feet, t is the thickness of the shell in inches, and w is the weight of the column per unit height in pounds per foot. This formula is suitable for columns with uniform diameter and weight distributions with height. Columns with variable weight distribution are discussed in the next section of this chapter.

Moment at Base. Given the base shear, the design equations estimate the moment at the base by assuming the shear forces to be triangularly distributed along the height of the column. An additional force at the top is included to account for higher modes. From these assumptions, the following equation for the moment at the base is obtained

$$M = \ell(0.07 + 2/3(1.0 - 0.07T))V \qquad (6.6)$$

or

$$M_b = C_2\ V. \qquad (6.7)$$

Bolt Stress. Some difficulties arise when calculating the bolt stress for a given applied moment and vertical load. An "exact" solution involves writing force and moment equilibrium equations for the base. Such equations cannot be solved in closed form. However, for design purposes the following approximation is used

$$\sigma_b = \frac{1}{A_b} \left(\frac{4\ M_b}{N\ D_b} - \frac{W}{N}\right) \qquad (6.8)$$

Where A_b is the cross-sectional area of each bolt, N is the number of bolts, D_b is the diameter of the circle of bolts and W is the total weight of the column. This equation is acknowledged to be fairly conservative.

Random Variables. A process for calculating the stress in the bolts for a given PGA has been outlined. In order to estimate the probability of failure the basic random variables must be identified. It was verified by sensitivity analysis that random variables with coefficients of variation of less

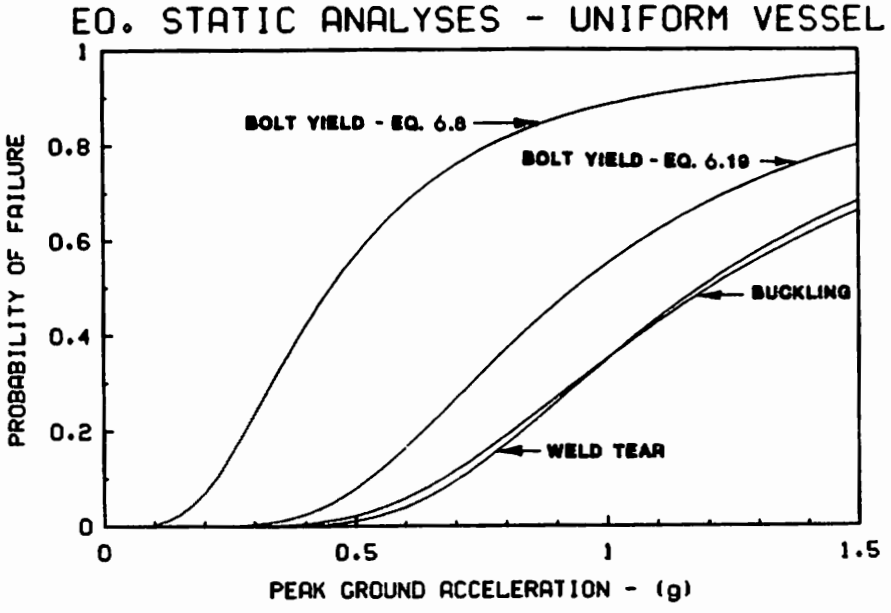


Figure 6.2 Fragility curve for equivalent static analysis

than five percent do not contribute significantly to the overall probability of failure. With that in mind, the following random variables are defined:

W - Weight of the column. The weight is assumed to be normally distributed. Discussion with SOCAL engineers revealed that the weight of the column would have a coefficient of variation (COV) of 10% when in operation. The weight will drop significantly when the vessel is emptied for maintenance. The column, however, will be in operation about 90% of the time and the loads will be considerably higher during operation. Thus, only the weight while the column is full is considered in the analysis.

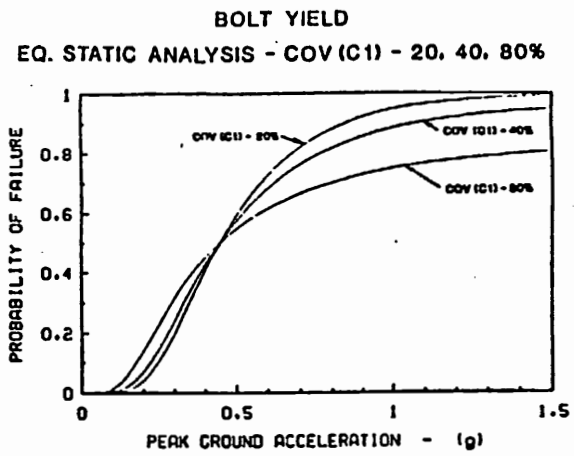
σ_y - Yield stress of the bolt. The yield stress is assumed to be normally distributed with a COV of 5%. This estimate is based on information on bolt tests performed by Kulak (1972).

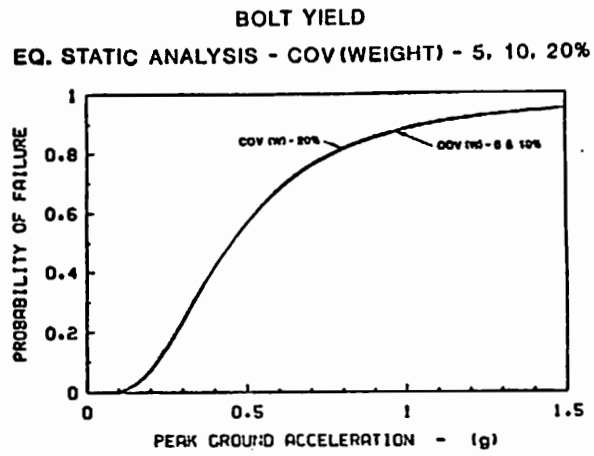
C_1 - Transfer function transforming PGA to base shear. Studies by Shah et al. (1975) show the COV of the mean DAF to be about 40%. C_1 is assumed normal.

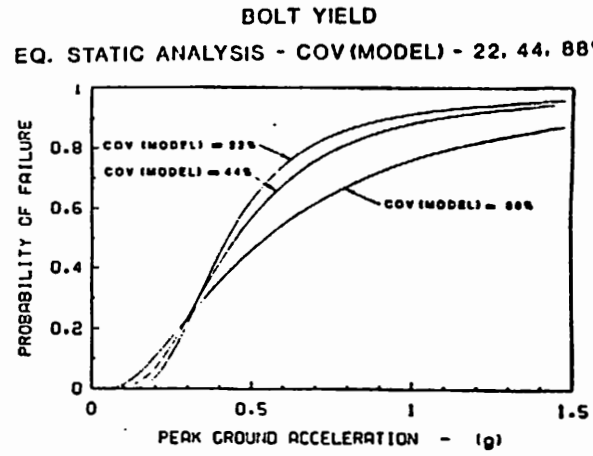
C_2 - Base shear to moment factor. Based on Rinne (1970) this factor is estimated to have a COV of 15% based on the accuracy of the assumed triangular mode shape and the contribution of the higher modes. C_2 is also assumed to be normal.

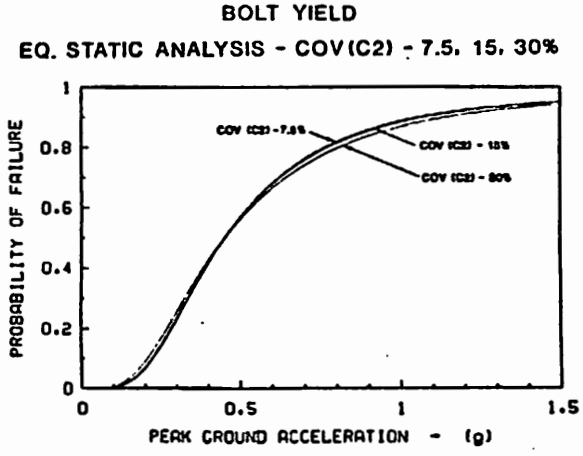
T - Period of the structure. It is noted that C_1 and C_2 are dependent on the period of the structure. The correlation between T and C_1 and C_2 is included in the analysis.

X_m - Modeling uncertainty. Based on an estimate of the overall variance in the random vibrations analysis, this random variable is assumed to have a mean of one and a COV of 44%. It is lognormally distributed.









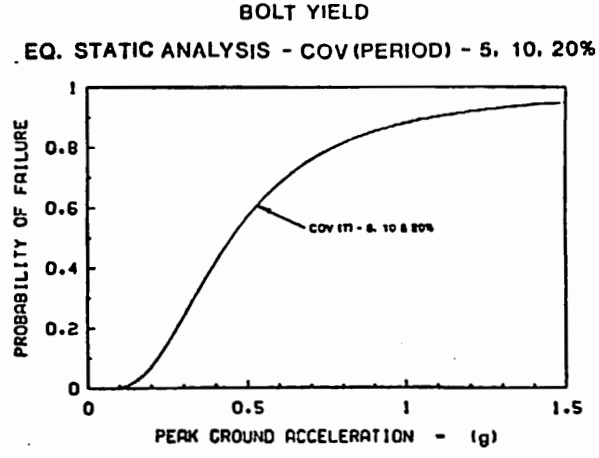


Figure 6.3 Sensitivity analyses for bolt yield

Other distributions could be used for the above variables. However, in view of the simplicity of the limit state formulation and the information from which these estimates were made such refinement is not justified.

Results. The first order reliability method outlined in Chapter 4 was used to obtain the fragility curves for equivalent static bolt yield. Figure 6.2 shows the resulting fragility curve. In order to study the effect of each random variable on the probability computation, additional analyses were carried out. The coefficient of variation of each random variable was increased or decreased by a factor of two. It was felt that a factor of two represented reasonable bounds on the estimates of the coefficient of variation. The results of these analyses are shown on Figure 6.3. It can be seen that the factor C_1 dominates the uncertainty and C_2 is the second largest uncertainty contributor.

A similar sensitivity analysis was performed for the anchor bolt design. The standard case of 12 bolts with 1-3/4 in. diameter was changed to 8 bolts at 2-1/4 in. diameter and 16 bolts at 1-1/2 inch diameter. The results are shown in Figure 6.4. The eight bolt design shows a decrease in probability of failure for a given level of PGA. This decrease is attributable to the fact

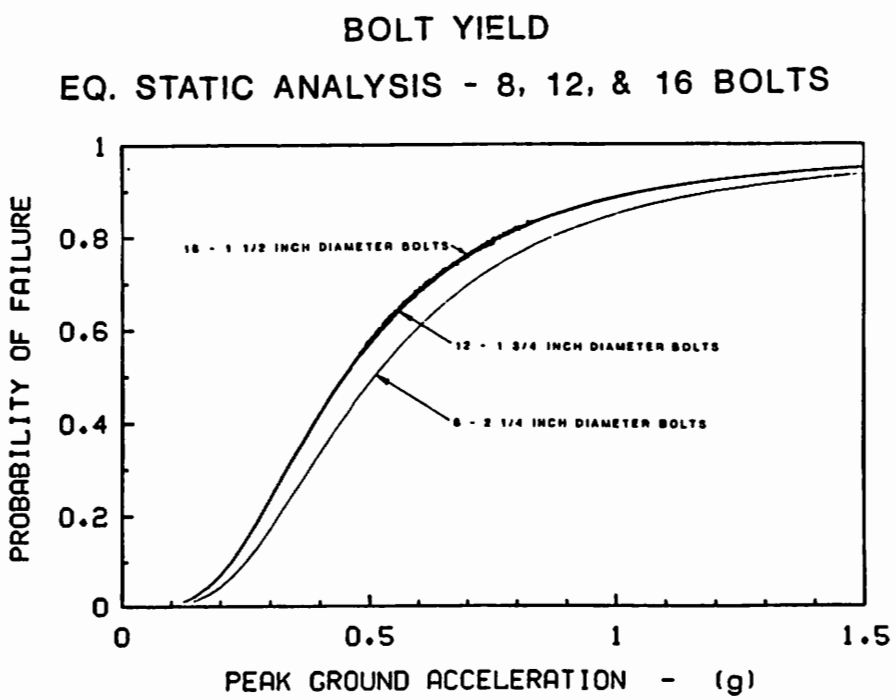


Figure 6.4 Sensitivity of bolt yield fragility to anchor bolt design

that anchor bolt diameters only come in standard increments. As a result it was necessary to specify bolts with a diameter larger than the minimum required by the design for the eight bolt configuration. The results of the equivalent static analysis will again be discussed in relation to the results of the random vibrations analysis.

6.2.2 Random Vibrations Analysis

A more rigorous definition of the limit state equation (equation 6.1) can be obtained from the theory of random vibrations. In this analysis the response of the column subjected to a random input motion is evaluated following the formulation of Shih and Chen (1984). The bending moment at the base of the column and the stress in the bolts are then computed in terms of first- and second-order statistics of the response motion of the column. The following is a brief summary of the main aspects of the reliability computations.

Equation of Motion. The equation of motion of a uniform vertical column subjected to vertical accelerations is given by (Iyengar and Shinozuka 1971):

$$EI \frac{\partial^4 y(x,t)}{\partial x^4} + m(g + \ddot{x}_g)\left[A(\ell - x) \cdot \frac{\partial^2 y(x,t)}{\partial x^2} - A \frac{\partial y(x,t)}{\partial x}\right] + c \frac{\partial y(x,t)}{\partial t} + m A \frac{\partial^2 y(x,t)}{\partial^2 t} = -m A \ddot{y}_g \qquad (6.9)$$

where y is the relative lateral displacement of the column, EI is the flexural rigidity, A is the cross-sectional area, ℓ is the height, c is the damping coefficient, and m is the mass per unit length of the column. The acceleration of gravity is represented by g; $\ddot{y}_g$ and $\ddot{x}_g$ are the horizontal and vertical accelerations at the base of the column respectively. The boundary conditions for this column are:

$$y(0,t) = \frac{\partial y(0,t)}{\partial x} = \frac{\partial^2 y(\ell,t)}{\partial x^2} = \frac{\partial^3 y(\ell,t)}{\partial x^3} = 0 \qquad (6.10)$$

and the initial conditions are zero displacement and velocity at t = 0. The ground motion is assumed to be a pair of nonstationary Gaussian white noise processes:

$$\ddot{y}_g(t) = e(t)\, W_1(t)$$

and $$\ddot{x}_g(t) = e(t)\, W_2(t) \qquad (6.11)$$

where e(t) is an envelope function, and $W_1(t)$ and $W_2(t)$ are Gaussian white noise processes. The autocorrelation functions for these processes are given as follows:

$$R_{W_1W_1}(s) = 2D_{11}\delta(s) \qquad (6.12a)$$

$$R_{W_2W_2}(s) = 2D_{22}\delta(s) \qquad (6.12b)$$

where $\delta(\cdot)$ is the dirac delta. The cross-correlation for these processes can be shown to be

$$R_{W_1W_2}(s) = 2(D_{11}D_{22})^{1/2}\delta(s) \qquad (6.12c)$$

if the earthquake is assumed to emanate from a point source (Shih and Chen, 1984). The equation of motion can be uncoupled by assuming a solution of the form:

$$y(x,t) = \sum_{j=1}^{\infty} f_j(x)q_j(t) \qquad (6.13)$$

where $f_j(x)$ is the jth mode shape and $q_j(t)$ is the jth generalized coordinate. The equations for the mode shapes, uncoupled equation of motion and the resulting stochastic differential equation of motion are given in Shih and Chen (1984). Of interst to the reliabilty problem are the first two moments of the column response motion. For the specific case of a uniform column, these moments are given by

$$\rho_i = E[Z_{ji}] \quad \text{and} \quad \rho_{ik} = E[Z_{ji} \cdot Z_{jk}] \qquad (6.14)$$

where $Z_{j1} = q(t)$, and $Z_{j2} = \dot{q}(t)$ and j denotes the specific mode under consideration. The solution process $[Z_{j1}, Z_{j2}]$ is jointly Markovian and the statistics given in equation 6.14 are determined by the corresponding Fokker-

Planck equations (Shih and Chen, 1984). For a column initially at rest $\rho_i = 0$ at $t = 0$.

Bending Moment Response. In order to determine the bending moment at the base of the column we define the bending moment mode shape as follows:

$$h_j = EI\ f''(x) \tag{6.15}$$

The first-order Taylor series approximation for the mean square of the moment is given by

$$E[M^2(x,t)] \approx \sum_{j=1}^{\infty} h_j^2(x) E[q_j^2(t)] \tag{6.16}$$

In this equation the correlation is assumed to be negligible. This assumption is reasonable since the dominant first modes for the column are in general not closely spaced (Kircher et al., 1978).

Input Ground Motions The ground motion is assumed to be nonstationary Gaussian white-noise process. The ground motion parameter used in the equivalent static analysis is the peak ground acceleration. To compare the two the PGA must be related to the parameters used in this formulation. Lai (1982) describes a procedure which correlates the PGA to the parameters of the Kanai-Tajimi power spectral density given by:

$$S(\omega) = S_0 \frac{(\omega_g^2 + 4\xi_g^2\omega^2)\omega_g^2}{(\omega_g^2 - \omega^2)^2 + 4(\xi_g\omega\omega_g)^2} \tag{6.17}$$

where S_0 is the earthquake intensity, ω_g and ξ_g are th site-dependent soil parameters. The value of $S(\omega)$ at the frequency of the mode in question can be used for the value of D_{11} in equation 6.12a. Since this parameter depends on the natural frequency of each mode, the analysis is no longer restricted to a white noise spectrum. Penzien and Watabe (1975) suggest a correlation between the horizontal and vertical power spectra which gives the value of D_{22} as one-half of the value of D_{11}.

The remaining ground motion parameters define the envelope function, e(t). For simplicity, the following form is suggested (Shinozuka and Sato, 1967)

$$e(t) = b(e^{-\alpha t} - e^{-\beta t}) \tag{6.18a}$$

where

$$b = \left[\frac{\beta}{\beta - \alpha}\right] \left[\frac{\alpha}{\beta}\right]^{\alpha/(\alpha-\beta)} \tag{6.18b}$$

The parameters α and β determine the shape of the envelope including the rate of buildup and decay of the ground motions as well as the total area under the envelope. Thus α and β can be related to the duration and intensity as defined by Vanmarke and Lai (1980). The value of b is chosen to give the envelope a maximum value of one. This ensures that the maximum parameters of the modulated Kanai-Tajimi spectrum match those of the unmodulated spectrum.

Stress in Bolts. The stress in the bolts is calculated form the bending moment and vertical force equilibrium equations. The following set of equations can be written:

$$W = B_1[A_1 - R^*A_2] - A_3 \tag{6.19a}$$

and

$$M_b = B_1[R_s^2 A_2 - R^*A_1]/2 + A_4 \tag{6.19b}$$

where

$$A_1 = \sqrt{x^*(2R_w - x^*)} \tag{6.20a}$$

$$A_2 \cos^{-1}(R^*/R_s) \tag{6.20b}$$

$$A_3 = E_s \varepsilon_{cm} A_b \left[\sum_{x_i < R^*} (R^* - x_i)^2/x^*\right] \tag{6.20c}$$

$$A_4 = E_s \varepsilon_{cm} A_b \left[\sum_{x_i < R^*} (R^* - x_i)^2/x^*\right] \tag{6.20d}$$

$$B_1 = 2R_s t E_s \varepsilon_{cm}/x^* \tag{6.20e}$$

$$R^* = R_s - x^* \tag{6.20f}$$

E_s is Young's modulus for steel, A_b is the cross-sectional area of the bolt as before, and ε_{cm} is the maximum compressive strain at the base. R_s, t, and x^* are dimensions illustrated in Figure 6.5. Equations 6.19a and b must be solved iteratively to find ε_{cm} and the neutral axis location, x^*. The maximum bolt stress can then be found from:

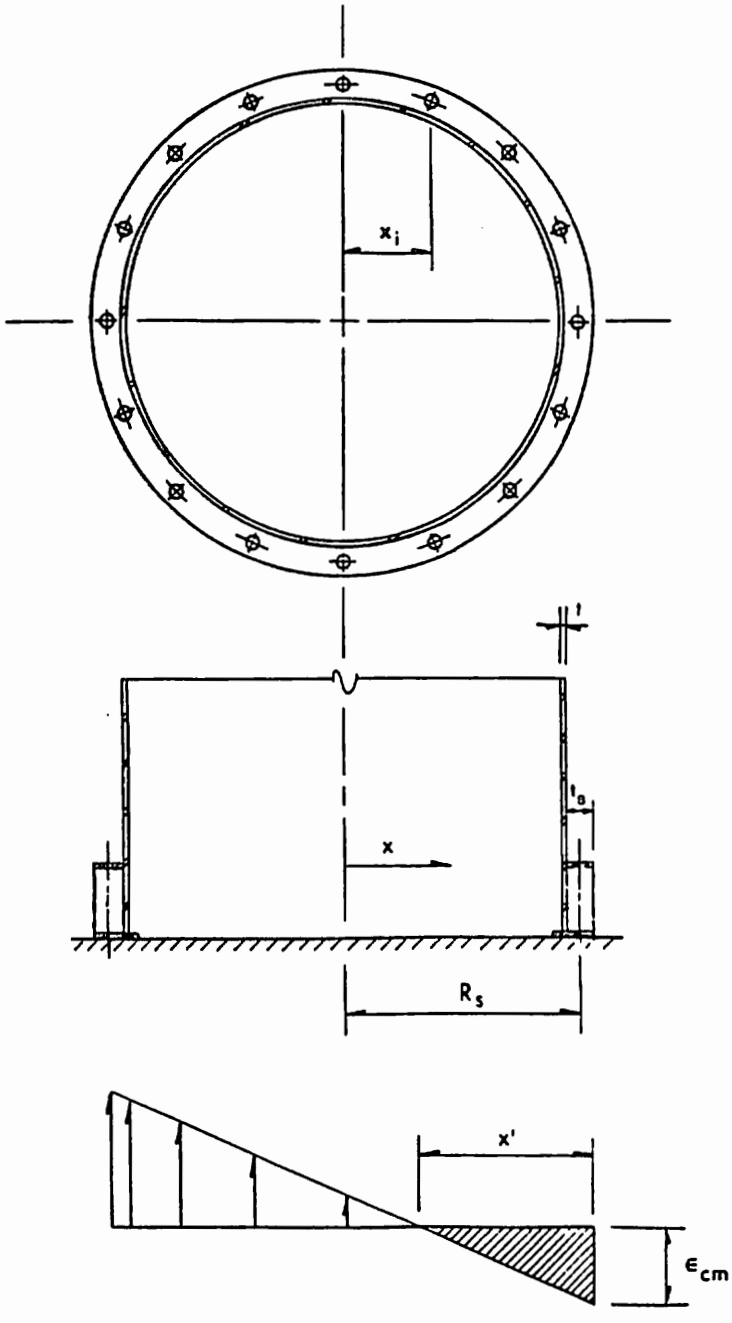


Figure 6.5 Cross section and stress distribution at base of supporting skirt

$$\sigma_{b,S} = E_s \varepsilon_{cm}(R^* + R_b)/x^* \qquad (6.21)$$

where R_b is the radius of the circle of bolts. The weight of the structure in equation 6.21 is also affected by the vertical accelerations discussed earlier. Specifically the weight is found from

$$W = mA\ell(g + \ddot{x}_g) \qquad (6.22)$$

The statistical properties of $\ddot{x}_g$ can be found from the power spectrum of the vertical accelerations as developed earlier.

Results. A full implementation of the random vibrations analysis has not been carried out. However, a comparison was made of the stress estimation when equation 6.19 is used instead of equation 6.8. In this comparison, the parameters for the column were defined as given in Section 6.2.1, and vertical accelerations (equation 6.22) were ignored. The results shown in Figure 6.6 indicate that the simplified equation greatly overestimates the stress, in the bolts for a given applied base moment, thus overestimating the probabilty of failure.

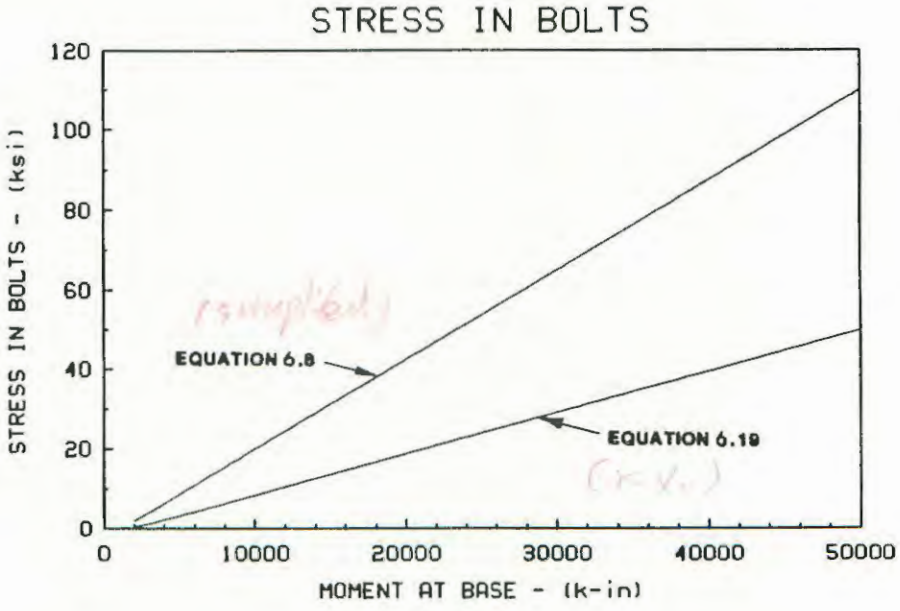


Figure 6.6 Stress in bolts versus applied base moment as predicted by equations 6.8 and 6.19

These results point out the need for a systems approach to the design problem. Although equation 6.8 is conservative for the bolt yield limit state, it may be unconservative for the overall system. The anchor bolts may be less likely to yield, but the column may be more likely to buckle because the bolts have not yielded to provide the anticipated energy dissipating mechanism. The designer must understand the overall behavior of the structure to properly anticipate the effects of his design decisions.

6.3 Skirt Buckling

The skirt buckling failure mode is fairly difficult to analyze. Since the buckling usually occurs after the bolts yield, the response of the column will be nonlinear due to the inelastic stretching of the bolts and the rocking motion at the base. Simplified empirical methods for defining inelastic response spectra based on energy considerations have been proposed (e.g., Newmark et al., 1973; and Newmark and Riddell, 1979). These methods have been incorporated into the ATC-03 design recommendations and will be used to analyze the buckling failure mode. The limit state equation for the buckling failure mode of the column is defined as:

$$g = \sigma_{buckle} - \sigma_b \tag{6.23}$$

where σ_{buckle} is the buckling stress and σ_b is the maximum stress at the base. The results of this analysis are presented after the derivation of the limit state equation.

Base Shear. The PGA to base shear factor, C_1, is modified to account for the inelastic behavior subsequent to bolt yield. Equations 6.2 and 6.3 will remain unchanged. However, the formula for B reflects the ductility due to bolt yield:

$$B = \frac{0.7}{\sqrt{2\mu - 1}} \tag{6.24}$$

where μ is the ductility of the column defined as:

$$\mu = \frac{\theta_{ultimate}}{\theta_{yield}} \tag{6.25}$$

Where $\theta_{ultimate}$ is the angular deflection at buckling and θ_{yield} is the angular deflection at bolt yield. The remaining factors in equation 6.2, D, Q, and W, are unchanged.

Moment at Base. The equation for transforming base shear into moment at the base is unchanged from equations 6.6 and 6.7.

Stress in Skirt. Typical diamond buckling anticipated in this failure mode will not occur right at the base. Rather it will occur at a short distance up the skirt. Thus, it is reasonable to assume that plane sections remaine plane and that the following equation defines the bending stress

$$\sigma_b = \frac{M_b}{S} + \frac{W}{A} \tag{6.26}$$

where S is the section modulus, and A is the area of the column.

Buckling Stress. According to classical buckling theory, buckling will occur when the stress reaches:

$$\sigma_{buckle} = \frac{2Et_s}{D'\sqrt{3(1-\nu^2)}} \tag{6.27}$$

where D' is the diameter of the skirt and ν is Poisson's ratio for the skirt. E is as defined in Section 6.2.2 and t_s is the thickness of the skirt. Experience has demonstrated that buckling actually begins at stresses far below those predicted by equation 6.27. This is attributed to imperfections in the shell (Timoshenko and Gere 1961). A series of tests on cylinders subjected to axial and bending leads (Donnel, 1934; and Donnel and Wen, 1950) correlated the reduction in buckling strength with the diameter-over-thickness ratio of the shell. A regression analysis performed on Donnel's data estimates the mean and variance of the reduction factor, ψ, as follows:

$$mean_\psi = 0.3644 - 1.069 \times 10^{-4} \left(\frac{D'}{2t_s}\right) \tag{6.28}$$

$$Var_\psi = \left[5.482 \times 10^{-3} + 1.963 \times 10^{-10} \left(\frac{D'}{2t_s} - 682.4\right)^2\right] \tag{6.29}$$

This approach is simiar to the simplified equivalent static formulations. For the range of D'/t_s used in these columns, the design equations predict a reduction factor of about 20%. Equation 6.28 predicts a reduction factor of about 34%. Again, the design equation proves to be overly conservative for purposes of reliability analysis.

Random Variables. Distributions and coefficients of variation for random variables W, T, C_1, and C_2 are as defined in Section 6.2.1. The reduction factor, ψ, is assumed to be lognormally distributed. The ductility is also assumed to be lognormally distributed and the distribution is transformed so that $f_\mu(\mu) = 0$ for $\mu < 1.0$. The mean is 1.271 based on analysis of the yield and ultimate deformations. The COV is 15% based on the results of sensitivity analyses of the ductility.

Results. The fragility curve generated by this analysis is plotted in Figure 6.2. Sensitivity analyses were carried out as before and the results are plotted in Figure 6.7. These results indicate that the uncertainty is dominated by the variable C_1; variables C_2 and ψ also contribute significantly.

6.4 Weld Tear

The weld tear limit state is also reached after the bolts have yielded. Thus the approximation for the nonlinear effects used in the preceeding section will be used in the equivalent static weld tear analysis. In this analysis the limit state equation is:

$$g = \sigma_{tear} - \sigma_{skirt} \tag{6.30}$$

where σ_{tear} is the stress at which the weld begins to tear and σ_{skirt} is the stress at the top of the skirt due to the earthquake.

Base Shear. The base shear factor, C_1, is calculated from equations 6.2 and 6.3 with the modification for B as given in equations 6.24 and 6.25.

Moment at Top of Skirt. The critical section in this case is at the top of the skirt where the weld connects the skirt to the shell. Therefore, the factor C_2 is modified as follows to evaluate the stress from the base to the top of the skirt.

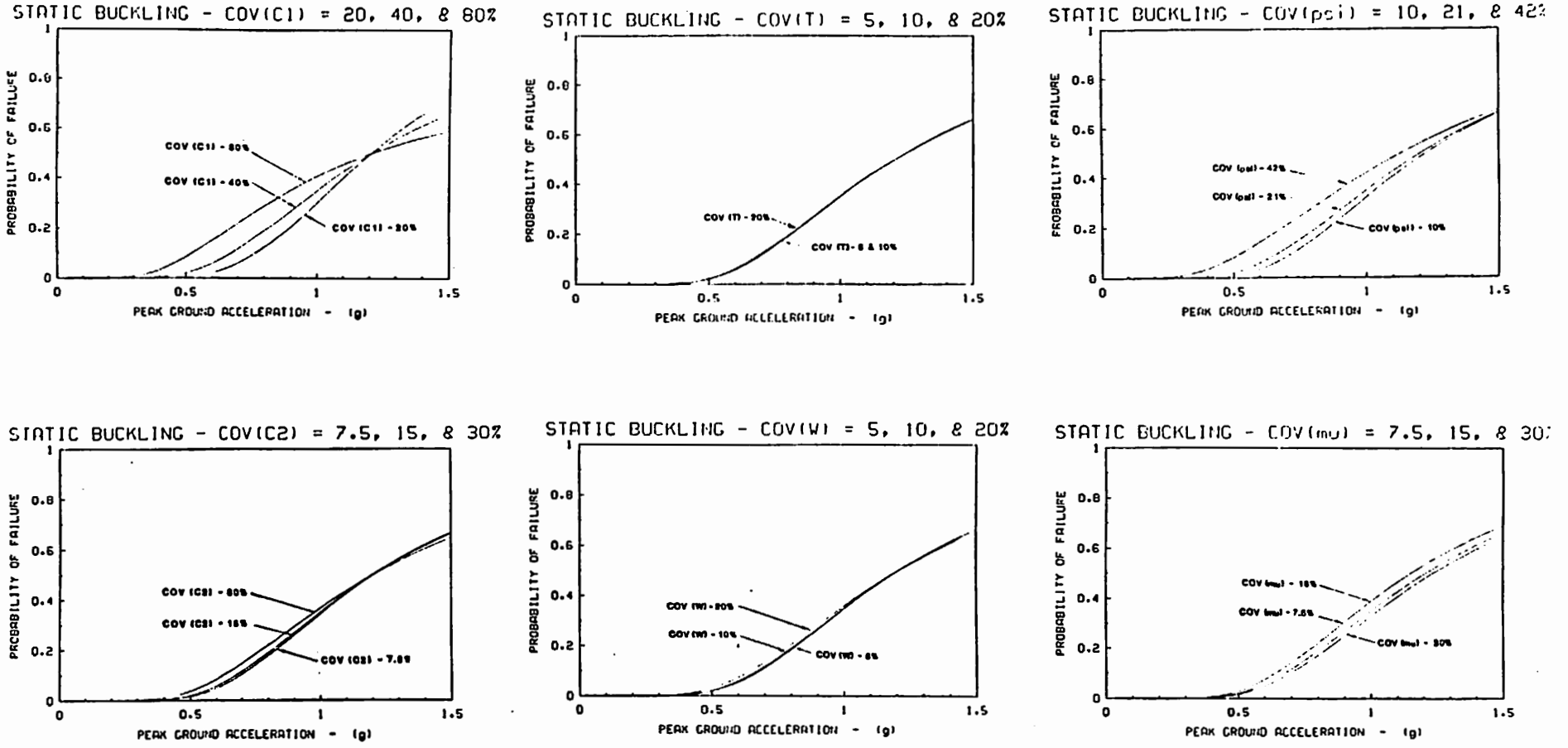


Figure 6.7 Equivalent static buckling fragility curve for uniform column

$$C_2 = h_{sh}[0.07T + (1-0.07T)(\ell-h^*)h^* + 2/3(1-0.07T)(h^*)^2] \quad (6.31)$$

where h_{sh} is the height of the shell not including the skirt, and h* is the ratio h_{sh}/ℓ.

Stress at Top of Skirt. The stress at the top of the skirt is calculated as a function of the moment and the axial force using the beam equation:

$$\sigma_{skirt} = \frac{M_{sk}}{S} - \frac{W^*}{A} \quad (6.32)$$

where W* is the weight at the top of the skirt and M_{sk} is the moment at this point. The variables S and A are respectively the section modulus and the cross-sectional area at the top of the skirt.

Yield Stress. The stress at which the skirt begins to yield is affected by two factors: the efficiency of the weld and the temperature of the material. The weld type chosen for this vessel places the skirt in line with the shell and has an efficiency of 100%. Lapping the shell with the skirt would reduce the efficiency.

The material chosen for the structure is ASME - SA36 which has a minimum yield of 27.8 ksi at the operating temperature of 650° F. The mean yield stress is assumed to be two standard deviations higher.

Random Variables. The basic random variables C_1, C_2, T, and W have the same distributions and coefficients of variation as presented in Section 6.2.1. The new factor, σ_{tear}, is assumed to be normally distributed with a COV of 10%.

Results. The results of this analysis are presented in Figure 6.2. A sensitivity analysis is again carried out and the results are plotted in Figure 6.8. This figure indicates that C_1 and C_2 again dominate the uncertainty in this analysis.

A comparison of the curves plotted in Figure 6.2 reveals that both bolt yield curves have higher probabilities of failure than the buckling or weld tear limit states. The curve corresponding to equation 6.19 for the bolt yield is much closer to the buckling and weld tear curves. The weld tear and buckling curves cross, with the flatter slope of the buckling curve reflecting greater uncertainty in the stress at buckling.

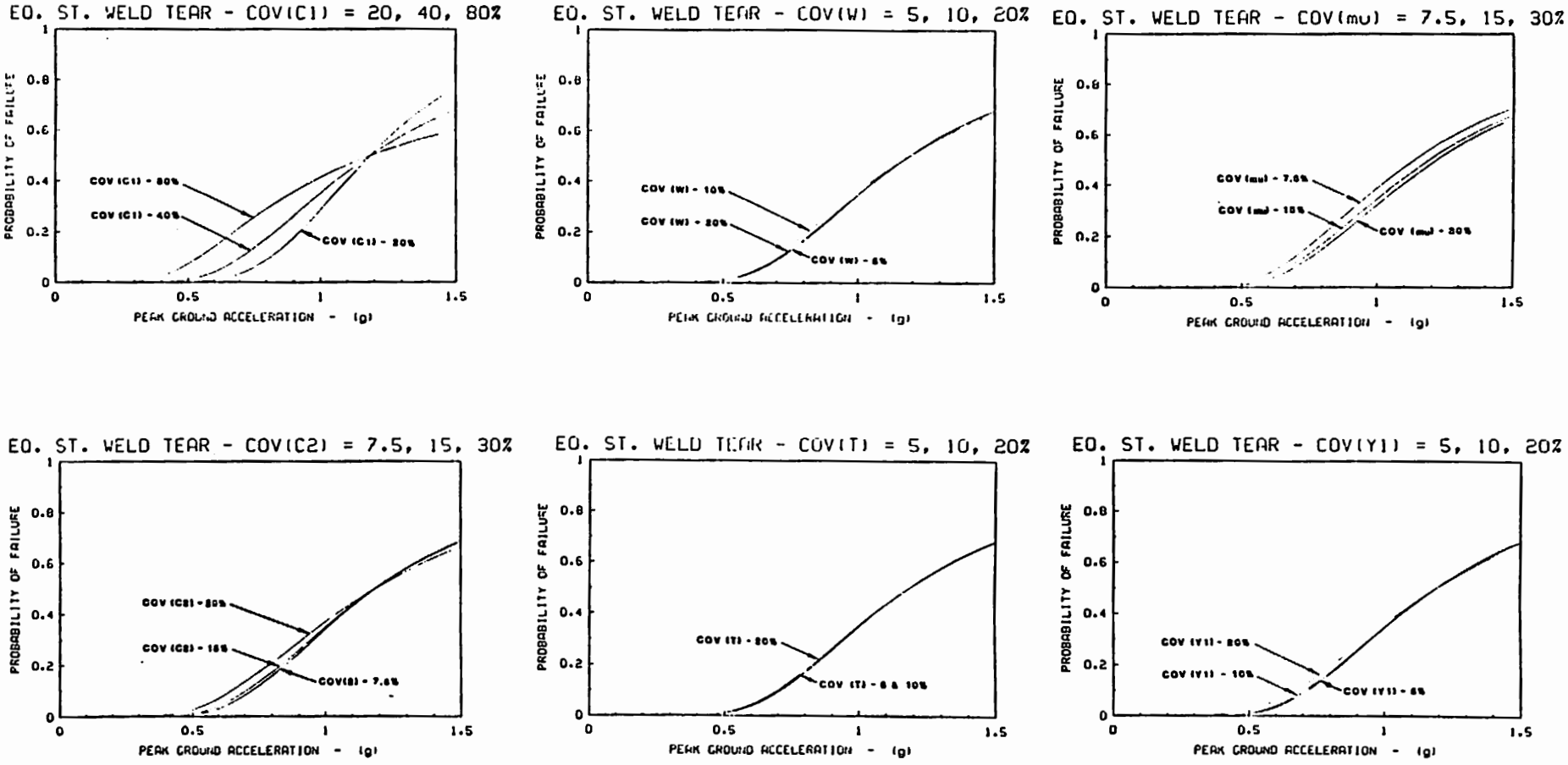


Figure 6.8 Sensitivity analysis for buckling of uniform column

6.5 Nonuniform Vessel

The column to be analyzed is a nonuniform vertical vessel illustrated in Figure 6.9. The reboiler is an additional piece of processing equipment supported by the skirt. The failure modes and the limit state functions are the same as described for the atmospheric column. The intent is to demonstrate the flexibility of the AFOR methods in dealing with a more complicated structure.

Base Shear. In these analyses, the transformation of PGA to base shear is performed using equations 6.2 and 6.3 with the factor B as defined in equations 6.24 and 6.25. Since the vessel is not uniform, equation 6.4 cannot be used to calculate the period of the structure. Instead, an equation proposed in RP-11 is used. In this formulation the structure is discretized and tabulated values are used to estimate the effects of the varying stiffness and mass on the fundamental period of the structure. In this case, the natural period was calculated to be 1.108 sec.

Moment at Base. The base shear to base moment factor is also calculated by discretizing the structure. The fundamental mode shape is assumed to be triangular and a portion of the base shear is applied at the top to account for higher modes of vibration. Thus the inertial force at each section is

$$F_i = (V - F_t)\left(\frac{W_i h_i}{\sum W_i h_i}\right) \tag{6.33}$$

where W_i is the weight of portion i of the structure, and h_i is the distance from the base to the centroid of portion i. V is the base shear and F_t is the force applied at the top:

$$F_t = 0.07TV \tag{6.34}$$

The inertial forces are multiplied by their moment arms, h_i, to find the moment at the base. The equation for C_2 is

$$C_2 = 63.51 + 2.13T \tag{6.35}$$

For the weld tear case, the moment is calculated at the top of the skirt. The moment arms are shortened and only those sections above the top of the skirt are included. Thus equation 6.35 becomes

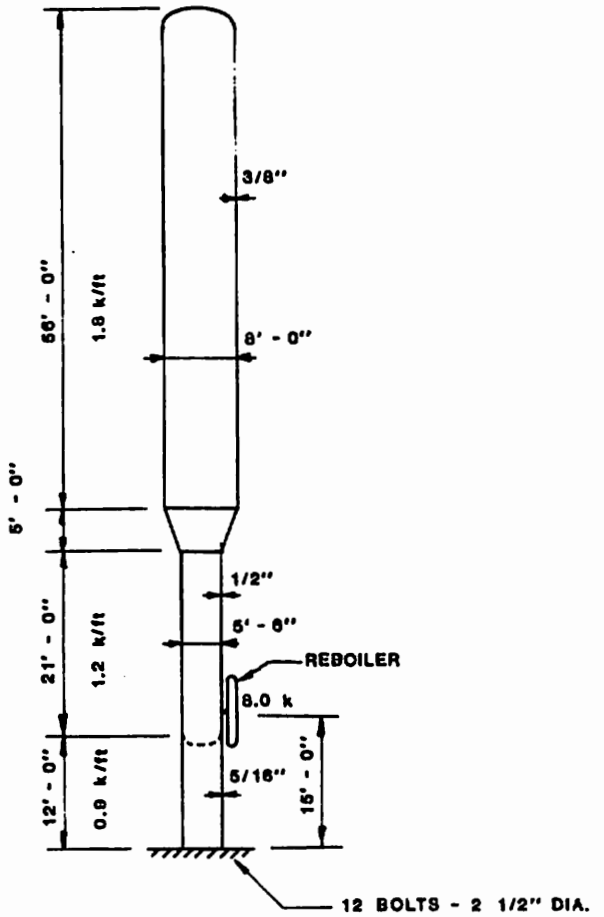


Figure 6.9 Nonuniform vessel

$$C_2 = 51.68 + 2.12T \qquad (6.36)$$

Resistance Parameters. The failure modes are the same as those discussed for the uniform column. For this reason the same formulations can be used to transform the base moment into the stress in a particular member. The stress in the bolts is calculated using equation 6.8 and equations 6.18 through 6.21 for the bolt yield limit state. For buckling, equation 6.25 was used to find the stress in the skirt and the stress at which buckling will occur is found from equation 6.27. The stress at the top of the skirt is calculated from equation 6.32.

Random Variables. The random variables are the same as defined in the equivalent static analyses of the uniform column. They are summarized in Table 6.1. The distributions and coefficients of variation are unchanged; the

mean values for C_1, C_2, W, T, and μ remain the same. The COV for the modeling uncertainty in the bolt yield analysis is based on the results of the uniform vessel analysis.

Results. The fragility curves generated by these analyses are plotted in Figure 6.10. This figure shows that although equation 6.8 predicts that bolts will yield first, equation 6.19 generates a bolt fragility curve below the buckling and the weld tear curves.

Table 6.1

Basic Random Variables for Analysis of Nonuniform Vessel

Random	Distribution	COV
C_1	normal	40%
C_2	normal	15%
T	normal	10%
W	normal	10%
σ_y	normal	5%
ψ	lognormal	See Section 6.3
μ	lognormal	15%

6.6 Summary and Conclusions

The analyses just presented demonstrate that the Advanced First Order Reliability methods outlined in Chapter 4 can be successfully used to develop fragility curves for use in subsequent system reliability analysis. The analysis can be greatly simplified through the use of design type equations. Analyses based on more rigorous approaches, however, demonstrate that conservatism in some design equations can adversely affect the accuracy of the analysis.

If the fragility curves must be in the lognormal format for subsequent systems analysis, the analyst can easily modify the numerical first order reliability analysis to search for the PGA's which correspond to the median

and median minus one standard deviation. These values are then used to find the parameters of a cumulative lognormal curve which passes through these two points. This process was carried out for the three limit states of the uniform vessel, and the results are shown in Figure 6.14. The fit is fairly good in the range of the median to median minus one for the PGA. At higher PGA's, however, the fit is not very good. These curves will be combined with a hazard analysis wherein the probability of occurrence of these PGA's is very low, and the errors arising from the poor fit in this region should be minimal.

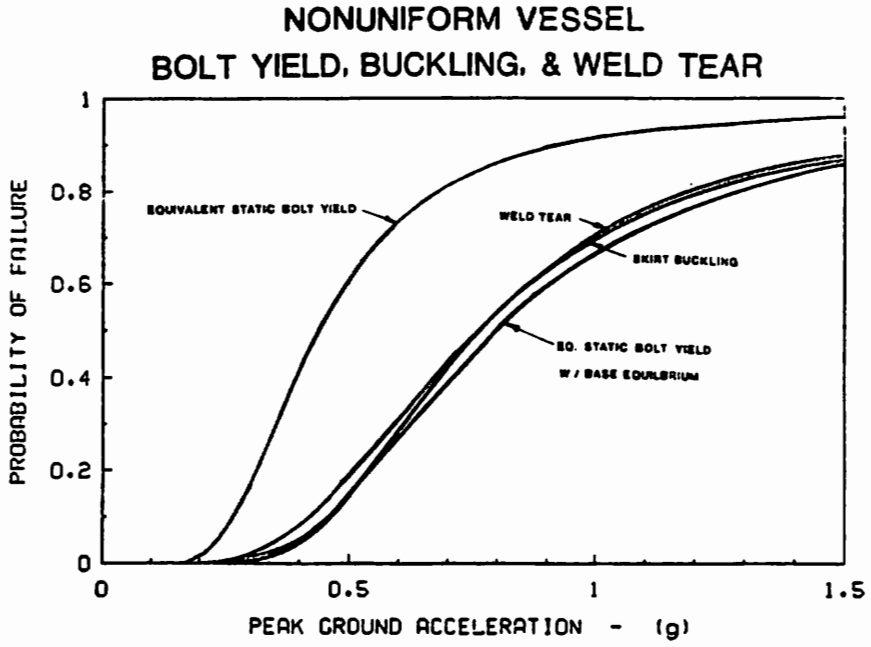


Figure 6.10 Fragility curves for equivalent static analysis of nonuniform column.

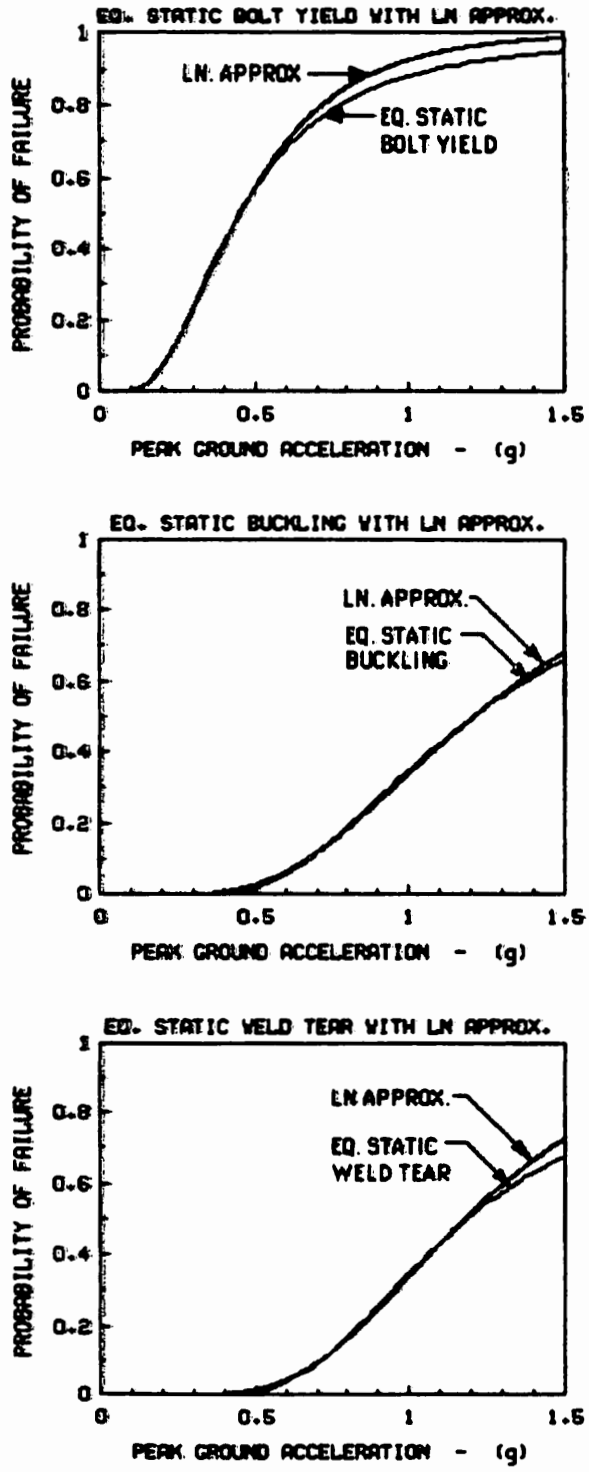


Figure 6.11 Lognormal approximations for fragility curves

CHAPTER 7

SUMMARY AND FUTURE WORK

7.1 Summary

The objective of this research is to develop a general methodology for the estimation of the risk from failures at large industrial facilities when subjected to major earthquakes. In this phase of the project the emphasis has been on reviewing existing methods for component and systems reliability analysis and introducing new methods for component reliability analysis.

In the effort to understand the behavior of large industrial facilities under severe earthquakes, a review of observed damage specifically at oil refineries was conducted. It was felt that the size, type of structures and production systems found at oil refineries are representative of other industrial facilities as well (e.g., chemical processing plants). The major conclusions from this review is that large cylindrical tanks and elevated tanks are most susceptible to damage and present the greatest hazard. The major risks associated with the failure of these structures is the potential for fire and the potential for the release of toxic substances. For oil refineries in particular, the potential for fire is greater than most other risks. For other major industries the release of toxic chemicals and contamination of ground water or air is of much greater concern. The consequences of these occurrences can be considerably more severe. The review and development of methods for the evaluation of the risk from such events will be the objective of subsequent studies.

Methods for systems reliability analysis are reviewed in Chapter 3. The main advantage of these methods over other existing systems analysis methods are that correlated failure modes, failure modes in cascade and correlated components can be included. The systems analysis approach will be implemented in Phase II of this study.

The emphasis in this report has been on the methods for the evaluation of component reliabilities (or probabilities of failure). Chapter 4 summarizes currently used first order second moment (FSOM) approach for fragility computations. Recently developed advanced first order reliability (AFOR) methods

are also presented in that chapter. The comparison of the two approaches reveals that the AFOR lends itself to just as simple formulation as the FSOM. However, uncertainties in the AFOR methods are usually related to basic random variables. These uncertainties are easier to quantify than uncertainties in safety factors. Furthermore, double counting for the same sources of uncertainties in resistance and load factors which are possible with FOSM fragility approach are avoided with the AFOR method. The most imporatant theoretical advantage of the AFOR method is that failure probability and reliability estimates are invariant with transformations of the limit state equation. For these and other reasons discussed more extensively in Chapter 4, the AFOR approach for fragility evaluation is considered. The feasibility of the AFOR approach in applications involving numerous component structures is demonstrated through specific examples.

Major component structures and equipment at oil refineries are identified in Chapter 5. The seismic design procedures for the structures are reviewed in that chapter. Potential failures and the consequences of failures are also discussed. The most critical structure for the oil production process is identified to be the isomerization columns.

In Chapter 6 failure probabilities are evaluated for tall isomerization columns with uniform and non-uniform cross sections. The objective in these examples is to evaluate failure probabilities using simple limit state equations which can be related to the seismic design procedure for that component. For comparison purposes, more detailed analytical techniques are employed to formulate the limit state equation. The significant observations from these analyses are summarized as follows:

- Simplified limit state equation can be modeled after specified design procedures based on equivalent static analyses. Failure probabilities estimated with these limit state equations are usually overestimated.

- Limit state equations using dynamic principles of structural analysis can be formulated at most structures of industrial facilities. A comparison between the design equation approach and the dynamic analsis show that failure probabilities from the equivalent static analysis may be overestimated by factors of two to three.

- Failure states which may be believed to be possible only in cascade are shown to have comparable failure probabilities when dynamic analysis is used to formulate the limit state equations.

- Failure probabilities conditional on the input ground motion as obtained from the AFOR methods are approximated by lognormal probability distributions preserving the median and median plus one standard deviation points on the distribution. The approximation appears to be close for the specific examples considered.

The lognormal approximation to the failure probability is particularly useful for subsequent systems analysis.

7.2 Future Work

Several major aspects of the seismic risk from major industrial facilities still remain to be investigated. These can be summarized as follows:

- Identify risk cirteria specific to various industries. These will provide the basis for event tree/fault tree formulations and subsequent systems analyses.

- Investigate the use of structural systems reliability techniques for the evaluation of large systems reliabilities. These will enable the treatment of dependent components and failure modes in cascade.

- Formulate systems reliability analysis methods. These methods should consider component correlations, and redundancies under common cause failures.

- Study the importance of component dependencies to the overall systems reliability.

- Study the effect of lognormal approximations of component failure probabilities to the systems failure estimates.

- Investigate existing methods and develop new methods for estimation of losses from components and systems failures.

- Conduct case studies in order to demonstrate the feasibility of various methods of analysis.

Phase II of the current study will concentrate on the systems evaluation methods considering component dependencies. Specifically, the feasibility of structural systems anaslysis approach will be investigated.

REFERENCES

Ang, A. H-S. and C.A. Cornell (1973). "Reliability Bases of Structural Safety and Design", in Modern Concepts of Structural Safety and Design, ASCE Structural Devision, Preprint 2023, pp. 1-29.

ATC-03 (1978). "Tentative Provisions for the Development of Seismic Regulations for Buildings," Applied Technology Council Publication ATC 3-06.

Bohn, M.P. et al. (1982). "Seismic Safety Margins Program", Progress Report No. 13, NUREG/CR -1120, Vol. 9, Lawrence Livermore Laboratory, Livermore, CA.

Committee on the Alaska Earthquake, Division of Earth Sciences, National Research Council (1973). The Great Alaskan Earthquake of 1964, National Academy of Sciences, Washingtoin, D.C..

Cornell, C.A. (1969). "A Probability-Based Structural Code", ACI-Journ, Vol. 66, pp. 974-985.

Cornell, C.A. (1967). "Bounds on the Reliability of Structural Systems", J. Struct. Div., ASCE, Vol. 93, pp. 171-200.

Ditlevesen, O. (1977), Fundamentals of Second Moment Structural Reliablity Theory, Int. Research Seminar on Safety of Structures, Trondheim, Norway.

Ditlevsen, O. (1979). "Narrow Reliability Bounds for Structural Systems", J. Struct. Mech., Vol. 7, pp. 435-451.

Donnel, L. H. and C.C. Wen (1950). "Effect of Imperfections on the Buckling of Thin Cylinders and Columns under Axial Compression," J. of Applied Mechanics, Vol. 17, No. 1, p. 73.

Donnel, L.H. (1934). "A New Theory for the Buckling of Thin Cylinders under Axial Compression and Bending," Transactions of the American Society of Mechanical Engineers, Vol. 56, p. 795.

Ferrer, G.W. (1975). "The Managua Earthquake of December 23, 1972," American Iron and Steel Institute.

Fussell, J.B. (1975). "Computer Aided Fault Tree Construction for Electrical Systems", in Reliability and Fault Tree Analysis, Barlow, R.E., J.B. Fussell, and N.D. Singpurwalla, eds., SIAM, Philadelphia, Penn., pp. 37-56.

Hasofer, A.M. and N. Lind, (1974). "An Exact and Invariant First Order Reliability Format", J. Eng. mech. Div., ASCE, Vol. 100, No. EM1, pp. 111-121.

Hohenbichler, M. and R. Rackwitz, (1981). "Non-Normal Dependent Vectors in Structural Safety", J. Eng. Mech. Div., ASCE, Vol. 107, EM6, pp. 1227-1238.

Hunter, D. (1976). "An Upper Bound for the Probability of a Union," J. of Applied Probability, Vol. 3, No. 3, 1976, pp. 597-603.

Iyengar, R.N., and M. Shinozuka (1971), "Effect of Self-Weight and Vertical Acceleration on the Behavior of Tall Structures During Earthquakes," Dept. of Civl Engg., Tech. Rep. No. 17, Columbia University, New York, N.Y.

Johnston, R.L. (1955). "Earthquake Damages to Oil Fields and to the Paloma Cycling Plant in the San Joaquin Valley," California Division of Mines and Geology, Bulletin No. 171, pp. 221-226.

Kawasumi, H. (1968). "General Report on the Niigata Earthquake of 1964," Tokyo Electrical Engineering College Press, Tokyo.

Kennedy, R.P., R.D. Campbell, G. Hardy and H. Banon (1982). "Systems Fragility, Seismic Safety Margins Program", NUREG/CR-2405, UCRL-15407, Lawrence Livermore Laboratory, Livermore, CA.

Kennedy, R.P., C.A. Cornell, R.D. Campbell, S. Kaplan, and H.F. Pesla, (1980). "Probabilistic Seismic Safety Study of an Existing Nuclear Power Plant", Nucl. Engr. Des., Vol. 59, pp. 315-338.

Kircher, C.A., et al. (1978), Seismic Analysis of Oil Refinery Structures, Part I, for John A. Blume Earthquake Engineering Center, Technical Report 31, Stanford University, Stanford, CA

Kulak, G.L., "Statistical Aspects of Strength of Connections," Safety and Reliability of Metal Structures, American Society of Civil Engineers, New York, 1972.

Lai, S.P. (1982), "Statistical Characteristics of Strong Ground Motions Using Power Spectral Density Function," Bull. Seism. Soc. Am., Vol 72, No. 1, pp. 259-274.

Leeds, D.J., ed., "Reconnaissance Report, Imperial County Earthquake, October 15, 1979," Earthquake Engineering Research Institute, Berkeley, CA, 1980.

National Board of Fire Underwriters (1933). "Report on Southern California Earthquake of March 10, 1933," NBFU, 1933.

Newland, D.E. (1975), An Introduction to Random Vibrations and Spectral Analysis. Longman, New York.

Newmark, N.M. and R. Riddell (1979). "A Statistical Study of Inelastic Response Spectra," Proceedings Second U.S. National Conference on Earthquake Engineering, Stanford, CA.

Newmark, N.M., W.J. Hall and B. Mohraz (1973). A Study of Vertical and Horizontal Earthquake Spectra, WASH 1255, Directorate of Licensing, U.S. Atomic Energy Commission, Washington, D.C.

Penzien, J., and Watabe, M. (1975), "Characteristics of 3-Dimensional Earthquake Ground Motions," Int. J. Earth. Engg. and Struct. Dyn., Vol. 3, pp. 365-373.

Powers, G.J., Tompkins, F.C. and S.A. Lapp (1975). "A Safety Simulation Language for Chemical Processes: A Procedure for Fault Tree Synthesis," in Reliability and Fault Tree Analysis, R. Barlow et al., eds. SIAM, Philadelphia, Penn., pp. 57-77.

PRA Guide (1982). PRA Procedures Guide, Review Draft, NUREG/CR-2300, Vol. 2, Rev. 1., U.S. Nuclear Regulatory Commission, Washington, D.C.

Rackwitz, R. (1978). "Close Bounds for the Reliability of Structural Systems", Berichte zur Zuverlassigkeitstheorie der Bauwerke, SFB 96, Heft 29, LKI, Technische Universitat, Munchen.

Reactor Safety Study, (1975), WASH-1400, NUREG-75/014, U.S. Nuclear Regulatory Commission, Washington, D.C.

Recommended Practice No. 11, Wind and Earthquake Design Standards (1980), Standard Oil Company of California, San Francisco, CA.

Rinne, J.E., (1970). "Design of Earthquake Resistant Structures: Towers and Chimneys," in Earthquake Engineering, R.L. Wiegel, ed., Prentice-Hall, Englewood Cliffs, NJ.

Shah, H.C., C.P. Mortgat, A. Kiremidjian and T.C. Zsutty (1975). "A Study of Seismic Risk for Nicaragua: Part I", Report No. 11, The J.A. Blume Earthquake Engineering Center, Stanford University, Stanford, CA.

Shih, T.Y., and Y.C. Chen, (1984) "Stochastic Earthquake Response of Tapered Columns," J. Engg. Mech., ASCE, Vol. 110, No. 8, pp. 1185-1210.

Shinozuka, M., and Sato, Y. (1967), "Simulation of a Nonstationary Process," J. Engg. Mech., ASCE, Vol. 93, EM1, pp. 11-40.

Smith, P.D. et al., (1981). "Seismic Safety Margins Program Overview", Final Report, Phase I., NUREG/CR-2015, Vol. I, UCRL - 53021, Vol. I, Lawrence Livermore Laboratory, Livermore, CA.

Steinbrugge, K. and D.F. Moran (1954). "An Engineering Study of the Southern California Earthquake of July 21, 1952 and Its Aftershocks," Bull. Seism. Soc. Am., Vol. 44, No. 28, pp. 270-278.

Stratta, J.L. (1980). "Greenville (Diablo-Livermore) Earthquakes of January 1980," Earthquake Engineering Research Institute Newsleter, Vol. 14, No. 2, pp. 20-90.

Thoft-Christensen, P. and J.D. Sorensen, (1982). "Reliability of Structural Systems with Correlated Elements", Appl. Math. Mod., Vol. 6.

Timoshenko, S.P. and J.M. Gere (1961). Theory of Elastic Stability, McGraw-Hill Book Company, New York.

Uniform Building Code, (1982). International Conference of Building Officials, Whittier, California.

Vanmarcke, E.H., and S.P. Lai (1980), "Strong-Motion Duration and RMS Amplitude of Earthquake Records", Bull. Seism. Soc. Am., Vol. 70, No. 4, pp. 1293-1307.

Veneziano, D. (1979). "New Index of Reliability," J. Eng. Mech., ASCE, Vol. 105, EM2, pp. 277-296.

Veneziano, D. (1974). "Second Moment Reliability", Research Report No. R74-33, Dept. of Civil Engineering, Mass. Inst. of Tech., Cambridge, Mass.

Yanev, P.L., ed. (1980). "Reconnaissance Report, Miyagi Ken-Oki, Japan Earthquake, June 12, 1978," Earthquake Engineering Research Institute, Berkeley, CA.

Yanev, P.I. and S. Swan (1982). "Program for the Development of an Alternative Approach to Seismic Equipment Qualification," Report to the Seismic Qualification Utility Group, EQE Rep. No. 52, EQE, San Francisco, CA.